Functional studies of selected actin binding proteins by point mutations and GFP fusions

Dissertation
der Fakultät für Biologie der
Ludwig-Maximilians-Universität
München

Soo Sim Lee

2000

Functional studies of selected actin binding proteins by point mutations and GFP fusions

Dissertation
der Fakultät für Biologie der
Ludwig-Maximilians-Universität
München

vorgelegt von

Soo Sim Lee
aus
Singapur

8. August 2000

Ehrenwörtliche Versicherung

Diese Dissertation wurde selbständig und ohne unerlaubte Hilfsmittel angefertigt.

München, August 2000

Soo Sim Lee

Dissertation eingereicht: 8. August 2000

Erstgutachter: **Dr. F. Siegert**
Zweitgutachter: **Prof. Dr. H.-U. Koop**
Sondergutachter: **Prof. Dr. M. Schleicher**

Tag der mündlichen Prüfung: 15. November 2000

Parts of this work were already being published:

Zimmermann, T., **Lee, S.S.**, Eichinger, L., Schleicher, M. and Siegert, F. *In vivo* localization of a severin GFP-fusion protein in *Dictyostelium* amoebae during endocytosis, cell motility and development. (submitted).

Lee, S.S., Karakesisoglou, I., Noegel, A.A., Rieger, D. and Schleicher, M. (2000). Dissection of functional domains by expression of point mutated profilins in *Dictyostelium* mutants. *Eur. J. Cell Biol*. **79**:92-103.

Eichinger, L., **Lee, S.S.** and Schleicher, M. (1999). *Dictyostelium* as model system for studies of the actin cytoskeleton by molecular genetics. *Microscopy Res. Technique* **47**:124-134.

The experimental parts of the work presented here were carried out in the laboratory of Prof. Dr. Michael Schleicher from April 1997 to February 2000 at the Adolf-Butenandt-Institute of Cell Biology, Ludwig-Maximilians-Universität München.

TABLE OF CONTENTS

i

ABBREVIATIONS vi

SUMMARY 1

ZUSAMMENFASSUNG 2

1 INTRODUCTION 3

1.1 The actin cytoskeleton 3

1.2 *Dictyostelium* as model organism 5

1.3 GFP as marker of gene expression 7

1.4 Profilin 9

1.5 Severin 11

1.6 Pathogens and the actin cytoskeleton 13

1.6.1 Actin-based motilities of pathogens 13

1.6.2 Rho modification by bacterial toxins 14

1.6.3 *Yersinia enterocolitica* and the actin cytoskeleton 15

1.7 Goals of project 19

2 MATERIALS AND METHODS 20

2.1 Materials 20

2.1.1 Enzymes for molecular biology 20

2.1.2 Antibodies 20

2.1.3 Protease inhibitors 20

2.1.4 Antibiotics 21

2.1.5 Chemical reagents 21

2.1.6 Media 21

2.1.6.1 Media for *D. discoideum* culture 22

2.1.6.2 Medium for *E. coli* culture 22

2.1.7 Buffers and other solutions 23

2.1.8 Bacterial strains 23
2.1.9 *Dictyostelium discoideum* strains 23
2.1.10 Mammalian cell line 24
2.1.11 Vectors 24
2.1.12 Equipment 24
2.1.13 Other materials 25
2.1.14 Centrifuges and rotors 26
2.1.15 Computer programmes 26
2.2 Cultivation of *Dictyostelium discoideum* 26
2.2.1 Growth in liquid medium 26
2.2.2 Growth on agar plates 27
2.2.3 Preservation of spores 27
2.2.4 Freezing of *Dictyostelium* cells 27
2.3 Mammalian tissue culture 28
2.3.1 Cell culture 28
2.3.2 Freezing of cells 28
2.4 Molecular biological methods 29
2.4.1 Preparation of plasmid DNA 29
2.4.1.1 Isolation of plasmid DNA by the method of Holmes and Quigley (1981) 29
2.4.1.2 Isolation of plasmid DNA by the method of Qiagen 29
2.4.2 Restriction digest 30
2.4.3 Agarose gel electrophoresis 30
2.4.4 Isolation of DNA fragments from agarose gels 31
2.4.5 Oligonucleotide primers 31
2.4.6 Polymerase chain reaction (PCR) 33
2.4.7 Purification of PCR products 33
2.4.8 Phosphatase treatment 34
2.4.9 DNA ligation 34
2.4.10 Preparation of electroporation competent cells 35
2.4.11 Electroporation of *E. coli* 35
2.4.12 Screening for positive *E. coli* transformants 35
2.4.13 *E. coli* permanent cultures 36
2.4.14 Transformation of *D. discoideum* 36
2.4.15 Cloning of transformants 36

2.4.16 Generation of severin-GFP *Dictyostelium* transformants 37
2.4.17 Generation of profilin-GFP *Dictyostelium* transformants 37
2.4.18 Transfection of mammalian cells 38
2.5 Biochemical methods 39
2.5.1 SDS-polyacrylamide gel electrophoresis (SDS-PAGE) 39
2.5.2 Coomassie Blue staining of proteins 40
2.5.3 Drying of SDS-PAGE gels 40
2.5.4 Western blotting 41
2.5.5 Bradford assay 42
2.5.6 Preparation of actin from rabbit skeletal muscle 42
2.5.7 Pyrene-labelling of actin 43
2.5.8 Partial purification of the severin-GFP fusion protein 43
2.5.9 Low shear viscometry 44
2.5.10 Severing activity of severin-GFP measured by fluorescence spectroscopy 44
2.5.11 Poly-(L)-proline binding assay 45
2.5.12 Inhibition of actin polymerization analyzed by fluorescence spectroscopy 45
2.5.13 Interaction of profilin-GFP with actin 45
2.6 Cell biological methods 47
2.6.1 Indirect immunofluorescence 47
2.6.2 Phagocytosis of yeast 48
2.6.3 *Yersinia* infection of COS7 cells 48
2.6.4 Confocal laser scanning microscopy (CLSM) 49
2.6.5 Growth curves of *D. discoideum* mutants 50
2.6.6 Development of *D. discoideum* mutants 50

3 RESULTS 51
3.1 Analyses of the point-mutated profilins in *D. discoideum* 51
3.1.1 The W3N and K114E point-mutated profilins 51
3.1.2 Poly-(L)-proline binding properties of W3N and K114E 51
3.1.3 Actin and PIP_2 binding characteristics of W3N and K114E 52
3.1.4 Cell morphology, cytokinesis and subcellular distribution of profilins 54
3.1.5 Development of DdW3N and DdK114E 54
3.1.6 Profilin localization at phagocytic cups 56

3.2 Analyses of profilin in *D. discoideum* via GFP fusion 57
3.2.1 Generation of profilin-GFP vector construct and *Dictyostelium* transformants 57
3.2.2 Western analysis of the GFP fusion proteins 59
3.2.3 Development of the profilin-GFP *Dictyostelium* transformant 60
3.2.4 Growth rate of profilin-GFP cells 60
3.2.5 Interaction between poly-(L)-proline and profilin-GFP 61
3.2.6 Interaction between profilin-GFP and actin 61
3.2.7 Cell morphology and subcellular distribution of profilin-GFP 65
3.2.8 *In vivo* distribution of the profilin-GFP fusion protein 67
3.3 Studies of severin in *D. discoideum* via GFP fusion 69
3.3.1 Generation of severin-GFP *Dictyostelium* transformants 69
3.3.2 Immunoblot analysis of the severin-GFP fusion protein 70
3.3.3 Partial purification of the severin-GFP fusion protein 70
3.3.4 Severing activity of the severin-GFP fusion protein 73
3.3.5 Localization of severin-GFP during macropinocytosis 74
3.4 *Yersinia* infection and the actin cytoskeleton 76
3.4.1 Indirect immunofluorescence analyses of selected cytoskeletal proteins during *Yersinia enterocolitica* infection 76
3.4.2 Studies of selected GFP-fused cytoskeletal proteins during *Yersinia* infection 81

4 DISCUSSION 92
4.1 The point-mutated profilins, W3N and K114E 92
4.1.1 *In vitro* analyses of W3N and K114E 92
4.1.2 Rescue of the profilin null phenotype by W3N and K114E 93
4.1.3 Profilin localization at phagocytic cups 93
4.1.4 Significance of the poly-(L)-proline binding property of profilin 94
4.2 Study of *D. discoideum* profilin via GFP fusion 96
4.2.1 Partial rescue properties of the profilin-GFP fusion protein 96
4.2.2 *In vitro* analyses of the profilin-GFP fusion protein 97
4.2.3 Profilin-GFP, a functional construct? 98
4.2.4 *Dictyostelium* profilin is involved in highly dynamic cellular processes 100
4.3 Study of *D. discoideum* severin via GFP fusion 101
4.3.1 Severin-GFP is a functional fusion construct 101

4.3.2 *In vivo* studies of severin dynamics 102

4.4 *Y. enterocolitica* infection and the actin cytoskeleton 104

4.4.1 Indirect immunofluorescence study of selected cytoskeletal proteins in *Y. enterocolitica* infected cells 105

4.4.2 *Y. enterocolitica* infection disrupts the actin cytoskeleton 105

5 REFERENCES 108

CURRICULUM VITAE 138

ACKNOWLEDGEMENT 139

ABBREVIATIONS

ATP	adenosine 5‘-trisphosphate
bp	base pair(s)
BSA	bovine serum albumin
CLSM	confocal laser scanning microscopy
Cy3	carboxymethyl-indole-cyanine
DEAE	diethylaminoethyl-cellulose
DIC	differential interference contrast
DMEM	Dulbeccos minimum essential medium
DMSO	dimethyl sulfoxide
DNA	deoxyribonucleic acid
DNase	deoxyribonuclease
dNTP	deoxyribonucleotide triphosphate
DTT	1,4-dithiothreitol
EDTA	ethylenediaminetetraacetic acid
EGTA	ethylene glycol-bis (2-aminoethyl ether)-N,N,N‘,N‘-tetraacetic acid
F-actin	filamentous (polymerized) actin
FITC	fluorescein isothiocyanate
g	ground acceleration; gram(s)
G-actin	globular actin (monomer)
GFP	green fluorescent protein
h	hour(s)
HEPES	N-2-hydroxyethylpiperazine-N‘-2-ethanesulfonic acid
IgG	immunoglobulin G
IPTG	isopropyl-ß-thiogalactopyranoside
kb	kilobase(s)
kDa	kilodalton
l	litre(s)
LMW	low molecular weight
µ	micro
M	molar

mAb	monoclonal antibody
MES	2-(N-morpholino)ethanesulfonic acid
min	minute(s)
ml	millilitres
µm	micrometer
mM	millimolar
MOPS	3-(N-morpholino)propanesulfonic acid
mS	millisiemens
nm	nanometer
NP40	nonylphenyl polyethyleneglycol
OD	optical density
PAGE	polyacrylamide gel electrophoresis
PBS	phosphate buffered saline
PC	phosphocellulose
PCR	polymerase chain reaction
PIP_2	phosphatidylinositol-4,5-diphosphate
PMSF	phenylmethylsulfonyl fluoride
psi	pounds per square inch, 1 psi = 6897 Pa
RNA	ribonucleic acid
RNase	ribonuclease
rpm	revolutions per minute
RT	room temperature
s	second(s)
SDS	sodium dodecyl sulfate
TEMED	N,N,N‘,N‘-tetramethylethylenediamine
Tris	Tris-(hydroxymethyl)-aminomethane
TRITC	tetramethylrhodamine isothiocyanate
Triton X-100	octylphenolpoly(ethyleneglycolether)$_n$
Tween 20	polyoxyethylene-sorbitanmonolaurate
U	unit(s)
V	volt
v/v	volume per volume
vol.	volume(s)
w/v	weight per volume

SUMMARY

Profilin is an ubiquitous cytoskeletal protein whose function is fundamental to the maintenance of normal cellular physiology. Site-directed mutagenesis of profilin II from *Dictyostelium discoideum* by PCR resulted in the point mutations W3N and K114E, whereby the W3N profilin is no longer able to bind to poly-(L)-proline concomitant with a slight reduction in actin-binding, whereas the K114E profilin shows profound decrease in its ability to interact with actin but its affinity for poly-(L)-proline remained unaltered. The *in vivo* properties of the point-mutated profilins were studied by expressing either W3N or K114E in the profilin-minus *D. discoideum* mutants which have defects in the F-actin content, cytokinesis and development (Haugwitz *et al*., 1994). Expression resulted in normal cell physiology, a reduction in the F-actin content, and a complete development. Interestingly, only cells which overexpressed W3N could restore the aberrant phenotype, while the K114E profilin with its fully functional poly-(L)-proline binding and its strongly reduced actin-binding activities rescued the phenotype at low concentrations. Both the wild-type and point-mutated profilins are enriched in phagocytic cups during uptake of yeast particles. These data suggest a) that a functional poly-(L)-proline binding activity is more important for suppression of the mutant phenotype than the G-actin binding activity of profilin, and b) that the enrichment of profilin in highly active phagocytic cups might be independent of either poly-(L)-proline or actin-binding activities.

To have a better understanding of the *in vivo* role of profilin, *D. discoideum* profilin II has been tagged at its C-terminus with the green fluorescent protein (GFP) with a 100-aa linker separating profilin and GFP. This fusion construct was introduced in *D. discoideum* profilin-minus cells and expression of the fusion protein could restore the aberrant phenotype partially. The partial rescue might be due to the uneven expression of the fusion protein leading to mixed populations even after repeated recloning. The profilin-GFP transformants showed normal cell morphology, could be cultivated in shaking suspensions, and could develop fruiting bodies which closely resembled those of the wild-type. *In vivo* studies revealed the distribution of the fusion protein in highly active regions of the cells such as phagocytic cups, macropinocytotic crowns, cell cortex and at the leading edges of locomoting cells. Thus profilin appears to play a significant role in the regulation of the dynamic actin-based cellular processes.

A second actin-regulatory protein from *D. discoideum* namely, severin, a Ca^{2+}-dependent F-actin fragmenting and capping protein, was also investigated via fusion to GFP at its C-

terminus. Although severin is a very active F-actin fragmenting protein in *in vitro* assays, the severin null *D. discoideum* mutant exhibits normal growth, cell motility, chemotaxis and development. Examination of the live dynamics of severin-GFP should clarify the *in vivo* role of severin and other functionally redundant cytoskeletal proteins. The 70 kDa severin-GFP fusion protein has been sufficiently expressed and partially purified from the severin null cells whereby *in vitro* assays confirmed the ability of this fusion protein to sever F-actin only in the presence of Ca^{2+}. Data from confocal microscopy showed that the fusion protein was transiently detected in macropinocytotic crowns, phagocytic cups, membrane ruffles, at the leading edges of motile cells and cell-cell contacts of aggregating cells in directed motion. These data suggest an *in vivo* role for severin in the remodulation of existing F-actin structures as supported by the *in vitro* data.

The highly dynamic cytoskeleton also plays a significant part in the defence of the cells against pathogens. The behaviour of the actin cytoskeleton of cultured mammalian cells in response to *Yersinia enterocolitica* infection was examined by confocal microscopy with the aid of GFP-tagged actin, cofilin and profilin II. The translocated *Yersinia* outer proteins (Yops) encoded by a virulence plasmid in the wild-type bacteria have been observed to disrupt the actin microfilaments, resulting in diffuse actin staining which subsequently disappeared completely upon prolonged bacterial infection. In addition, F-actin structures resembling phagocytic cups were found at the sites of bacterial adherence, suggesting the likelihood of the involvement of the Rho family of small GTPases in the regulation of the actin cytoskeleton. The secreted Yops appeared to have no major effect on the distribution of GFP-profilin whereas the staining pattern of GFP-cofilin seemed to be modified by the Yops, resulting in a decrease in length of the actin-cofilin rods and a diffuse localization of cofilin. The exact mechanisms of interaction between the Yops and their host targets remain to be determined. However, a clearer insight into the interaction between pathogens and the host cytoskeleton will certainly aid in the cellular defence and the prevention of pathogenesis.

ZUSAMMENFASSUNG

Profilin ist ein ubiquitäres Zytoskelettprotein, dessen Funktion für die Zellphysiologie von fundamentaler Bedeutung ist. Durch gerichtete Mutagenese von Profilin II aus *Dictyostelium discoideum* wurden die Punktmutationen W3N und K114E erzeugt. Das W3N-Profilin interagiert nicht mehr mit poly-(L)-Prolin und zeigt geringfügig verminderte Aktinbindung. Dagegen ist die Aktinbindung des K114E-Profilin stark reduziert, während seine Affinität zu poly-(L)-Prolin unverändert bleibt. Die *in vivo* Eigenschaften der punktmutierten Profiline wurden durch Expression von W3N- bzw. K114E-Profilin in *D. discoideum* Profilin-Nullmutanten (Haugwitz *et al*., 1994) untersucht, die Defekte im Aktingehalt, der Cytokinese und der Entwicklung aufweisen. Die Expression führte zur Wiederherstellung eines normalen Phänotyps. Interessanterweise ist dafür eine W3N-Profilin-Überexpression erforderlich, während K114E-Profilin mit seiner stark reduzierten Aktin-, aber voll funktionellen poly-(L)-Prolin-Bindung den mutanten Phänotyp schon in geringen Mengen aufhebt. Sowohl das Wildtyp-Profilin als auch die beiden punktmutierten Profiline sind während der Phagozytose von Hefezellen in „phagocytic cups“ angereichert. Diese Befunde sprechen dafür, dass a) eine funktionelle poly-(L)-Prolin-Bindungsaktivität für die Suppression des mutanten Phänotyps wichtiger ist als die G-Aktin-Bindungsaktivität, und b) die Anreicherung von Profilin bei der Phagozytose weder von seiner poly-(L)-Prolin-Bindung, noch von einer intakten Aktinbindung abhängt.

Für ein besseres Verständnis der Funktion von Profilin *in vivo* wurde *D. discoideum* Profilin II am C-Terminus über ein 100 Aminosäuren langes Verbindungsstück mit dem grün-fluoreszierenden Protein (GFP) verknüpft. Die Expression dieses Fusionskonstrukts in der *D. discoideum* Profilin-Nullmutante führte zu weitgehender Kompensation des mutanten Phänotyps. *In vivo* Untersuchungen zeigten die Lokalisation des Fusionsproteins in hochaktiven Regionen der Zelle, wie z. B. in Phagozytose Strukturen, dem Zellkortex und Pseudopodien. Profilin scheint also eine signifikante Rolle bei der Regulation dynamischer, Aktin-abhängiger, zellulärer Prozesse zu spielen.

Severin, ein weiteres Aktin-regulatorisches Protein aus *D. discoideum* mit Ca^{2+}-abhängiger Aktin-Fragmentierungs- und „Capping"-Aktivität, wurde ebenfalls mit Hilfe C-terminaler Verknüpfung an GFP untersucht. Das 70 kDa große Severin-GFP Fusionsprotein wurde in den Severin-Nullmutanten ausreichend stark exprimiert und aus diesen Zellen angereichert. Dabei zeigten *in vitro* Versuche, dass die Fragmentierung von F-Aktin durch das Fusionsprotein nur in Gegenwart von Ca^{2+} erfolgt. Die Ergebnisse der Konfokalmikroskopie belegten die transiente Lokalisation des Fusionsproteins in aktiven Regionen bei der Zellbewegung. Diese Befunde deuten auf eine Rolle von Severin beim Umbau bereits existierender Aktinstrukturen *in vivo* hin.

Das hochdynamische Zytoskelett spielt auch eine bedeutende Rolle bei der Verteidigung von Zellen gegen pathogene Organismen. Durch Konfokalmikroskopie an kultivierten Säugerzellen wurde das Verhalten des Aktin-Zytoskeletts als Antwort auf eine *Yersinia enterocolitica* Infektion mit Hilfe von GFP-verknüpftem Aktin, Cofilin und Profilin II untersucht. Es wurde beobachtet, dass die von einem Virulenzplasmid der Wildtyp-Bakterien kodierten Yops (*Yersinia* outer proteins) die Aktin-Mikrofilamente abbauen, was sich zunächst in einer diffusen Aktinfärbung äußerte. Zusätzlich wurden an den Stellen bakterieller Anheftung F-Aktin-Strukturen gefunden, die Phagozytose Strukturen ähnlich sahen. Dies macht eine Beteiligung der Rho-Familie kleiner GTPasen bei der Regulation des Aktin-Zytoskeletts wahrscheinlich. Die sezernierten Yops hatten keinen deutlichen Effekt auf die Verteilung von GFP-Profilin, dagegen schien das Färbungsmuster von GFP-Cofilin durch die Yops modifiziert zu werden, was zu einer Verkürzung der Aktin-Cofilin-Stäbchen und diffuser Lokalisation von Cofilin führte. Der genaue Mechanismus der Interaktion der Yops mit den Zieldomänen der Wirtszelle ist noch unbekannt, aber ein genauerer Einblick in die Interaktionen zwischen pathogenen Organismen und dem Zytoskelett der Wirtszelle kann sicherlich zum Schutz der Zellen und der Prävention der Pathogenese beitragen.

1 INTRODUCTION

1.1 The actin cytoskeleton

Cells vary greatly in shapes and sizes, from the almost spherical lymphocyte, to amoeboid cells such as macrophages, to flattened spindle-shaped fibroblasts or polygonal epithelial cells, to neuronal cells with complex extensions like the dendrites and the axons. Such cellular architecture is constructed and maintained by the cytoskeleton, a dynamic network comprising of three major types of proteinaceous structural elements, namely, the actin microfilaments (about 6-10 nm in diameter), tubulin microtubules (about 25 nm in diameter) and intermediate filaments (about 10 nm in diameter). The cytoskeleton is responsible for cell shape, motility, migration, cytokinesis, cell polarity, intracellular transport, and last but not least, it is involved in protection of cells against bacterial and viral infections.

In contrast to the well organized and stably structured actin cytoskeleton in a striated muscle cell, the highly motile cells, such as leukocytes, platelets and other cell types which migrate on a surface or through tissues, possess a very dynamic cytoskeleton whereby the actin filaments can quickly undergo polymerization and depolymerization, depending on the cytoplasmic ionic conditions and regulated by a large number of actin binding proteins (Stossel *et al*., 1985; Pollard and Cooper, 1986; Noegel and Luna, 1995; Schleicher *et al*., 1995) which are functionally conserved from lower eukaryotes to mammals. These actin regulatory proteins are able to maintain the steady-state equilibrium between monomeric or G- and filamentous or F-actin by reversibly controlling the turnover rate of G-actin into filaments. In addition, they also govern the three-dimensional organization of the microfilament network. They are in turn regulated by various factors such as Ca^{2+}, phospholipids, phosphorylation and pH. Depending on their interaction with G- or F-actin, these actin modulatory proteins can be grouped into five major classes, (a) monomer binding proteins, (b) F-actin fragmenting and capping proteins, (c) F-actin crosslinking proteins, (d) membrane anchors and (e) the myosin motor proteins (Fig. 1).

Usually small and ubiquitous, G-actin associating proteins reversibly remove polymerizable actin from the equilibrium with F-actin, thus reducing the viscosity in the cytoplasm by lowering the number and lengths of filaments. Representatives of this monomer sequestering protein family are profilin (Carlsson *et al*., 1977; Haugwitz *et al*., 1991; Christensen *et al*., 1996; Rothkegel *et al*., 1996), cofilin (Aizawa *et al*., 1995, 1997; Theriot, 1997), adenylyl cyclase-associated protein or CAP (Gottwald *et al*., 1996), and ß-thymosins (Nachmias, 1993).

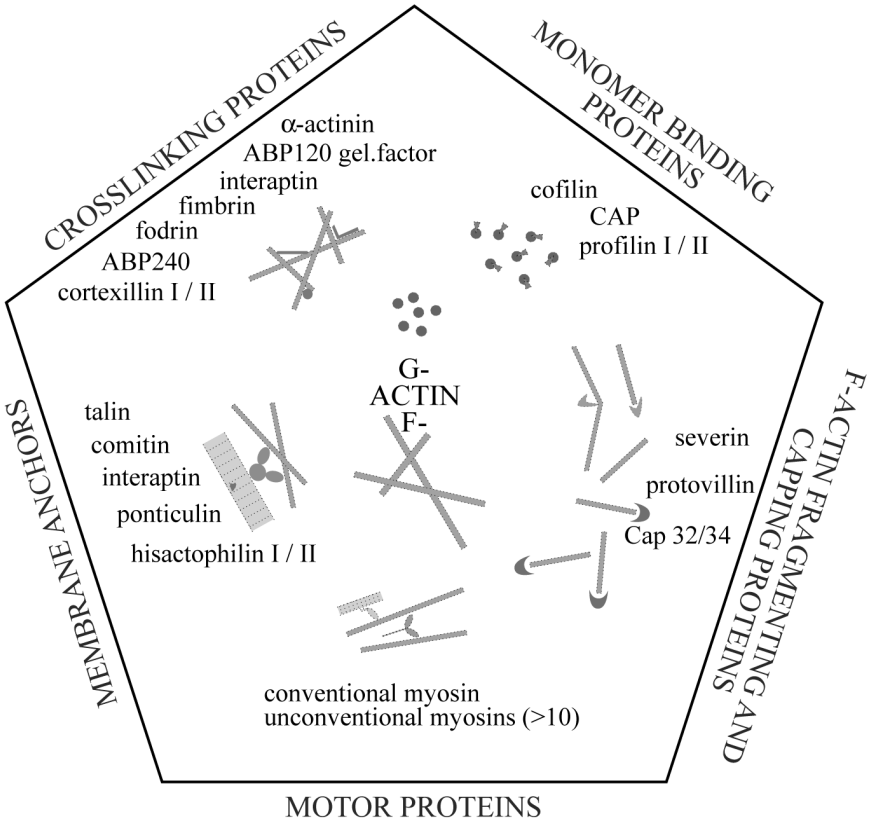

Fig. 1 An overview of the actin-binding proteins in *Dictyostelium* (Eichinger *et al*., 1999)
As in other non-muscle cells, a *Dictyostelium* amoeba is able to maintain an approximate 1:1 molar equilibrium between monomeric (G-) and polymerized (F-) actin due mainly to the monomer binding proteins and proteins which sever or cap the microfilaments. The myosins are motor proteins responsible for contractility. Membrane anchors connect actin filaments to membranes, and F-actin crosslinking proteins are able to strengthen the viscoelasticity of filamentous networks. Many actin-binding proteins are composed of different domains which are essential for self-regulation or for distinct subcellular distribution.

Free barbed ends are a prerequisite for all actin-based motile processes, as they allow for the regulated assembly and disassembly of actin filaments. Filament number and lengths are controlled by the group of F-actin fragmenting and capping proteins which acts by either capping the barbed (+) ends of filaments only, or by severing filaments, which is usually followed by capping of the newly created (+)-end, thus maintaining short filaments and lowering cell viscosity. Their activity is regulated by Ca^{2+}, polyphosphoinositides, pH, and phosphorylation. The best investigated examples of this group are gelsolin (Yin and Stossel, 1979; Witke *et al*., 1995; Sun *et al*., 1997), villin (Janmey and Matsudaira, 1988; Finidori *et al*., 1992; Pope *et al*., 1994), protovillin (Hofmann *et al*., 1993), severin (Eichinger *et al*., 1991; Eichinger and Schleicher, 1992), fragmin (Hasegawa *et al*., 1980; Gettemans *et al*., 1992) and the heterodimeric capping protein Cap32/34 (Hartmann *et al*., 1989; Eddy *et al*., 1996).

The group of F-actin stabilizing proteins consists of generally large, abundant, cytosolic proteins which can bind along the side of filaments, thereby stabilising actin filaments themselves, as in the case of tropomyosin (Lehman *et al*., 1994). In addition, the availability of at least two F-actin binding sites enables them to crosslink filaments and form bundles as well as three-dimensional actin networks. The two actin binding sites are either arranged in tandem on a single polypeptide chain like fimbrin (Matsudaira *et al*., 1983; Kuebler and Riezman, 1993; Prassler *et al*., 1997), or they are found on separate polypeptide chains which form parallel or antiparallel dimers such as α-actinin (Condeelis and Vahey, 1982; Fechheimer *et al*., 1982; Noegel *et al*., 1987), or gelation factor/ABP120 (Noegel *et al*., 1989; Rivero *et al*., 1996; Fucini *et al*., 1997) and filamin (Hock and Condeelis, 1987). The majority of F-actin cross-linking proteins discovered in *Dictyostelium*, including two recent members, namely Cortexillin I and II (Faix *et al*., 1996) and interaptin (Rivero *et al*., 1998), belongs to the α-actinin/spectrin superfamily of proteins.

Myosins, characterized by a well conserved motor domain, are responsible for contractility and transport of cargoes along actin filaments. They are classified as either conventional or unconventional myosins. Possessing a common structure, the conventional, class II or double-headed myosins from muscle or non-muscle cells are able to assemble into bipolar filaments (Manstein, 1993). On the other hand, the unconventional myosins are a very diverse group of motor proteins, consisting of the generic motor domain adhered to a multitude of structurally and functionally distinct tail domains (Uyeda and Titus, 1997; Baker and Titus, 1998).

Another important group of proteins helps to maintain the cell integrity and control motile processes by anchoring actin filaments to membranes. Well-studied membrane anchors of actin include the pH-regulated hisactophilin I and II (Scheel *et al*., 1989; Hanakam *et al*., 1996; Stoeckelhuber *et al*., 1996), the Golgi and vesicle associated comitin (Weiner *et al*., 1993; Jung *et al*., 1996a), the integral plasma membrane protein, ponticulin (Hitt *et al*., 1994; Schutt *et al*., 1995), and talin, a protein involved in linking the actin cytoskeleton to sites of cell-to-substrate adhesion (DePasquale and Izzard, 1991; Kaufmann *et al*., 1992; Kreitmeier *et al*., 1995; Niewoehner *et al*., 1997).

1.2 *Dictyostelium* as model organism

Single cell motility has long since been studied in tissue culture systems or higher eukaryotes. Isolated more than 60 years ago (Raper, 1935) the highly motile *Dictyostelium discoideum* amoeba, whose motility properties parallel those of human leukocytes (Devreotes and Zigmond, 1988), appears to be an appealing and versatile model system for analysing cell

movement both at the single cell and multicellular stage by a wide variety of genetic, biochemical, and cell biological methods. Besides cell motility, a multitude of cellular processes such as cell differentiation, signal transduction, cytokinesis, chemotaxis and phagocytosis can be studied with ease.

Residing naturally in the upper soil layer of decaying leaves, these free-living, unicellular amoebae feed on bacteria. Upon starvation, a developmental cycle is initiated whereby up to 100,000 cells are able to chemotactically aggregate to form a multicellular structure which undergoes morphogenesis and cell-type differentiation. Development culminates in the generation of fruiting bodies containing resistant spores which later on give rise to individual amoebae (Loomis, 1996). The life cycle of *Dictyostelium* is summarized in Fig. 2.

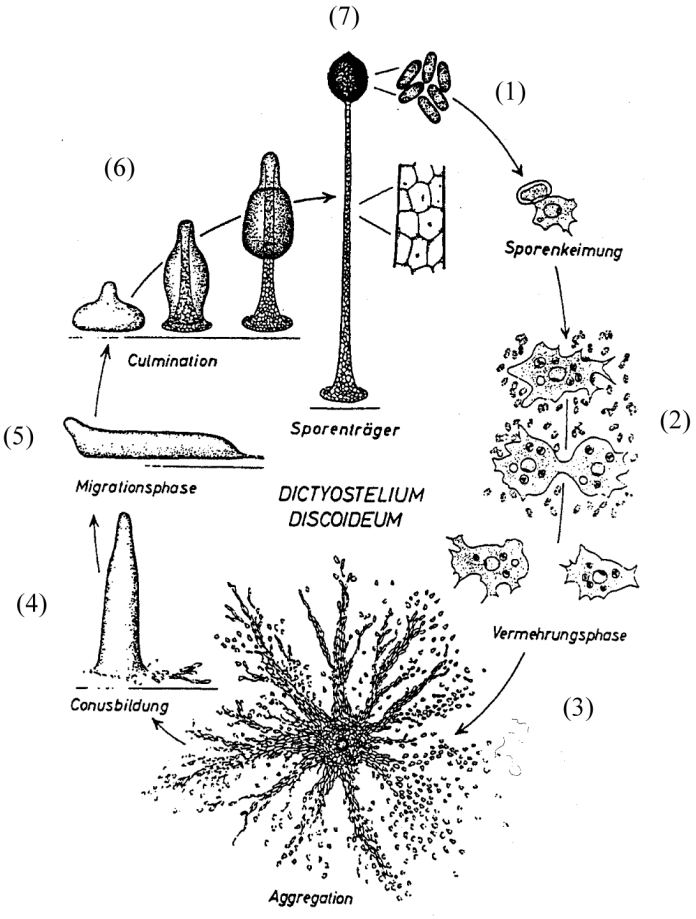

Fig. 2 The life cycle of *Dictyostelium discoideum*
(1) Spores germinate to give rise to individual amoebas (2) which feed on bacteria as food source and the vegetative cells divide and multiply. (3) Upon depletion of the food source, the cells chemotatically aggregate to form a cell mass that elongates to form the "first finger" (4) which then either migrates as a slug (5) or directly enters the culmination stage (6) leading to the formation of a fruiting body (7) consisting of the terminally differentiated stalk cells and the spores which can initiate another round of the cycle. Under laboratory conditions, development from the onset of starvation to the mature fruiting body can be accomplished within 24 h.

Several advantages offered by *Dictyostelium* firmly establish its role as laboratory organism. Firstly, large amounts of genetically identical cells can be easily cultivated over a period of three days for biochemical analysis; proteins of interest can be investigated at the unicellular and multicellular level; a small genome of about 34 Mb of DNA should facilitate the molecular studies of genes involved in growth and development; development should be

rapid, synchronous and easy to control and observe; its haploid genome allows isolation and characterization of mutants with ease. Last but not least, the availability of convenient transformation protocols (Nellen *et al*., 1984; Howard *et al*., 1988) greatly facilitates the genetic manipulation of this organism. The existence of various selection markers such as neomycin (Nellen *et al*., 1984), hygromycin (Egelhoff *et al*., 1989), 5-fluoroorotic acid (Kalpaxis *et al*., 1991), phleomycin (Leiting and Noegel, 1991) and blasticidin (Adachi *et al*., 1994) enables isolation of single, double, triple , or even quadruple mutants.

Furthermore, a wide variety of improved genetic approaches are available to generate mutants for studying the cytoskeleton of *Dictyostelium* amoebae (Fig. 3). These include targeted gene disruption and gene replacement by homologous recombination (Manstein *et al*., 1989), antisense-mediated gene inactivation (Knecht and Loomis, 1987; Liu *et al*., 1992), tagging of disrupted genes with easily detectable antigenic and biochemical markers (Doering *et al*., 1991), the transponson tagging like mutagenesis by restriction enzyme-mediated integration (REMI) of DNA (Kuspa and Loomis, 1992; Karakesisoglou *et al*., 1999), and the tagging of cytoskeletal proteins with GFP to allow *in vivo* monitoring of gene expression in prokaryotic or eukaryotic cells (Chalfie *et al*., 1994; Wang and Hazelrigg, 1994; Ludin and Matus, 1998) which has all but transformed cell biological research in living *Dictyostelium*.

1.3 GFP as marker of gene expression

The green fluorescent protein (GFP) of 238 amino acid residues from the jellyfish *Aequorea victoria* (Prasher *et al*., 1992; Chalfie *et al*., 1994) has generated much attention as the tool of choice in visualizing live molecular events in real time in a large and ever-growing number of species, including bacteria, amoebae, fungi, plants, insects, nematodes, *Drosophila* and the higher mammalian cells (Chalfie *et al*., 1994). GFP-tagged proteins are ideally suited for studying cytoskeletal dynamics *in vivo*, in terms of being able to conveniently visualize their subcellular distributions and more importantly, to detect transient alterations of cellular processes during dynamic remodelling of the cytoskeleton. Excitation at 395 nm yields an emission maximum at 508 nm. GFP mutants harbouring altered excitation and emission spectra (Heim and Tsien, 1996) greatly broaden the field of applications, whereby an improved emission of fluorescence (Heim *et al*., 1995) allows better visualization. In addition, GFP mutants with varied color properties make it possible to perform double labelling of subcellular structures to distinguish multiple cellular events simultaneously (Heim *et al*., 1994; Rizzuto *et al*., 1996). Also, the GFP mutants can serve as donors and acceptors for

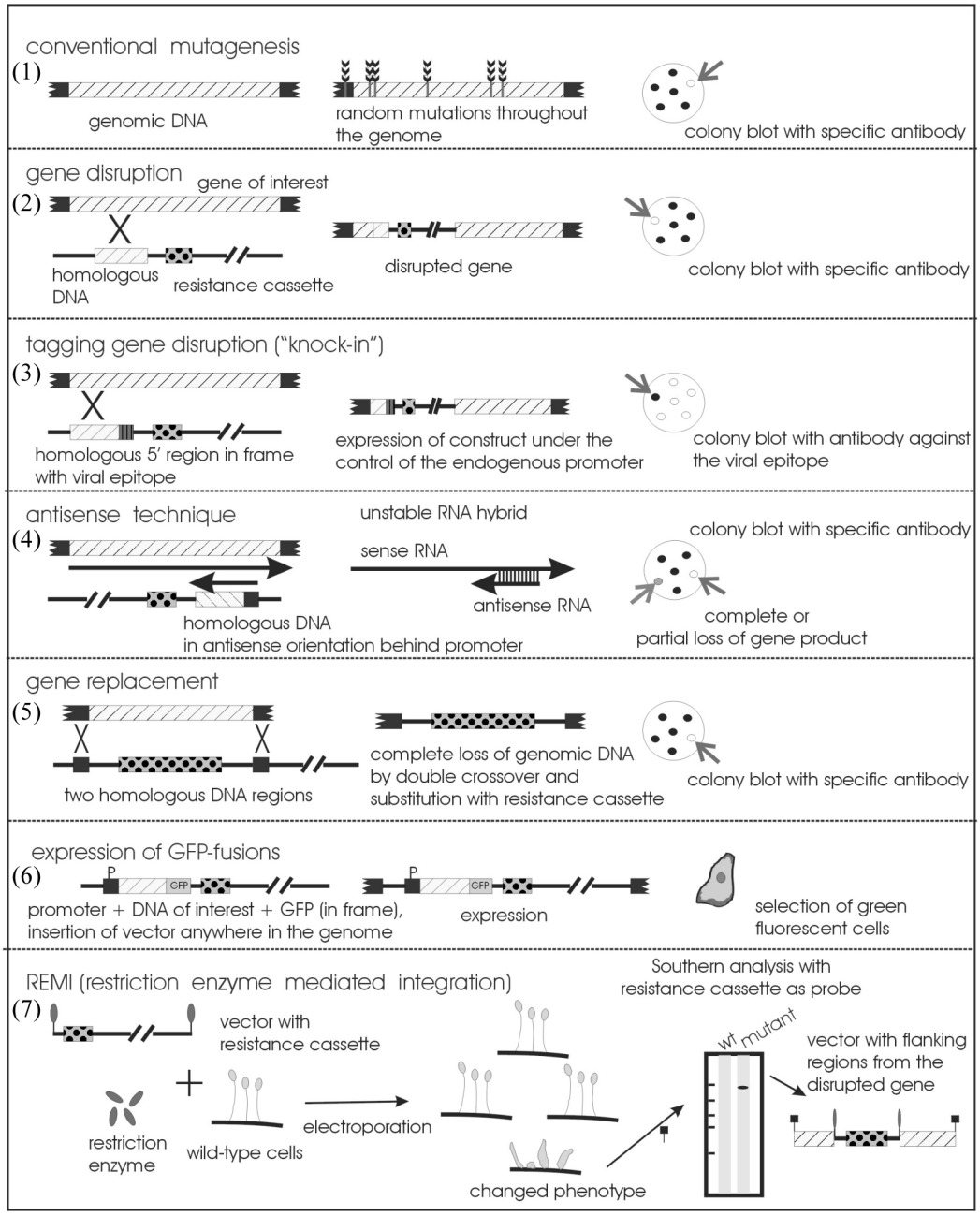

Fig. 3 Genetic approaches to study the cytoskeleton of *Dictyostelium* amoebae (Eichinger *et al*., 1999)
(1) Conventional mutagenesis leading to random point mutations throughout the entire genome. The loss of gene product could be detected with a specific antibody. (2) The current method of choice is a targeted gene disruption. The circular vector aligns with the endogenous gene via a homologous piece from the gene of interest, and the vector could be inserted up to several times in tandem into the genomic DNA. Transformants carrying the resistance cassette can be detected with an antibody. (3) A "knock-in" method can be used to disrupt the gene of interest when an antibody is unavailable. The homologous piece of DNA from the extreme 5' coding region can be fused in frame e.g. to a viral epitope. Only disruption of the target gene at the proper site would the epitope be expressed. (4) The disruption of an essential gene is often lethal, thus an antisense method could remove unstable RNA hybrids, allowing the isolation of transformants that still express a low level of gene product. (5) To avoid undesired recombinational events, a complete or partial removal of genomic DNA can be achieved by a gene replacement construct which recombines via two homologous DNA regions with flanking parts of the target gene, looping out the mismatched interregional piece by substitution with the resistance cassette. (6) *Dictyostelium* is a well-suited system for the expression of GFP fused target genes. (7) With REMI, cells are transformed with a restriction enzyme-linearized vector carrying a resistance cassette in the presence of the same restriction enzyme. Consequently, the vector with its appropriate sticky ends can be inserted into the randomly-cut genome whereby an altered phenotype might indicate by chance that a specific gene has been disrupted, and one could then recover the gene by isolating the vector including flanking genomic DNA from the transformant.

fluorescence resonance energy transfer (FRET) to monitor protein-protein interactions *in vivo* (Heim and Tsien, 1996).

A main consideration of using GFP has been that the tagging of GFP might alter the function of the fusion partner. However, this has been resolved by the successful labelling of highly conserved proteins like tubulin (Neujahr *et al*., 1998) and actin (Westphal *et al*., 1997). A major proportion of GFP tagged proteins has been cytoskeletal proteins. With the aid of GFP-actin, the microfilament dynamics has been well studied in yeast (Doyle and Botstein, 1996), *Dictyostelium* (Westphal *et al*., 1997) and mammalian cells (Choidas *et al*., 1998). Some other examples of the constantly increasing number of GFP-fused cytoskeletal proteins include ß1-integrin (Smilenov *et al*., 1999), myosin heavy chain (Moores *et al*., 1996), coronin (Gerisch *et al*., 1995; Maniak *et al*., 1995; Hacker *et al*., 1997), cortexillin (Weber *et al*., 1999), FtsZ (Ma *et al*., 1996), α-tubulin (Straight *et al*., 1997; Neujahr *et al*., 1998), kinesin (Pierce *et al*., 1997), microtubule-associated protein MAP4 (Olson *et al*., 1995), and Ncd (Endow and Komma, 1997).

1.4 Profilin

Profilins are abundant, low molecular weight (12-15 kDa), cytoplasmic proteins found in all eukaryotic cells examined so far. They are able to bind to actin monomers (Carlsson *et al*., 1977), poly-(L)-proline stretches (Tanaka and Shibata, 1985), the vasodilator-stimulated phosphoprotein (VASP) (Reinhard *et al*., 1995) and polyphosphoinositides (Lassing and Lindberg, 1985; 1988). Depending on the conditions, profilin can either upregulate or downregulate the polymerization of actin monomers (Carlsson *et al*., 1977; Pantaloni and Carlier, 1993). Besides sequestering G-actin, profilins are capable of enhancing the rate of ADP/ATP exchange in the actin monomer (Mockrin and Korn, 1980; Nishida, 1985) and thus promote actin polymerization. If the barbed ends of actin filaments are capped, profilin acts like a sequestering protein. However, when free barbed ends are available, profilin is able to assist, in the presence of ß-thymosin, polymerization of actin (Pantaloni and Carlier, 1993; Theriot and Mitchison, 1993; Carlier and Pantaloni, 1994). Furthermore, binding of profilin to phospholipids and to target proline-rich proteins suggests a role in signal transduction pathways to the cytoskeleton (Sohn and Goldschmidt-Clermont, 1994; Sun *et al*., 1995; Carlier and Pantaloni, 1997).

Genetic analyses confirmed the importance of profilins as components of the microfilament system essential for the regulation of normal cellular roles and cell viability (Haarer *et al*., 1990, 1993; Cooley *et al*., 1992; Witke *et al*., 1993; Balasubramanian *et al*., 1994; Haugwitz

et al., 1994; Rothkegel *et al*., 1996; Schlueter *et al*., 1998; Ostrander *et al*., 1999). *In vivo* studies had demonstrated the significance of the specific molecular environment on the actual role played by profilin. For example, microinjected birch-pollen profilin was characterized in *Tradescantia blossfeldiana* cells as a sequestering protein (Staiger *et al*., 1994), but it was found to have a stabilizing effect on the F-actin network in BHK cells (Rothkegel *et al*., 1996). In addition, various *Drosophila* profilin mutants had stressed the importance of profilin in normal cell development (Verheyen and Cooley, 1994).

Atomic configurations of bovine (Schutt *et al*., 1993; Cedegren-Zeppezauer *et al*., 1994), human (Metzler *et al*., 1993) or *Acanthamoeba* profilin (Vinson *et al*., 1993; Fedorov *et al*., 1994) showed that profilins share an analogous three-dimensional fold despite highly divergent sequences. The key feature of the profilin molecule is an antiparallel ß-pleated sheet flanked on one side by the amino- and carboxy-terminal α-helices and some smaller α-helices and ß-strands on the opposite side. Both co-crystallization studies of bovine profilin:ß-actin complexes (Schutt *et al*., 1993) and crosslinking experiments (Vandekerckhove *et al*., 1989) showed that profilin binds to the subdomains 1 and 3 of G-actin in a 1:1 complex. The predominant contact areas in profilin are helices 3, 4 and strands 4-6 (Fig. 4). Lysine (Lys) #125 of bovine profilin forges an intermolecular electrostatic interaction with the glutamic acid (Glu) residue #364 of actin. This lysine residue is homologous to the highly conserved Lys #115 of *Acanthamoeba* profilin which has earlier been chemically crosslinked to Glu #364 of actin via a zero length crosslinker (Vandekerckhove *et al*., 1989).

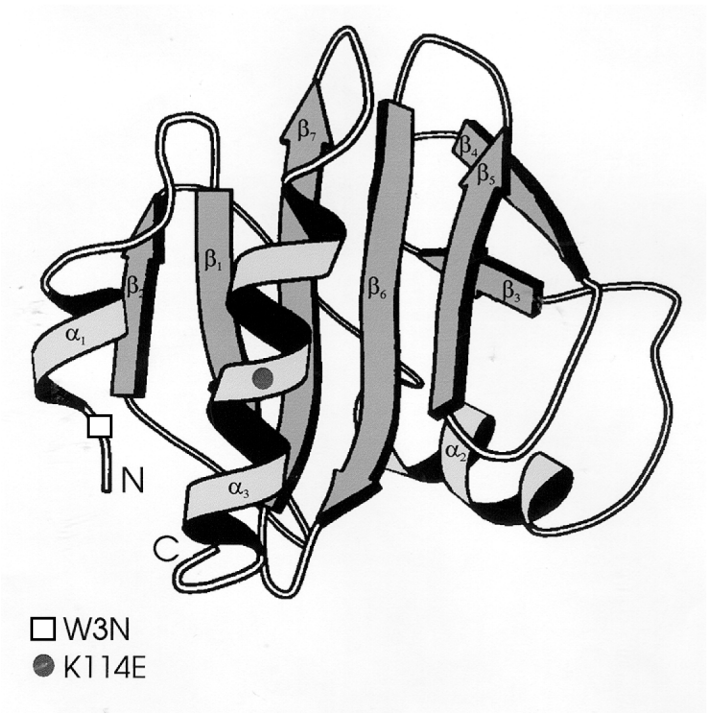

Fig. 4 Three-dimensional structure of *Acanthamoeba* profilin (Vinson *et al*., 1993) showing the locations of the point mutations W3N (square) and K114E (filled circle).

A hallmark of all eukaryotic profilins is their ability to interact with poly-(L)-proline sequences, due to highly conserved aromatic residues which create a hydrophobic cleft between profilin's amino- and carboxy-terminal helices and the upper face of its antiparallel ß-sheet (Bjoerkegren *et al*., 1993; Haarer *et al*., 1993; Metzler *et al*., 1993; Schutt *et al*., 1993; Archer *et al*., 1994; Kaiser and Pollard, 1996). Currently, only the profilin-like molecule from the *Vaccinia* virus has been known to lose its ability to bind poly-(L)-proline stretches due to aromatic substitutions (Machesky *et al*., 1994). So far, two proline-rich biological ligands of profilin have been well characterized, VASP (Reinhard *et al*., 1995) and Mena, a relative of VASP (Gertler *et al*., 1996). However, the knowledge of the relevance and the physiological role of profilin's interaction with poly-(L)-proline is still inadequate.

Dictyostelium possesses two profilin isoforms, profilin I and II, with 55% identity in their amino acid sequences (Haugwitz *et al*., 1991). *In vitro* studies showed that both isoforms bind G-actin with slightly differing affinities and are able to delay the onset of actin polymerization by shifting the critical concentration for actin polymerization to a higher level. Cells which lack only one isoform are indistinguishable from wild-type cells (Haugwitz *et al*., 1994). Only the disruption of both genes gave rise to an aberrant phenotype with an increased F-actin content, abnormal cytokinesis and development. These profilin deficient cells exhibit reduced motility, are up to ten times larger than wild-type cells, often multinucleate, could grow on surfaces but not in shaking suspension, and their development is blocked prior to fruiting body formation (Haugwitz *et al*., 1994). The increase of F-actin by 60-70% suggests that *Dictyostelium* profilin acts *in vivo* primarily as an actin sequestering protein.

While profilins have been thoroughly studied *in vitro*, their *in vivo* roles remain elusive. The expression of point mutated profilins or GFP-tagged profilins in profilin null cells should help further in elucidating the *in vivo* functions of profilin.

1.5 Severin

The dynamic remodelling of actin-based cytoskeletal structures usually requires the fragmentation of existing filaments and filament bundles. Severin, the major severing protein from *D. discoideum* (Brown *et al*., 1982; Yamamoto *et al*., 1982), is a 40 kDa protein with sequence homologies to other members of the group of F-actin fragmenting proteins found in lower and higher eukaryotes. These include the vertebrate proteins gelsolin (Yin and Stossel, 1979) and villin (Bretscher and Weber, 1979), or fragmin from *Physarum polycephalum* (Hasegawa *et al*., 1980). A characteristic feature of severin-like proteins is the segmental organization into three (severin, fragmin) or six (gelsolin, villin) homologous domains which

might have evolved through sequential gene duplications prior to the evolutionary branching off of *Dictyostelium* (Janmey and Matsudaira, 1988; Hofmann *et al*., 1993). The presence of micromolar Ca^{2+} allows these proteins to nucleate actin assembly, sever actin filaments, and cap the fast growing barbed ends of actin filaments (Matsudaira and Janmey, 1988).

Based on sequence homology to human gelsolin, two additional members have been isolated from *Dictyostelium*. Protovillin is a villin prototype which caps but does not sever actin filaments (Hofmann *et al*., 1993), and the 190 kDa villidin is a multidomain protein harbouring WD repeats at the N-terminal region, followed by a PST (proline, serine, threonine) rich stretch and sequence homology to vertebrate villin at the C-terminal domain (unpublished data).

The Ca^{2+}-activated, PIP_2-inhibited actin-binding, severing and capping activities of *D. discoideum* severin have been correlated with its highly conserved three-domain structure by *in vitro* studies (Eichinger *et al*., 1991; Eichinger and Schleicher, 1992). It was found that severin possesses a capping site in domain 1, and two F-actin side-binding regions in domains 2+3. Two distinct Ca^{2+}-binding activities are associated with domains 1 and 2, while two PIP_2-binding sites have been determined separately in domain 1 and domains 2+3. Severin was also found to be inhibited by other negatively charged phospholipids besides PIP_2. Domain 2 of severin consisting of a Ca^{2+}-dependent actin interacting site, was determined to have a stable and conserved three-dimensional structure similar to that of profilins and the segment I of gelsolin (Pollard *et al*., 1994; Schnuchel *et al*., 1995).

Recently, a *Dictyostelium* protein kinase isolated from cytosolic extracts was found to belong to the family of Ste20p- or p21-activated protein kinase (PAK) (Sells *et al*., 1997; Tapon and Hall, 1997). This novel kinase which specifically phosphorylates severin and exhibits highest homology to human SOK-1 (Ste20/oxidant stress response kinase) has been characterized by Eichinger *et al*. (1998).

Although *in vitro* assays revealed severin as a very active F-actin fragmenting protein, the severin null *Dictyostelium* mutant (HG1132) isolated by chemical mutagenesis, exhibits normal growth rate, cell motility, chemotaxis, and development (André *et al*., 1989). This suggests the redundancy of the cytoskeletal network, whereby removal of a single actin-binding protein could be functionally compensated by others (Witke *et al*., 1992). There is increasing evidence that *in vivo* F-actin severing proteins are involved in signal transduction (Barkalow and Hartwig, 1995; Kwiatkowski, 1999), hence the tagging of severin with GFP should aid further in revealing its *in vivo* role in the transient, dynamic processes of the cytoskeleton.

1.6 Pathogens and the actin cytoskeleton

1.6.1 Actin-based motilities of pathogens

Phagocytosis constitutes the first step for the uptake and degradation of particles. This process occurs in "professional" phagocytes like macrophages and neutrophils, and also to a lesser extent, in non-professional phagocytes such as fibroblasts, endothelial and epithelial cells. Once inside the host cells, intracellular pathogens are able to control the fate of their membrane-bound compartments, evade host defences and further degradation, and at the same time, transform their environments to allow survival. Various pathogens have evolved different mechanisms to replicate successfully within host cells and to spread from cell to cell. The high plasticity of the actin cytoskeleton enables active exploitation by many pathogens during entry into cells and in some cases during dissemination of these pathogens in cells and tissues. Although rearrangements of the cytoskeleton appear to be an essential requirement for entry of most pathogens, the manipulation of the cytoskeleton at a later intracellular stage of infection seems to be restricted to several intracellular pathogens, the best studied ones such as *Listeria*, *Shigella*, *Rickettsias* and *Vaccinia*.

Studies of the actin-based motility of pathogens have offered insights into events occurring at the leading edge of motile cells (Machesky, 1997; Welch *et al*., 1998). Intracellular bacteria like *Listeria monocytogenes* (Tilney and Portnoy, 1989; Cossart and Kocks, 1994), *Shigella flexneri* (Bernardini *et al*., 1989; Zeile *et al*., 1996), spotted fever group *Rickettsia* (Gouin *et al*., 1999) and also the *Vaccinia* virus (Cudmore *et al*., 1995; 1996) are able to interact with the cellular machinery leading to local polymerization of host actin into "comet tail" structures which propel the pathogens within the cytoplasm. Once the pathogens reach the plasma membrane, they form long protrusions which are engulfed by neighbouring cells thus allowing infection to spread from cell to cell. Identification of pathogenic factors responsible for actin-based motilities led to the ActA protein from *L. monocytogenes* (Domann *et al*., 1992; Kocks *et al*., 1992; Pistor *et al*., 1994) and the IcsA protein from *S. flexneri* (Bernardini *et al*., 1989; Goldberg *et al*., 1993). The genes responsible for the actin polymerization process in *Rickettsia* and the *Vaccinia* virus have yet to be found. Host actin cytoskeletal proteins implicated in bacterial actin-based motility include the Arp 2/3 (actin-related protein) complex (Welch *et al*., 1997) and VASP (Chakraborty *et al*., 1995) for *L. monocytogenes*, and vinculin (Kadurugamuwa *et al*., 1991; Suzuki *et al*., 1996; Laine *et al*., 1997) and N-WASP (neural Wiskott-Aldrich syndrome protein) for *S. flexneri* (Suzuki *et al*., 1998; Egile *et al*., 1999). In contrast to *Listeria* and *Shigella*, *Rickettsia* appears to use a different mechanism for

actin assembly since *Rickettsia* tails have a distinct structure from that of *Listeria* and *Shigella*. Two host proteins, VASP and alpha-actinin were found to colocalize with actin in the *Rickettsia* tails (Gouin *et al*., 1999). In the case of the *Vaccinia* virus, a host phosphotyrosine protein was found to be responsible for actin-based motility (Frischknecht *et al*., 1999) of the virus within host cytoplasm.

Actin-based motility of extracellular bacteria is best studied in the enteropathogenic *Escherichia coli* (EPEC), a causative agent of infantile diarrhoea. These bacteria adhere to the surface of host cell and induce localized formation of actin bundles beneath the attachment sites. The actin filaments become organized into membrane encased protrusions which can extend up to 6 μm above the cell surface, generating actin pedestals on which the bacteria lie. These EPEC pedestals can bend and undulate, changing in length while remaining tethered in place (Sanger *et al*., 1996), while some adhered EPEC can also move along the cell surface. Thus actin assembly in the pedestals is essential for the translocation of EPEC on the host cell surface. All genes required for pedestal formation during EPEC infection are encoded by the bacterial chromosome, as well as many virulence effectors, including several EPEC-secreted proteins (Esps), some of which are secreted into the host cell and are important for signal transduction. A two-protein complex has been identified to be involved in the attachment of EPEC. A bacterial protein, Tir, is initially inserted in the host's plasma membrane, which can in turn act as a receptor for bacterial intimin which mediates adherence of bacteria to the host cell (see review Goosney *et al*., 1999).

1.6.2 Rho modification by bacterial toxins

GTP-binding proteins of the Rho family are regulators of the actin cytoskeleton and molecular switches in various signal transduction pathways. The Rho proteins are often targets for intracellular bacterial protein toxins which either inactivate GTPases by ADP-ribosylation or glucosylation, or activate them by deamidation. Rho proteins are essential for host cell invasion by bacteria. These small GTPases are targets for bacterial ADP-ribosylating toxins belonging to the C3 exoenzyme family (Aktories *et al*., 1992), some members including the *Clostridium botulinum* C3 ADP-ribosyl-transferase (Aktories *et al*., 1987; Rubin *et al*., 1988), and a transferase produced by *Staphylococcus aureus* (Sugai *et al*., 1990). The RhoA GTPase has been shown to be glucosylated by the toxin B of *Clostridium difficile*, leading to disaggregation of actin filaments (Lyerly *et al*., 1988; Kelly *et al*., 1994; Just *et al*., 1995).

All *Bordetella* species are able to produce heat-labile toxins known as dermonecrotic toxins (DNTs) (Horiguchi *et al*., 1995). The *Bordetella pertussis* toxin interferes with the adenylate

cyclase system by ADP-ribosylating the alpha subunit of heterotrimeric G proteins (Katada and Ui, 1982). *Cholera* toxin and a heat-labile enterotoxin from *E. coli*, both with structures resembling that of *B. pertussis* toxin, also ADP-ribosylate G proteins (Cassel and Selinger, 1977; Sixma *et al*., 1991). DNT from *Bordetella*, which shares homologous sequences with the cytotoxic necrotizing factors (CNFs) of *E. coli* (Oswald *et al*., 1994) at the carboxy-terminal, modifies and activates Rho by deamidation (Horiguchi *et al*., 1997), leading to actin filament assembly and formation of focal adhesions. On the other hand, the N-terminal of CNF shows sequence homology to *Pasteurella multocida* toxin (PMT) (Oswald *et al*., 1994). It has been suggested that activation of Rho mediates PMT-stimulated tyrosine phosphorylation of focal adhesion kinase as well as formation of stress fibres and focal contacts in fibroblasts (Lacerda *et al*., 1996). The *E. coli* CNF toxins were also reported to deaminate and activate Rho (Flatau *et al*., 1997; Schmidt *et al*., 1997).

Exoenzyme S (ExoS), an exotoxin secreted by the opportunistic pathogen *Pseudomonas aeruginosa* (Yahr *et al*., 1996), belongs to the family of ADP-ribosylating toxins (Kreuger and Barbieri, 1995). ExoS has been shown *in vitro* to ADP-ribosylate various proteins, such as vimentin and members of the Ras family (Coburn *et al*., 1989a; Coburn and Gill, 1991). *In vivo*, ExoS was reported to ADP-ribosylate Ras (McGuffie *et al*., 1998) and uncouple a Ras-mediated signal transduction pathway (Ganesan *et al*., 1998). The amino-terminal half of ExoS exhibits homology to the secreted YopE (*Yersinia* outer protein E) cytotoxin of pathogenic *Yersinia* species (Forsberg and Wolf-Watz, 1990; Yahr *et al*., 1995). Similar to YopE, intracellular targeting of ExoS results in disruption of the actin microfilament system and resistance to phagocytosis (Rosqvist *et al*., 1991; Frithz-Lindsten *et al*., 1997). Recently, the small GTP-binding proteins have been implicated in actin filament disruption by ExoS (Pederson *et al*., 1999).

1.6.3 *Yersinia enterocolitica* and the actin cytoskeleton

Three species of the gram-negative *Yersinia* bacteria are human pathogens, namely, *Y. pestis*, the causative agent of bubonic plague, while *Y. pseudotuberculosis* and *Y. enterocolitica* are well-known pathogens responsible for food-borne enteric diseases that are usually self-limiting. These orally transmitted pathogens proliferate mainly in the lymphoid tissue and their primary site of infection is the lymphoid follicles of the small intestine (Hanski *et al*., 1989). The best-studied invasion system is that of *Y. pseudotuberculosis* and *Y. enterocolitica* (Falkow *et al*., 1992), which possesses a chromosomal gene encoding an outer membrane protein, invasin, that mediates adherence and entry into non-phagocytic mammalian cells

(Isberg *et al*., 1987). Invasin is maximally expressed at 28°C (Isberg *et al*., 1988), suggesting its involvement in early infection (Simonet and Falkow, 1992). The cellular receptor for invasin was identified as a ß1 integrin (Isberg and Leong, 1990), which mediates cell-cell interactions as well as adhesion to the extracellular matrix. The high affinity interaction between invasin and ß1 integrins guides extension of the host cell membrane around the bacterium to form a tight-fitting phagosome which internalizes the bacterium in a "zipper"-like process (Isberg and Leong, 1990; Swanson and Baer, 1995). Another invasin encoded by enteropathogenic *Yersinia* is the YadA protein (Boelin *et al*., 1982). YadA is a virulence plasmid-encoded fibrillar adhesin (Kapperud *et al*., 1987) which is maximally expressed by *Y. pseudotuberculosis* and *Y. enterocolitica* at 37°C (Boelin *et al*., 1982; Lambert de Rouvroit *et al*., 1992), and like invasin, YadA binds to ß1 integrins (Schulze-Koops *et al*., 1993) and provides bacterial attachment and entry into eukaryotic cells (Heesemann and Grueter, 1987; Isberg, 1989; Bliska *et al*., 1993).

Besides coding for YadA, the 70 kb *Yersinia* pYV virulence plasmid (Cornelis *et al*., 1998) also encodes various secreted *Yersinia* outer proteins or Yops (Michiels *et al*., 1990; Straley *et al*., 1993; Forsberg *et al*., 1994) which are optimally synthesized at 37°C (Lambert de Rouvroit *et al*., 1992; Straley *et al*., 1993). At this temperature, bacteria entry into host cells via invasin and YadA is inhibited by the antiphagocytic activities of several Yops (Lian *et al*., 1987; Visser *et al*., 1995; Ruckdeschel *et al*., 1996). Thus during active infection, invasin and YadA probably function mainly as adhesins as the wild-type *Yersinia* species remain extracellular but firmly affixed to the host cell surface (Faellman *et al*., 1995). The Yops are only expressed upon intimate contact with the eukaryotic target cell, and while the pathogen remains at the cell surface, the Yop effectors are translocated across the plasma membrane by a unique polarized transfer mechanism (Forsberg *et al*., 1994; Rosqvist *et al*., 1994; Sory and Cornelis, 1994; Sory *et al*., 1995). The Yops are secreted without post-translational processing by a virulence plasmid-encoded secretion system (*ysc*). This type III secretion machinery (Michiels *et al*., 1990; Michiels and Cornelis, 1991; Forsberg *et al*., 1994; Lee, 1997) constitutes about 22 proteins (Michiels *et al*., 1991; Allaoui *et al*., 1995). Similar machineries have been found in all major gram-negative pathogens, indicating that the type III secretion pathway is a universal strategy for the pathogenesis of bacterial infections (Bergman *et al*., 1994; Russel, 1994; Rosqvist *et al*., 1995). Yop secretion also requires cytosolic Syc proteins, which appear to function as chaperones that bind to Yops and maintain them in a secretion-competent, degradation-resistant state (Wattiau *et al*., 1996).

The secreted Yops have been divided into effectors, translocators and regulators according to their functions (Cornelis and Wolf-Watz, 1997). So far, a set of at least six effector Yops, namely, YopE, YopH, YopM, YopT, YopO/YpkA and YopP/YopJ and at least four proteins, YopB, YopD, LcrV and YopK/YopQ (Holmstroem *et al*., 1995), implicated in the correct assembly of the translocation apparatus, have been identified. YopN (Forsberg *et al*., 1991; Cornelis *et al*., 1998) and TyeA (Iriarte *et al*., 1998) have been reported to be involved in the regulation of Yop secretion. YopB and YopD are involved in translocation of Yops into host cells (Hakansson *et al*., 1993; Rosqvist *et al*., 1994), whereby YopB was reported to be able to create pores in the eukaryotic cell membrane through which other Yops are translocated (Hakansson *et al*., 1996a). LcrV also plays a role in translocation where it can bind to YopB and YopD and a LcrV deletion mutant is defective in YopB and YopD secretion (Bergman *et al*., 1991; Sarker *et al*., 1998). YopP/YopJ has roles in apoptotic induction (Mills *et al*., 1997) and inhibition of cytokine expression (Schesser *et al*., 1998). YopO/YpkA is a protein kinase with homology to the eukaryotic serine/threonine protein kinases essential for bacterial virulence (Galyov *et al*., 1993) and it has been suggested to be involved in interference with signal transduction and cytoskeletal reorganization (Hakansson *et al*., 1996b). YopE and YopH work in concert to prevent phagocytosis by macrophages (Rosqvist *et al*., 1988; 1990). According to Black and Bliska (1997) and Persson *et al*. (1997), YopH is a protein tyrosine phosphatase reported to dephosphorylate $p130^{Cas}$ (Sakai *et al*., 1994; Burnham *et al*., 1996) and the focal adhesion kinase or FAK (Richardson and Parsons, 1995). Dephosphorylation of these focal adhesion proteins by YopH seemed to impair bacterial uptake by host cells. A list of *Yersinia* secreted proteins is summarized in Table 1.

So far, YopE and YopT have been identified as actin microfilament disrupting cytotoxins (Rosqvist *et al*., 1991; Iriarte and Cornelis, 1998). YopE is a cytotoxin which induces rounding and detachment of cultured cells from the extracellular matrix (Rosqvist *et al*., 1990). It mediates a contact dependent cytotoxicity leading to depolymerization of the actin microfilament network of the host cell without affecting the microtubule network and the intermediate filaments (Rosqvist *et al*., 1991). Either secretion of YopE by wild-type *Yersinia* or microinjection of YopE into the host cell resulted in the alteration of the ordered actin filaments to a disordered granular appearance, whereby prolonged incubation led to disappearance of the granular pattern suggesting complete disruption of the microfilaments. However, the molecular target of YopE remains unknown and this actin dissembly effect is probably secondary since YopE does not affect actin polymerization *in vitro* (Rosqvist *et al*., 1991). Given the homology to exoenzyme S, it is possible that YopE targets small GTP-

binding proteins as exoenzyme S has been reported to modify these signalling molecules (Coburn *et al*., 1989b).

Table 1. *Yersinia* proteins secreted via the type III secretion pathway

Secreted protein	Biochemical activity	Effect on host cell	Comments	References
YopE		Cytotoxic, F-actin disruption	Translocated	Forsberg and Wolfwatz, 1990; Rosqvist *et al*., 1991
YopH	PTPase dephosphorylates FAK, $p130^{Cas}$	Inhibition of phagocytosis	Translocated	Michiels and Cornelis, 1988; Black and Bliska, 1997; Persson *et al*., 1997
YopO/YpkA	Protein serine/threonine kinase		Translocated	Galyov *et al*., 1993; Hakansson *et al*., 1996b
YopM	Binds to thrombin		Translocated	Boland *et al*., 1996
YopP/J		Apoptotic induction in macrophages		Galyov *et al*., 1994; Mills *et al*., 1997; Schesser *et al*., 1998
YopB	Pore-forming translocase		Translocation	Hakansson *et al*., 1993; 1996a
YopD			Translocation	Hakansson *et al*., 1993
YopK/Q			Modulation of translocation efficiency	Holmstroem *et al*., 1995
YopN			Putative surface sensor, regulation of Yops secretion	Forsberg *et al*., 1991; Cornelis *et al*., 1998
YopT		Cytotoxic, F-actin disruption	Translocated	Iriarte and Cornelis, 1998
LcrV		Suppression of immune response	Regulatory function	Bergman *et al*., 1991; Sarker *et al*., 1998
LcrG			Regulation of secretion	Bergman *et al*., 1991
LcrQ/YscM 1/YscM2			Involved in feedback transcriptional regulation	Michiels *et al*., 1991; Rimpilaeinen *et al*., 1992; Stainier *et al*., 1997

Recently, a new *Y. enterocolitica* effector protein, YopT, has been shown to be delivered into the host cytoplasm and resulted in disruption of the actin filament structure (Iriarte and Cornelis, 1998) whereby actin appeared as dispersed patches in the cytosol. The need for YopE and YopT for actin-disrupting activity raises several speculations. The two cytotoxins could reinforce each other via different signalling pathways involving the small GTP-binding proteins (Ridley and Hall, 1992; Aktories, 1997). Secondly, YopE and YopT may target different cell types or these two cytotoxins could act on the same cell types but at different stages of their development. Recently, specific modification and inactivation of the RhoA GTPase by YopT was demonstrated (Zumbihl *et al*., 1999).

1.7 Goals of project

The two major aims of this thesis are:

firstly, to study the *in vivo* roles of two selected actin binding proteins from *Dictyostelium discoideum*, namely the G-actin sequestering protein profilin and the F-actin fragmenting protein severin, via fusion of these cytoskeletal proteins to the green fluorescent protein (GFP). Point mutated profilins allowed the determination of the significance of functional domains essential for normal cell physiology.

Secondly, the behaviour of the actin cytoskeleton in mammalian cells was investigated with the aid of actin-GFP and other GFP-fused cytoskeletal proteins, in the course of infection by the pathogenic bacteria *Yersinia enterocolitica*.

2 MATERIALS AND METHODS

2.1 Materials

2.1.1 Enzymes for molecular biology

Calf intestine alkaline phosphatase	Boehringer
DNA polymerase I (Klenow fragment)	Boehringer
Lysozyme	Sigma
Restriction enzymes	Amersham, Boehringer, Eurogentec, Gibco-BRL, New England Biolabs, Promega
RNase A	Sigma
T4 DNA ligase	Gibco-BRL, Promega
Taq polymerase	Amersham

2.1.2 Antibodies

Anti-Actin (mAb Act1)	(Simpson *et al*., 1984)
Anti-Profilin II (mAb 174-380-3)	(Haugwitz *et al*., 1991)
Anti-Severin (mAb 102-425-1)	(André *et al*., 1988)
Goat anti-mouse IgG antibody, coupled with peroxidase	Dianova
Goat anti-mouse IgG antibody, conjugated with Cy3 or FITC	Dianova

2.1.3 Protease inhibitors

Benzamidine	Sigma
PEFA-block	Roth
Phenylmethylsulfonylfluoride (PMSF)	Serva
Protease inhibitor cocktail (P2714)	Sigma

2.1.4 Antibiotics

Ampicillin	Roth
Blasticidin S	ICN Biomedicals
Geneticin (G418)	ICN Biomedicals
Hygromycin B	Calbiochem
Kanamycin	Sigma
Nalidixic acid	Sigma
Penicillin/Streptomycin	Sigma

2.1.5 Chemical reagents

Unless otherwise stated, chemicals were obtained from Fluka, Merck, Pharmacia, Roth, Serva or Sigma and have the purity grade of "p.a.".

Agarose (SeaKem ME)	FMC Bioproducts
Bacto-agar, -peptone, -tryptone	Difco
Chloroform p.a.	Riedel de Haen
DE52 (Diethylaminoethyl-Cellulose)	Whatman
Hydroxylapatite	Bio-Rad
IPTG (Isopropyl-ß-D-thiogalacto-pyranosid)	Gerbu
Oligonucleotides	MWG-Biotech
Peptone	Oxoid
Phenol	Appligene
Phosphocellulose (P11)	Whatman
Proteose peptone	Oxoid
Triton X-100	Pierce
Yeast extract	Oxoid

2.1.6 Media

All media and buffers were made with deionized water and sterilized by autoclaving at 120°C for 20 min. Antibiotics were added to media when cooled to about 50°C.

2.1.6.1 Media for *D. discoideum* culture

AX medium (pH 6.7)

(Claviez *et al*., 1982)

14.3 g peptone

7.15 g yeast extract

50 mM glucose

3.5 mM Na_2HPO_4

3.5 mM KH_2PO_4

SM agar plates (pH 6.5)

9 g agar

10 g peptone

50 mM glucose

1 g yeast extract

4 mM $MgSO_4$

16 mM KH_2PO_4

5.7 mM K_2HPO_4

-Both media were filled up to 1 litre (l) with dH_2O.

Soerensen phosphate buffer (pH 6.0)

(Malchow *et al*., 1972)

14.6 mM KH_2PO_4

2 mM Na_2HPO_4

Salt solution

10 mM NaCl

10 mM KCl

2.7 mM $CaCl_2$

HL-5 medium

10 g yeast extract

20 g proteose peptone

50 mM glucose

8.5 mM KH_2PO_4

1.25 mM Na_2HPO_4

-Filled up to 2l with dH_2O.

Phosphate agar plates (pH 6.0)

15 g Bacto agar

-Filled up to 1l with Soerensen buffer.

2.1.6.2 Medium for *E. coli* culture

LB medium (pH 7.4)

(Sambrook *et al*., 1989)

10 g bacto-tryptone

5 g yeast extract

86 mM NaCl

-pH adjusted with NaOH and medium filled up to 1l with dH_2O.

For LB-agar plates, 1.5% (w/v) agar was added into the medium and selection was provided by introducing 50 mg/l ampicillin and/or 25 mg/l kanamycin.

2.1.7 Buffers and other solutions

Those not shown here will be described in their corresponding sections under Methods.

100 x Denhardt's reagent
2% Ficoll 400
2% polyvinylpyrrolidon
2% bovine serum albumin

TE buffer (pH 8.0)
10 mM Tris/HCl
1 mM EDTA
-autoclave

10 x NCP buffer (pH 8.0)
100 mM Tris/HCl
1.5 M NaCl
5 ml Tween 20
0.02% NaN_3
-Filled up to 1l with dH_2O

10 x TBE buffer (pH 8.3)
890 mM Tris
890 mM Boric acid
20 mM EDTA
-autoclave

PBS (pH 7.2)
70 mM Na_2HPO_4
150 mM NaCl
30 mM KH_2PO_4
2.7 mM KCl
-autoclave

Tris-Phenol (pH 8.0)
-1 vol. melted phenol was equilibrated with 1 vol. 1 M Tris/HCl, pH 8.0.

2.1.8 Bacterial strains

E. coli JM83	(Vieira and Messing, 1982)
E. coli XL1 Blue	(Sambrook *et al*., 1989)
Klebsiella aerogenes	***(Williams and Newell, 1976)***
Yersinia enterocolitica, WA-P (wild-type, serotype O8, human isolate)	(Heesemann, 1987)
Y. enterocolitica, WA-C (virulence plasmid-cured derivative of WA-P)	(Heesemann, 1987)

2.1.9 *Dictyostelium discoideum* strains

AX2-214 (can be cultivated under axenic conditions	(Raper, 1935)

or on bacteria lawn; derived from the free-living soil isolate NC4)	
HG1132 (severin minus mutant obtained by chemical mutagenesis)	(André *et al*., 1989)
pI/II-minus (mutant lacking both profilin isoforms)	(Haugwitz *et al*., 1994)

2.1.10 Mammalian cell line

COS-7 cells (derived from monkey kidney)	American Type Culture Collection

2.1.11 Vectors

pDexRH	(Faix *et al*., 1992)
pHyx	(Karakesisoglou *et al*., 1996)
pIMS6	(Simon *et al*., 1988)
pUC19	(Yanisch-Perron *et al*., 1985)
T84/bsr	(provided by Annette Erdmann)

2.1.12 Equipment

Axiophot microscope	Zeiss
CCD camera (C5985-10)	Hamamatsu
Conductivity meter (LF 537)	WTW
Confocal laser scanning microscope	Leica
Diavert inverse microscope	Leica
Digital color video CCD camera (TK-C1380)	JVC
Dounce homogenizer	Braun
Eagle Eye II	Stratagene
Electroporation apparatus	BioRad
Fluorescence spectrophotometer (Aminco Bowman)	Sopra
FPLC device (BioLogic)	BioRad
Nuclepore filter	Costar
Parr bomb	Parr Instrument Company
PCR thermal cycler	Biometra

pH meter	Knick
Protein fraction collector	Pharmacia
Rotary shaker	GFL
Semi-dry protein transfer Trans-Blot SD	BioRad
SMART system	Pharmacia
Spectrophotometer	Pharmacia
Speed-Vac concentrator	Bachhofer
Stereomicroscope (MZ12)	Leica
Ultrafiltration Centricon	Amicon
Vortex	Bender & Hobein
Water baths	GFL
Weighing machines	Sartorius
X-ray film developing machine (Curix 60)	AGFA

2.1.13 Other materials

2.2 ml sterile tubes for freezing of cells	Nunc
3MM filter paper	Whatman
4-well borosilicate glass chamber slides (for tissue culture and direct fluorescence microscopy)	Nunc
24-well plates	Costar
Dialysis membranes	Biomol
Eppendorf tubes (0.1 ml, 0.5 ml, 1.5 ml)	Eppendorf
Falcon centrifuge tubes (15 ml, 50 ml)	Falcon
Nitrocellulose membranes (BA85)	Schleicher & Schuell
Petri dishes	Greiner
Polaroid film (667)	Polaroid
Polyallomer ultracentrifuge tubes 1.5 ml	Beckman
Quartz cuvettes	Hellma
Sterile filters (0.22 μm, 0.45 μm)	Millipore
Tissue culture flasks	Nunc
X-ray films (X-omat)	Kodak

2.1.14 Centrifuges and rotors

Centrifuges	
J2-21M/E	Beckman
J6-HC	Beckman
G6-SKR	Beckman
Optima LE-80K ultracentrifuge	Beckman
Optima TL100 ultracentrifuge	Beckman
Table-top centrifuge (5415)	Eppendorf
Rotors	
JA 14, JA 20, JS-4.2, Ti 45, Ti 70, TLA 100.3	Beckman

2.1.15 Computer programmes

Windows NT	
Bilddatenbank system	Leica
Sigma Plot 2.01	Jandel Scientific
Winword 7.0	Microsoft
Macintosh	
Illustrator 8.0	Adobe
NIH Image 1.60	National Institutes of Health
Photoshop 5.0	Adobe
UNIX	
UWGCG package program (University of Wisconsin Genetics Computer Group)	(Devereux *et al*., 1984)

2.2 Cultivation of *Dictyostelium discoideum*

2.2.1 Growth in liquid medium (Claviez *et al*., 1982)

From spores or bacterial lawns on SM-agar plates, the wild-type strain AX2 was inoculated into AX or HL-5 medium containing the antibiotic streptomycin sulfate (400 µg/ml) in order to be free of the contaminating *K. aerogenes*. The generation time at 21°C and 150 rpm is about 10 hours. For large-scale generation of cells for protein purification, cells cultivated in 4

x 2.5 l cultures up to a density between 5 x 10^6 to 1.2 x 10^7 cells/ml were harvested after centrifugation giving normally a yield of about 100 g wet weight. As for cell biological studies, cells were allowed to grow maximally up to a density of 5 x 10^6 cells/ml to avoid the stationary phase.

2.2.2 Growth on agar plates

Isolation of transformant clones was carried out on SM agar plates. 100 µl of a suspension of *K. aerogenes* in salt solution were placed on each agar plate, spread evenly together with the *Dictyostelium* cells, and the plates were kept at 21°C for about 2 days. The doubling time is around 3-4 h and the *Dictyostelium* colonies appeared as round clearings on the bacteria lawn.

2.2.3 Preservation of spores

Cells from axenic culture were harvested by centrifugation at 300 g for 10 min, washed once with cold Soerensen buffer and resuspended at a cell density of 2 x 10^8 cells/ml. 500 µl of the cell suspension was spread out onto each phosphate agar plate, and the cells were able to develop into fruiting bodies within 2-3 days. The spores were then harvested by knocking onto the lid of the petri dish and taken up in 10 ml of cold Soerensen buffer. 1 ml aliquots were dispensed into Nunc tubes (2.2 ml), shock-frozen in liquid nitrogen and stored at –70°C. For inoculation of spores, an aliquot was thawed at room temperature and cultured in AX medium, whereby after 3 days at 21°C and 150 rpm, a cell density of about 5 x 10^6 cells/ml was reached.

2.2.4 Freezing of *Dictyostelium* cells

For preservation of *Dictyostelium* cells, axenic cultures were harvested and resuspended at a cell density of about 5 x 10^7 cells/ml in ice-cold freezing medium (AX or HL-5 medium + 1% (v/v) penicillin-streptomycin solution + 5% (v/v) DMSO), and distributed as 1 ml aliquots into Nunc tubes (2.2 ml) pre-cooled on ice. The aliquots were then placed into the wells of a pre-cooled (4°C) brass block (10 x 9 x 5 cm) and kept at –70°C for a period of at least 15 h and subsequently stored at –70°C. To revive the cells, a frozen vial was thawed rapidly under cold running water, the cells washed once with cold AX medium, and then cultivated in AX medium in petri dishes or 24-well plates. For the transformant clones, growth medium was changed after 24 h and replaced with medium containing suitable antibiotics for selection.

2.3 Mammalian tissue culture

2.3.1 Cell culture

Adherent COS-7 cells (derived from monkey kidney) were cultivated under aseptic conditions in tissue culture flasks (Nunc, 200 cm^2) in 15 ml of Dulbeccos minimum essential medium (DMEM; Nunc) supplemented with 10% (v/v) foetal calf serum (heat-inactivated at 56°C for 1 h; Nunc), 2 mM L-glutamine (Nunc), and penicillin-streptomycin solution (100 U/ml penicillin, 100 µg/ml streptomycin; Nunc). The flasks were then incubated at 37°C in the presence of 5% CO_2 and the growth medium was changed every 2-3 days. The cell-line can be maintained by repassaging continuously. At 80-90% confluency, the cells were split in a ratio of 1:10 to 1:15 into new culture flasks in the following manner. Old medium was removed and the cells were washed once with sterile PBS buffer. 2 ml of trypsin/EDTA solution (Nunc; 1x, stock solution of 10x diluted in PBS) was introduced and the culture flask was incubated for 5 min at 37°C or until cells detached from the surface of the flask. 10 ml of DMEM containing 10% serum was then added to inactivate the activity of trypsin and the cells were centrifuged at 400 g for 5 min at room temperature, after which the medium was discarded and the cells resuspended in 10-15 ml of fresh growth medium. 1 ml of cell suspension per flask was dispensed into new culture flasks already containing fresh medium.

2.3.2 Freezing of cells

Cells were harvested from culture flasks via the action of trypsin as described above. After centrifugation (400 g, 5 min, RT), the medium was removed and the cells resuspended in ice-cold freezing medium (DMEM supplemented with 10% (v/v) serum and 10% (v/v) DMSO) at a concentration of 1 x 10^7 cells/ml. 1 ml aliquots of cell suspension were dispensed into Nunc tubes (2.2 ml) and the tubes placed into wells of a brass block (10 x 9 x 5 cm) pre-cooled at 4°C. This was then kept at –70°C for 24 h after which the ampules of cells were transferred to liquid nitrogen for long-term storage.

For revival of cells, a frozen ampule was thawed rapidly in a 37°C water bath and the contents emptied into a 50 ml Falcon tube containing 15 ml of medium prewarmed at 37°C. Following centrifugation (400 g, 5 min, RT), the supernatant was discarded and the cells resuspended in a suitable volume of growth medium and dispensed into new culture flasks.

2.4 Molecular biological methods

2.4.1 Preparation of plasmid DNA

2.4.1.1 Isolation of plasmid DNA by the method of Holmes and Quigley (1981)

An inoculum of bacteria was taken from a streak culture and suspended in 200 µl of STET/lysozyme buffer. Alternatively, 1 ml of bacteria from a fresh overnight shaking culture was harvested using a table-top centrifuge (5000 rpm, 1 min, RT), the supernatant discarded and the pellet resuspended in STET buffer. The suspension was boiled in a water bath for 1 min, centrifuged (14,000 rpm, 10 min, RT), and the insoluble cell debris removed using a sterile toothpick. The nucleic acids in the supernatant were precipitated with 200 µl of isopropanol for 5 min at RT and sedimented using a table-top centrifuge (14,000 rpm, 30 min, RT). The DNA pellet was then washed with 70% ethanol, vacuum-dried with a Speed-vac concentrator, and dissolved in 30 µl of TE buffer.

STET buffer (pH 8.0)
50 mM Tris/HCl
50 mM EDTA
5% Triton-X 100
8% sucrose
1 mg/ml lysozyme (added prior usage)

2.4.1.2 Isolation of plasmid DNA by the method of Qiagen

Large-scale preparation of plasmid DNA from *E. coli* was carried out with the Midi-kit purchased from the Qiagen company. Bacteria were cultivated in 150 ml of LB medium containing 50 µg/ml ampicillin overnight at 37°C with agitation. The cells were harvested by centrifugation (4,000 g, 5 min, 4°C) and resuspended in 10 ml of buffer P1. For cell lysis, 10 ml of buffer P2 was introduced and the resultant mixture was gently mixed by inverting the tube several times. After incubation for 5 min at RT, 10 ml of chilled buffer P3 was added, the suspension mixed gently by inverting tube, and then incubated on ice for 15 min. Following centrifugation (35,000 g, 30 min, 4°C), the sediment of proteins and cell debris was discarded, while the supernatant containing the plasmid DNA was centrifuged for a further period of 15 min. The clear supernatant was passed through a Qiagen tip 100 column previously

equilibrated with 5 ml of buffer QBT. After washing twice with 10 ml each of buffer QC, the plasmid DNA was eluted with 5 ml of buffer QF, precipitated with 0.7 vol. of isopropanol, spun down (30,000 g, 30 min, 4°C), and the DNA pellet washed with 70% ice-cold ethanol, air-dried and dissolved in 200 µl of 0.1x TE buffer.

The DNA concentration was determined using a spectrophotometer whereby an OD_{260} of 1.0 corresponds to 50 µg of DNA. The ratio of OD_{260}/OD_{280} should be between 1.8 and 2.0.

P1 buffer	P2 buffer	P3 buffer
50 mM Tris/HCl (pH 8.0)	200 mM NaOH	3 M K-acetate (pH 5.5)
10 mM EDTA	1% SDS	
100 µg/ml RNase A		

QBT buffer	QC buffer	QF buffer
750 mM NaCl	1 M NaCl	1.25 M NaCl
50 mM MOPS (pH 7.0)	50 mM MOPS (pH 7.0)	50 mM Tris/HCl (pH 8.5)
0.15% Triton-X 100	15% ethanol	15% ethanol

2.4.2 Restriction digest

Digestions of DNA with restriction enzymes were performed according to the manufacturer's instructions using recommended buffer systems and at the appropriate reaction temperatures. Generally, 2-10 U of enzymes were needed per µg DNA. Plasmid DNA was usually digested for 1-2 h, and chromosomal DNA for 3-12 h. The completion of the reaction could be monitored by agarose gel electrophoresis.

2.4.3 Agarose gel electrophoresis (Sambrook *et al*., 1989)

Electrophoretic separation of DNA was carried out using 0.7-1.5% (w/v) agarose gels prepared in 1x Tris-borate buffer. The gel buffer and running buffer are identical. Gels were cast in chambers of various sizes (4 x 7 to 20 x 20 cm, Eigenbau), and the DNA to be separated was mixed with 0.2 vol. of DNA sample buffer and loaded onto the gels. Separation occurs at 1-5 V/cm. At the end of the run, the gel was stained in a solution of ethidium bromide (5 µg/ml) for 10-30 min, followed by destaining in water for 30 min. Subsequently gels could be observed under UV light at 312 nm and photos taken with the Eagle-eye system (Stratagene, Heidelberg).

DNA sample buffer

40% sucrose

0.5% SDS

0.25% Bromophenol blue

-Taken up in TE buffer.

DNA molecular weight standards:

*Hin*d III-restricted λDNA (BRL): 23130 bp, 9416 bp, 6557 bp, 4361 bp, 2322 bp, 2027 bp, 564 bp, 125 bp

Hae III-restricted ΦX174-RF DNA (BRL): 1353 bp, 1078 bp, 872 bp, 603 bp, 310 bp, 281/271 bp, 234 bp, 194 bp, 118 bp, 72 bp

2.4.4 Isolation of DNA fragments from agarose gels

Extraction and purification of DNA from agarose gels in Tris-borate buffer were performed using the QIAquick gel extraction kit (Qiagen) according to the manufacturer's instructions. Buffers are provided by the kit and all centrifugation steps were carried out at 14,000 rpm at RT in a table-top microcentrifuge. The DNA fragment was excised from the agarose gel with a clean scalpel, the gel slice weighed, and 3 vol. buffer QG were added to 1 vol. gel (100 mg ~ 100 µl). The tube was then incubated in a heating block at 50°C for 10 min or until the gel slice had entirely dissolved. To increase the yield of DNA fragments (<0.5 kb and >4 kb), 1 gel vol. isopropanol was added to the sample and mixed. The sample was then applied to a QIAquick spin column (Qiagen) and centrifuged for 1 min in order to bind DNA to the column. The flow-through was collected in a 2 ml collection tube and discarded. For washing of DNA, 0.75 ml of buffer PE was added to the column and spun down for 1 min. The flow-through was removed and the column centrifuged for an additional 1 min to remove completely residual ethanol. The column was then placed into a clean 1.5 ml tube and the DNA eluted by the addition of 50 µl of buffer EB (10 mM Tris/HCl, pH 8.5) or dH_2O to the column followed by centrifuging for 1 min. The DNA could be concentrated by precipitating with 2 vol. ethanol.

2.4.5 Oligonucleotide primers

Oligonucleotide primers for sequencing and polymerase chain reaction (PCR) were synthesized from MWG-Biotech (Ebersberg) and delivered as lyophilized forms. The oligonucleotides were each dissolved in 50 µl of sterile dH_2O and their concentrations

determined at an optical density (OD) of 260 nm. An OD_{260} of 1.0 corresponds to 25 µg of a chain of oligonucleotides.

Profilin-GFP construct

Oligonucleotide primers for PCR

FPpIIuni	5‘-CGC GCC GCG GAA GCT TGA GCT CAA AAA TGA CTT GGC AAG CAT ACG TC-3‘
FPpIIrev	5‘-CGC GGA TCC ACA GTT GTT GTC AAT TAA ATA ATC G-3‘
FPgel4uni	5‘-CGC GGA TCC GCT GAT CCA GAG AAA TCA TAC-3‘
FPgel4rev	5‘-CGC GAA TTC GGC TGG TTT AAC GGT AAC AG-3‘
CTRgel4uni	5‘-CGC GCC GCG GAA GCT TGG ATC CAA AAA TGG CTG ATC CAG AGA AAT C-3‘
FPbgfpuni	5‘-CGC GAA TTC ATG AGT AAA GGA GAA GAA C-3‘
FPbgfprev	5‘-GCG CAA GCT TGC GGC CGC TTA TTT GTA TAG TTC ATC CAT G-3‘

Oligonucleotide primers for sequencing

BluescriptT3uni	5‘-AAT TAA CCC TCA CTA AAG GG-3‘
BluescriptT7rev	5‘-GTA ATA CGA CTC ACT ATA GGG C-3‘

Severin-GFP construct

Oligonucleotide primers for PCR

NSEV-GFP	5‘-CGC GAA TTC AAA AAT GAT TAA GAA TAG AAA ATT AG-3‘
C4SEV-GFP	5‘-CGC GAA TTC AGC TTC ACC TGA AGC AGA TAA TAA AGT TTC AAA TG-3‘

Oligonucleotide primers for sequencing

NSEV-GFP	5‘-CGC GAA TTC AAA AAT GAT TAA GAA TAG AAA ATT AG-3‘
CDS378rev	5‘-TAA GCA GCA GTG CCA GC-3‘
CDS847rev	5‘-CGC GAA TTC TTA GGC AGT TTC GTG TTT AGC AGC G-3‘
GFP 5rev	5‘-TTG CCC ATT AAC ATC GCC-3‘

2.4.6 Polymerase chain reaction (PCR)

PCR was employed to amplify and generate suitable restriction sites for the *Dictyostelium* profilin II and severin DNA fragments using profilin II cDNA (Haugwitz *et al*., 1991) and severin cDNA (André *et al*., 1988) as PCR templates respectively. With the aid of a thermal cycler (Biometra UNO) the reaction was performed in 50 µl volume, overlaid with mineral oil at the surface to avoid evaporation. Based on the number of guanine and pyrimidine nucleotides, the annealing temperature (Tm) of a particular oligonucleotide primer could be calculated according to the formula of Suggs *et al*. (1981): 4(G+C) + 2(A+T) –10 = Tm (°C)

Reaction conditions

Denaturation: 94°C, 60 sec
Annealing: 55-60°C, 60 sec
Elongation: 72°C, 60 sec
No. of cycles: 25

Reaction components

0.5 µg plasmid DNA
20 pmol 5‘-oligonucleotide
20 pmol 3‘-oligonucleotide
2 µl dNTP mix (5 mM each)
1 U *Taq* polymerase (Eurogentec)
5 µl 10 x PCR buffer
-Filled up to 50 µl with dH_2O.

First denaturation step: 94°C, 120 sec
(to allow complete denaturation of the DNA)
Last elongation step: 72°C, 120 sec
(to ensure complete polymerization of the products)

10 x PCR buffer

100 mM Tris/HCl (pH 8.3)
500 mM KCl
15 mM $MgCl_2$
0.1% (w/v) gelatine

2.4.7 Purification of PCR products

For cloning purposes, the PCR products were purified using the QIAquick PCR purification kit (Qiagen) following the manufacturer’s protocol. Buffers used were provided by the kit and all centrifugation steps were done at 14,000 rpm at RT using a table-top microcentrifuge. 5 vol. PB buffer were added to 1 vol. of the PCR reaction and mixed. The sample was applied to a QIAquick spin column and centrifuged for 1 min to bind DNA to the column while the flow-through collected in 2 ml collection tube was discarded. DNA was washed with 0.75 ml of PE buffer by centrifuging for 1 min. Residual ethanol was removed by centrifuging for an extra 1 min. The spin column was then placed in a clean 1.5 ml eppendorf tube and the DNA eluted by the addition of 50 µl of dH_2O to the column and centrifuging for 1 min. The purified

DNA was subsequently used for restriction digest for 2-6 h and finally purified from agarose gel with the aid of the QIAquick gel extraction kit from Qiagen (2.4.4).

2.4.8 Phosphatase treatment (Sambrook *et al.*, 1989)

In order to prevent self-ligation of a linearized vector, the phosphate group at the 5‘ end was removed using alkaline phosphatase from calf intestine. Dephosphorylation was performed in a 50 µl reaction volume, whereby 1-5 µg of linearized vector DNA was incubated with 1-2 U of alkaline phosphatase in 1 x phosphatase buffer at 37°C for 1 h. Reaction was stopped with 5 mM EDTA followed by heat-inactivation of the enzyme at 75°C for 10 min. The DNA was then extracted twice with equal volume of phenol/chloroform/isoamyl alcohol (25:24:1) and precipitated with 2 vol. of ethanol.

10 x phosphatase buffer (pH 9.0)

500 mM Tris/HCl

10 mM $MgCl_2$

1 mM $ZnCl_2$

10 mM spermidine

2.4.9 DNA ligation

DNA fragments were connected using T4 DNA ligase in a reaction volume of 10 µl. The concentrations of vector (dephosphorylated) and insert DNA fragment were estimated from an analytical agarose gel. In general, for successful ligation of small insert fragments (< 1000 bp), a 10-fold excess of insert over vector DNA was necessary, whereas for large fragments, equal amounts of vector and insert DNA were used for ligation. Cohesive-end ligation was carried out at RT for 12-16 h.

Reaction components

Linearized vector DNA (200-400 ng)

Insert DNA fragment

2 µl 5 x ligation buffer

1 U T4 DNA ligase

-Filled up to 10 µl with dH_2O.

5 x ligation buffer (pH 7.6)

100 mM Tris/HCl

25 mM $MgCl_2$

25 mM DTT

2.5 mM ATP

250 µg/ml BSA

2.4.10 Preparation of electroporation competent cells

1l LB medium was inoculated with 10 ml of an overnight culture of the *E. coli* strain of choice and cultivated at 37°C with shaking at 220 rpm until an OD_{600} of 0.6 was reached. All tubes and solutions subsequently used were sterilized and cooled to 4°C. Good cooling was essential to obtain competent cells of a good quality. The cells were cooled on ice, harvested by centrifuging (4,000 g, 15 min, 4°C) and resuspended in 1l dH_2O. Following another centrifugation step, the cells were resuspended in 0.5l dH_2O, pelleted again, washed with 20 ml of 10% glycerol and finally resuspended in 2-3 ml of 10% glycerol. 100 µl aliquots were shock-frozen in liquid nitrogen and stored at –70°C.

2.4.11 Electroporation of *E. coli*

For transformation, electroporation competent *E. coli* cells were thawed on ice. 45 µl of cells were mixed with 1-5 µl of DNA or the ligation mixture resolubilized in dH_2O, and placed in a pre-chilled electroporation cuvette (Eurogentec; 2 mm gap between electrodes). After a pulse of 2.5 kV, 200 Ω and 25 µF, 1 ml of SOC medium (Sambrook *et al*., 1989) was added instantly and the cells regenerated at 37°C for 45 min with agitation. 1, 10 and 100 µl of cells were plated out on LB agar plates containing 50 µg/ml of ampicillin or 25 µg/ml of kanamycin and incubated overnight at 37°C.

SOC medium

2% Bacto-tryptone
0.5% yeast extract
10 mM NaCl
2.5 mM KCl
10 mM $MgCl_2$
10 mM $MgSO_4$
20 mM glucose

2.4.12 Screening for positive *E. coli* transformants

To isolate *E. coli* colonies carrying the desired DNA fragment, colonies were selected and mini preparations of plasmid DNA were performed (2.4.1.1) followed by restriction analyses (2.4.2) to determine the correct orientation of the DNA insert. Finally the authenticity of the DNA sequence was verified by sequencing (Toplab, Martinsried).

2.4.13 *E. coli* permanent cultures

Important transformants were preserved as permanent cultures. An inoculum of bacteria was resuspended in 1 ml of LB medium containing 7% of DMSO. The cells were shock frozen in liquid nitrogen and stored at –70°C.

2.4.14 Transformation of *D. discoideum*

Dictyostelium cells were electro-transformed with profilin- or severin-GFP DNA constructs. Recombinant gene expression in *D. discoideum* was regulated by a plasmid harbouring the *Dictyostelium* actin 15 promoter (A15P) and actin 8 terminator (A8T) sequences. The presence of an appropriate antibiotic resistance cassette on the expression plasmid allowed for selection of transformants with geneticin or blasticidin.

For transformation, *Dictyostelium* cells cultivated to a density of 2-3 x 10^6 cells/ml were harvested by centrifugation (300 g, 5 min, 4°C), washed once with cold Soerensen buffer, followed by washing twice with ice-cold electroporation buffer and the cells finally resuspended in chilled electroporation buffer at a density of 1 x 10^8 cells/ml. 500 µl of the cell suspension were mixed with 15-30 µg of the desired plasmid DNA in a pre-chilled electroporation cuvette (4 mm gap between electrodes). After a pulse at 1.0 kV and 3 µF with the aid of an electroporation device (Gene Pulser, Biorad), the cells were immediately transferred to a petri dish and incubated at RT for 10 min, after which $CaCl_2$ and $MgCl_2$ were added to an end concentration of 1 mM each and the cells incubated for an additional 15 min at RT with gentle agitation. Finally, the cells were diluted with HL-5 medium to a density of 1 x 10^6 cells/ml and allowed to recover at 21°C for 24 h before selection pressure was added.

Electroporation buffer (pH 6.1)

50 mM sucrose

10 mM KH_2PO_4

-pH was adjusted with KOH solution, and the buffer sterilized by filtration.

2.4.15 Cloning of transformants

Following 10-15 days of selection, the transformants were washed out from the petri dishes, diluted, and plated out together with an aliquot of *K. aerogenes* suspension in salt solution onto SM agar plates. The transformants were diluted to the extent of about 50-100 cells per plate for better isolation of single colonies. Within 2-3 days at 21°C, single round clearings were observed, and the plates were screened directly under low magnification (5 x) at 488 nm

(FITC filter) using an Axiophot microscope (Zeiss) for clones that exhibited green fluorescence. These were picked with toothpicks and cultured in 24-well plates in AX or HL-5 medium containing selection pressure for the transformants and streptomycin sulfate (400 µg/ml) to remove the contaminating bacteria. The axenic cultures were then grown in larger quantities, harvested and preserved as described (2.2.4) until further analysis.

2.4.16 Generation of severin-GFP *Dictyostelium* transformants

Using severin cDNA (André *et al*., 1988) as a template and a pair of oligonucleotide primers containing the *Eco*RI restriction site for PCR, the resulting 1.1 kb of severin DNA consisting of the complete coding region was cloned into the *Eco*RI site of the expression vector pDEXRH (Faix *et al*., 1992), already harbouring a red-shifted S65T GFP inserted in the *Hin*dIII site of the vector. Correct sequence and orientation were confirmed by sequencing. Severin was thus fused to the N-terminal of the GFP separated by a linker of 10 amino acid residues, SGEAEFKKLK. Expression of the fusion protein is controlled by the *D. discoideum* actin 15 promoter. The recombinant vector was introduced by electroporation into AX2 wild-type and the HG1132 severin null (André *et al*., 1989) *D. discoideum* cells. Transformants were selected with 10 µg/ml of G418 for 2 weeks. For culture conditions, the *D. discoideum* strains AX2, HG1132 and the transformants were cultivated at 21°C axenically in liquid medium rotary shaken at 150 rpm. For the transformed cells, G418 was added to a final concentration of 10 µg/ml.

2.4.17 Generation of profilin-GFP *Dictyostelium* transformants

The profilin II gene from *Dictyostelium* was fused to the amino-terminal of the W7 blue-shifted mutant of GFP (Heim and Tsien, 1996) via a linker of 100 amino acid residues derived from the segment 4 (rod 4) of the six 100-residue repetitive segments of the rod domain of the gelation factor (ABP-120) from *D. discoideum* (Fucini *et al*., 1997) whose 3-D structure was recently determined by NMR spectroscopy. Essentially the 3 DNA fragments namely, profilin II, rod 4 and W7 GFP were sequentially cloned into the pBluescript II SK vector (a derivative of pUC19) with the aid of oligonucleotide primers for generating suitable restriction sites via PCR. Using a pair of primers FPpIIuni (*Sac*II, *Hin*dIII, *Sac*I) and FPpIIrev (*Bam*HI), the profilin II gene was amplified from a cDNA template (Haugwitz *et al*., 1991) and cloned into the *Sac*II and *Bam*HI sites of pBluescript. The rod 4 sequence was amplified from the entire coding sequence of ABP-120 in the pIMS6 vector (Simon *et al*., 1988) with the primer pair FPgel4uni (*Bam*HI) and FPgel4rev (*Eco*RI) and then cloned into pBluescript via *Bam*HI and

*Eco*RI sites. As for the W7 GFP gene, it was cloned via the *Eco*RI and *Hin*dIII sites into pBluescript using the primers FPbgfpuni (*Eco*RI) and FPbgfprev (*Not*I, *Hin*dIII) from the W7 GFP-pRSET B recombinant plasmid kindly provided by Roger Tsien. The authenticity of the profilin-GFP sequence was determined by restriction digests followed by sequencing with the gene-specific primers and the vector-specific T3uni and T7rev primers. The entire profilin-GFP construct was then digested with *Hin*dIII and cloned into the T84/bsr *Dictyostelium* expression vector. After confirmation of the correct insert orientation by restriction analyses, the fusion construct was used for transformation and subsequent fusion protein expression in profilin null cells.

As control, only the 100-residue linker was fused to the amino-terminal of GFP. The rod 4 sequence was amplified with a primer pair CTRgel4uni (*Sac*II, *Hin*dIII, *Bam*HI) and FPgel4rev (*Eco*RI) and cloned via *Sac*II and *Eco*RI restriction sites into pBluescript. The GFP was cloned as described above and the rod 4-GFP construct was eventually recloned into the *Hin*dIII site of the T84/bsr *Dictyostelium* expression vector and transformed into profilin null cells.

2.4.18 Transfection of mammalian cells

COS-7 cells were transfected with selected EGFP-fused cytoskeletal constructs whereby gene expression was driven by the human cytomegalovirus (CMV) promoter and SV40 (simian virus) polyadenylation signals. The enhanced GFP (EGFP) gene has been codon-optimized for maximal expression and fluorescence intensity in mammalian cells. Using a modified protocol of Graham and van der Eb (1973), transient transfection was performed via a calcium phosphate-DNA precipitate adhering to the cell surface thus allowing uptake of plasmid DNA by the cell monolayer. 18-24 h prior to transfection, an almost confluent cell monolayer was split 1:15 into 4-well chamber slides or onto coverslips placed in 24-well plates (~2 x 10^4 cells/well), and allowed to grow overnight in DMEM supplemented with 10% serum in an incubator at 37°C and 5% CO_2. 2-4 h before transfection, old medium was replaced. 500 µl of 2 x HBS solution was placed in a sterile 50 ml Falcon tube. In a tube, 60 µl of 2M $CaCl_2$ were mixed with ~20 µg of plasmid DNA prepared from the Qiagen Midi-kit (2.4.1.2) and the volume adjusted to 500 µl with sterile dH_2O. While using a sterile plugged pipette to bubble the 2 x HBS, the DNA/$CaCl_2$ solution was added dropwise to the HBS. After 30 min of incubation at RT, the precipitate was distributed evenly over the cells in wells (24 µl/well) and the plates or chamber slides gently agitated to mix precipitate and medium. The cells were incubated for 12-16 h under standard growth conditions, after which medium was

removed and the cells washed twice with PBS solution and replaced with fresh growth medium. The cells were analysed after 48-72 h.

2 x HEPES-buffered saline (HBS) solution (pH 7.05-7.12)

16.4 g NaCl

11.9 g HEPES (N-2-hydroxyethylpiperazine-N‘-2-ethanesulfonic acid)

0.21 g Na_2HPO_4

-800 ml dH_2O was added, pH adjusted to 7.05-7.12 with 5 N NaOH and filled up to 1l with dH_2O. The solution was subsequently sterilized by filtration through a 0.45 µm filter and stored at –20°C in 10 ml aliquots.

2.5 Biochemical methods

2.5.1 SDS-Polyacrylamide gel electrophoresis (SDS-PAGE)

Protein mixtures were separated by discontinuous SDS-PAGE (Laemmli, 1970). For this purpose, 12% or 15% resolving gels with 3% stacking gels were used (7.5 x 10 x 0.05 cm). The stacking gel deposits the polypeptides to the same starting level at the surface of the resolving gel, and subsequently the SDS-polypeptide complexes are separated in the resolving gel according to size under uniform voltage and pH. Prior to SDS-PAGE, 1/3 vol. 3 x SDS gel loading buffer was added to the protein samples to be separated and boiled for 3 min. Electrophoresis was carried out at a constant voltage of 150 V, after which the gel could be stained with Coomassie Blue dye and destained for direct observation of the protein bands or proteins from the gel could be blotted onto nitrocellulose membranes and detected indirectly via antibodies. As standard, a mixture of proteins of defined molecular masses was electrophoresed.

Stacking gel

125 mM Tris/glycine (pH 6.8)

0.1% SDS

3.3% acrylamide:bisacrylamide (30:0.8)

Resolving gel

380 mM Tris/glycine (pH 8.8)

0.1% SDS

12%/15% acrylamide:bisacrylamide (30:0.8)

Per 16 ml:	Per 42 ml:
240 µl 20% ammonium persulfate (APS)	480 µl 20% APS
8 µl N,N,N‘,N‘-tetramethylethylenediamine (TEMED)	12 µl TEMED

10 x SDS-PAGE running buffer (pH 8.3)	3 x SDS gel loading buffer
250 mM Tris	150 mM Tris/HCl (pH 6.8)
1.9 M glycine	30% glycerol
1% SDS	6% SDS
	15% ß-mercaptoethanol
	0.3% bromophenol blue

Molecular weight standards:

LMW (“low molecular weight“, Biorad)
92.5 kDa, 68 kDa, 45 kDa, 33 kDa, 20 kDa, 14 kDa

“See blue“ (Novex)
250 kDa, 98 kDa, 64 kDa, 50 kDa, 36 kDa, 30 kDa, 16 kDa, 6 kDa, 4 kDa

2.5.2 Coomassie Blue staining of proteins

Following SDS-PAGE, gels were stained in Coomassie Blue solution for at least 30 min with agitation, after which the unbound dye was removed by shaking in a destaining solution.

Coomassie Blue solution	Destaining solution
0.1% Coomassie Brilliant Blue R250	10% ethanol
50% methanol	7% glacial acetic acid
12% glacial acetic acid	
-Solution filtered via a Whatman filter	

2.5.3 Drying of SDS-PAGE gels

For permanent recording, SDS-polyacrylamide gels after Coomassie Blue staining were washed in water with agitation with a couple of changes of water to remove the destaining solution. The gels were then shaken in a drying solution for 20 min, after which each gel was

placed between 2 dialysis membranes pre-wetted in the drying solution and then air-dried overnight.

Drying solution for polyacrylamide gels

24% ethanol

5% glycerol

2.5.4 Western blotting

Following separation of proteins by SDS-PAGE, the proteins were transferred from gels onto nitrocellulose membranes (Schleicher & Schuell BA85) according to the modified protocol of Towbin *et al*. (1979) with the aid of a protein transfer apparatus (Trans-Blot SD, BioRad). In this "semi-dry" method, the gel and its attached nitrocellulose filter were sandwiched between pieces of Whatman 3MM filter paper which had been soaked in transfer buffer and protein transfer was carried out at RT at 12 V for 40 min, after which the nitrocellulose filter was blocked overnight at 4°C in 5% (w/v) milk powder in 1 x NCP buffer. The membrane was then washed thrice (each 15 min) with NCP buffer (without sodium azide) and incubated with primary antibody (hybridoma supernatant diluted 1:100-1:1000 in NCP buffer) for 2 h. After washing several times with NCP buffer, the membrane was incubated with a secondary antibody (diluted 1:10,000 in NCP buffer) for 1 h. For the experimental purposes, goat anti-mouse IgG conjugated with peroxidase (Dianova) was used as the secondary antibody. Finally the membrane was washed a few times with NCP buffer and protein bands were detected via chemiluminescence by incubating the membrane in enhanced chemiluminescence reagents (ECL, Amersham) for 1 min and then exposed to X-ray films (X-omat AR5, Kodak).

Transfer buffer

25 mM Tris/HCl (pH 8.5)

190 mM glycine

20% methanol

0.02% SDS

20 x NCP buffer (pH 7.2)

48.4 g Tris

348 g NaCl

20 ml Tween 20

-Filled up to 2 l with dH_2O.

Chemiluminescence reagents (light sensitive)

200 µl Luminol (250 mM in DMSO; Luminol: 3-amino-phthalazinedione)

89 µl p-Coumaric acid (90 mM in DMSO)

2 ml Tris/HCl (1 M, pH 8.5)

-Filled up to 20 ml with dH_2O and prior to use, 6.1 µl H_2O_2 (30%) was added.

2.5.5 Bradford assay

Protein quantitation was performed according to the method of Bradford (1976). In principle, the Coomassie brilliant blue G 250 dye interacts primarily with arginine residues of proteins and causes a shift in the absorbance peak from 465 nm to 595 nm. Bovine serum albumin was used to make a standard colour response curve from which the concentrations of protein samples could be determined.

2.5.6 Preparation of actin from rabbit skeletal muscle

Actin was prepared from rabbit skeletal muscle according to the methods described by Spudich and Watt (1971) as well as by Pardee and Spudich (1982). The back and upper thigh muscles of a freshly bled rabbit were sliced into pieces and extracted with high-salt extraction buffer for 10 min with agitation. The mixture was centrifuged (4,000 g, 10 min) and re-extracted to remove myosin, after which the sediment was resuspended in water and the pH adjusted to between 8.2 and 8.5 with 1 M Na_2CO_3 solution. Following centrifugation (4,000 g, 10 min), the supernatant was discarded and the process repeated until swelling of the sediment was observed. The sediment was then washed with cold acetone, dried overnight, extracted once with chloroform and dried again. Finally the acetone powder was stored at -20°C for subsequent actin preparation.

10 g of muscle acetone powder were extracted with 200 ml of G-buffer at 0°C for 30 min, filtered through a nylon net and re-extracted at 0°C for 10 min. The filtrate was centrifuged (30,000 g, 30 min, 4°C) and the actin in the supernatant allowed to polymerize for 2 h at 4°C after addition of KCl (50 mM), $MgCl_2$ (2 mM) and ATP (1 mM). For removal of tropomyosin, solid KCl was then slowly introduced until a final concentration of 0.8 M was reached, and the actin filaments were then sedimented by centrifugation (150,000 g, 3 h, 4°C). For depolymerization, the F-actin pellet was dialyzed against several changes of G-buffer and further purified using a Sephacryl S300 gel filtration column (2.5 x 45 cm, Pharmacia). From its optical density at 290 nm, the G-actin concentration could be calculated easily from the ratio of $OD_{290}/0.65$, whereby 26,000 is the extinction coefficient value of actin at 290 nm (Wegner, 1976). The G-actin prepared could be stored at 4°C up to 3 weeks for active applications.

Extraction buffer

0.5 M KCl

0.1 M K_2HPO_4

G-buffer (pH 8.0)

2 mM Tris/HCl

0.2 mM $CaCl_2$

0.2 mM ATP

0.02% NaN_3

0.5 mM DTT

2.5.7 Pyrene-labelling of actin

Actin was labelled with N-(1)pyrenyliodoacetamide (pyrene) following the protocol of Kouyama and Mihashi (1981). After the ultracentrifugation step in the course of preparation of actin from acetone powder as described above, 2/3 of the supernatant were carefully collected and dialyzed thrice against 1l buffer P. Actin polymerization was initiated by the addition of KCl (150 mM) and $MgCl_2$ (2 mM) and 3-5 fold molar excess of pyrene (in DMSO) was introduced immediately to the actin while stirring. From this step onwards, all activities were carried out in the dark, since pyrene is light-sensitive. The solution was then shaken in a Falcon tube at RT overnight after which the actin filaments were sedimented (150,000 g, 3 h, 4°C). The F-actin pellet was homogenized in G-buffer and dialyzed three times against 1l G-buffer to allow depolymerization of actin. After a second centrifugation step (150,000 g, 3 h, 4°C), the pyrene-labelled G-actin was purified by gel filtration and later stored at –70°C.

Buffer P (pH 7.6)

1 mM $NaHCO_3$

0.1 mM $CaCl_2$

0.2 mM ATP

2.5.8 Partial purification of the severin-GFP fusion protein

For purification of the fusion protein from the HG1132 cells transformed with severin-GFP, cells cultivated under G418 selection in shaking suspension up to a density of 5 x 10^6 cells/ml were harvested, and the cell pellet resuspended in a homogenization buffer (30 mM Tris/HCl, 4 mM EGTA, 2 mM EDTA, 2 mM DTT, 30% sucrose, 5 mM benzamidine, 0.2 mM ATP, 1 mM PEFA-block, 0.5 mM PMSF; pH 8.0). Cells were lysed using a Parr bomb at 750 psi (pounds per square inch) for 30 min at 4°C. After centrifugation at 4°C for 1.5 h at 100,000 g, the supernatant was adjusted to pH 8.0 and loaded onto a DEAE anion-exchange column

(DE52, Whatman, Maidstone; 2.5 x 8 cm) equilibrated with TEDABP buffer (10 mM Tris/HCl, 1 mM EGTA, 1 mM DTT, 0.02% NaN_3, 1 mM benzamidine, 0.5 mM PMSF; pH 8.0). Under the conditions used, the fusion protein did not bind to the resin and the flow-through was adjusted to pH 6.5 with the addition of solid MES (2 [N-morpholino] ethane sulfonic acid) to a final concentration of 10 mM, after which it was loaded onto a phosphocellulose column (P11, Whatman; 2.5 x 6 cm) pre-equilibrated with MEDABP buffer (10 mM MES, 1 mM EGTA, 1 mM DTT, 0.02% NaN_3, 1 mM benzamidine, 0.5 mM PMSF; pH 6.5). The flow-through fraction containing the fusion protein was precipitated with solid ammonium sulphate and proteins precipitating between 50-80% of saturation were separated on a Sepharose 6B-CL gel filtration column (Pharmacia; 2.5 x 110 cm) equilibrated in IEDANBP buffer (10 mM imidazole, 1 mM DTT, 1 mM EGTA, 0.02% NaN_3, 0.2 M NaCl, 1 mM benzamidine, 0.5 mM PMSF; pH 7.6). Active fractions were pooled, dialyzed against MEDABP buffer and chromatographed on a hydroxylapatite column (Biorad; 1.5 x 3 cm, equilibrated in MEDABP, pH 6.5) using a linear gradient (2 x 125 ml, 0-1 M KCl in the presence of 10 mM potassium phosphate in column buffer) whereby the fusion protein, as determined by Western blotting, was eluted between 18-24 mS.

2.5.9 Low shear viscometry

Low shear viscometry was performed after 20 min of incubation at 25 °C in a falling ball viscometer (MacLean-Fletcher and Pollard, 1980). The reaction mixture (160 µl) contained usually 0.5 mg/ml rabbit skeletal muscle actin, and polymerization was initiated by the addition of G-actin to buffered $MgCl_2$ (final concentration: 2 mM $MgCl_2$, 10 mM imidazole, pH 7.2, 1 mM ATP, 0.2 mM $CaCl_2$, or 1 mM EGTA). The data shown are the average values of duplicate experiments.

2.5.10 Severing activity of severin-GFP measured by fluorescence spectroscopy

Pyrene-labelled actin (8 µM) was polymerized for 15 min in G-buffer (2 mM Tris/HCl, pH 8.0, 0.2 mM $CaCl_2$, 0.2 mM ATP, 0.01% NaN_3, 0.5 mM DTT, 2 mM $MgCl_2$) for use in the fluorescence measurements carried out with an Aminco Bowman luminescence spectrometer (Sopra GmbH, Buettelborn, FRG). All measurements were done in a sample volume of 800 µl at 25 °C with an excitation wavelength of 365 nm and an emission wavelength of 386 nm in G-buffer with or without 2 mM EGTA and at a final actin concentration of 0.8 µM. The slow depolymerization of actin filaments is drastically increased if a severing activity raises the number of pointed ends. Individual experiments were performed in duplicates. Measured

arbitrary relative fluorescence values were plotted against time and the slopes of these plots were calculated in the linear range of fluorescence decrease which were subsequently plotted versus increasing concentrations of the partially purified severin-GFP fusion protein.

2.5.11 Poly-(L)-proline binding assay

Interaction of the recombinant profilins with poly-(L)-proline stretches was investigated by affinity chromatography using poly-(L)-proline coupled agarose beads. The poly-(L)-proline residues were covalently conjugated to CNBr-activated agarose beads (BioRad) according to the manufacturer's instructions and the coupled beads were resuspended and stored in PBS (70 mM Na_2HPO_4, 30 mM KH_2PO_4, 150 mM NaCl, 0.1% NaN_3, pH 7.0). Total protein extracts from *D. discoideum* cells were prepared by incubating 2 x 10^6 cells with 200 µl lysis buffer (1% NP-40, 2 mM $MgCl_2$, 5 mM EGTA, 150 mM KCl, 2 mM KH_2PO_4, 10 mM ß-glycerophosphate, 5 mM ATP and 10 mM Hepes, pH 7.2) for 15 min on ice. Following centrifugation using a table-top microcentrifuge (14,000 rpm, 15 min, 4°C), 160 µl each of the supernatants were incubated with 100 µl of poly-(L)-proline/PBS mixture at 4°C for 3 h with agitation. Subsequently, the samples were sedimented with a table-top microcentrifuge (14,000 rpm, 15 min, 4°C), and the pellets washed twice with PBS before being resuspended in 60 µl each of 1 x SDS gel loading buffer. The supernatants and the pellet fractions were then analyzed by SDS-PAGE (2.5.1).

2.5.12 Inhibition of actin polymerization analyzed by fluorescence spectroscopy

Interactions of the recombinant profilins with either actin or PIP_2 (Sigma) were examined with the aid of pyrene-labelled G-actin (2.5.7) using a luminescence spectrometer (Sopra GmbH) in a final reaction volume of 800 µl at 25°C. The PIP_2 was sonicated in 10 mM Tris/HCl (pH 7.5) until an optically clear solution was obtained. In the kinetic studies, polymerization of 3 µM G-actin usually including 10-20% pyrene-actin was initiated by the addition of 2 mM $MgCl_2$ in the absence or presence of varying concentrations of recombinant profilins. All measurements were performed at an excitation wavelength of 365 nm and an emission wavelength of 386 nm, and the arbitrary fluorescence units were subsequently plotted against time. Data were confirmed with duplicate experiments.

2.5.13 Interaction of profilin-GFP with actin

Due to difficulty in obtaining large amounts of cells for protein purification, the affinity of the fusion protein for actin could not be pursued by fluorescence spectroscopy. Instead the

interaction between profilin-GFP and actin was investigated by molecular sizing via gel filtration utilizing the intrinsic ability of profilin to form profilactin complex with actin. The shift in the elution profile of the fusion protein detected by immunoblotting would be an indication of the presence of interaction between the fusion protein and actin.

300 ml of profilin II-GFP transformed *D. discoideum* cells, cultivated in HL-5 medium containing 5 µg/ml blasticidin to a density of 3 x 10^6 cells/ml at 21°C and 150 rpm, were harvested by centrifugation (300 g, 5 min, 4°C), washed in cold Soerensen buffer, and the cell pellet resuspended in 2 vol. homogenization buffer (30 mM Tris/HCl, 4 mM EGTA, 2 mM EDTA, 2 mM DTT, 5 mM benzamidine, 0.2 mM ATP, 1 mM PEFA-block, 0.5 mM PMSF; pH 8.0). The cells were then lyzed via several passages through Nuclepore filters (5 µm pore size), after which the lysate was ultracentrifuged at 100,000 g (Ti70 rotor, 4°C, 1.5 h). After adjustment to pH 8.0, the supernatant consisting of soluble cytosolic proteins was loaded onto an anion-exchange monoQ column (0.75 x 5 cm, 1 ml vol., Pharmacia) pre-equilibrated with TEDABP buffer (10 mM Tris/HCl, 1 mM EGTA, 1 mM DTT, 0.02% NaN_3, 1 mM benzamidine, 0.5 mM PMSF; pH 8.0) and chromatography was performed with the aid of a FPLC setup (BioLogic, BioRad). Protein was eluted with a linear NaCl gradient (0-400 mM in TEDABP) and fractions of 0.5 ml were collected throughout the run which were later analyzed by immunoblotting. Using antibodies specific for the fusion protein [anti-profilin II (174-336-8), anti-GFP (264-236-2)] and for *Dictyostelium* actin (Act-1; Simpson *et al*., 1984), a fraction with only profilin-GFP and another one containing both the fusion protein and actin were selected for subsequent gel filtration.

For gel filtration chromatography, the 2 monoQ-eluted fractions were separately loaded onto a Superose 12 column (1.5 x 30 cm, Pharmacia) equilibrated in IEDANBP buffer (10 mM imidazole, 1 mM EGTA, 1 mM DTT, 0.02% NaN_3, 200 mM NaCl, 1 mM benzamidine, 0.5 mM PMSF, pH 7.6) and 0.5 ml-fractions were eluted using the BioLogic FPLC equipment. The elution profiles of the 2 monoQ fractions after gel filtration could then be compared via immunoblotting using an antibody specific for the fusion protein. Alternatively, a more sensitive micro-separation method by the SMART system (Pharmacia) was used for gel filtration chromatography. The 2 monoQ fractions, 1 with profilin-GFP only and the second with both actin and the fusion protein, were separately loaded (50 µl sample vol.) onto a Superose 6 PC 3.2/30 column (3.2 x 300 mm, 2.4 ml vol., Pharmacia) whose optimal molecular weight separation ranges from 5000 to 5 x 10^6 Da. Proteins eluted with IEDANBP buffer at a flow rate of 40 µl/min were collected in 50 µl-fractions which were subsequently analyzed via Western blotting and the elution patterns compared. The elutions of marker

proteins, whose absorptions were confirmed at 280 nm, were performed to make a standard algorithm curve. Data were analyzed with the SMART Manager software for OS/2 (Pharmacia).

Standards:
Ferritin (450 kDa), Catalase (240 kDa), Aldolase (158 kDa), BSA (68 kDa) and Chymotrypsinogen (25 kDa)

2.6 Cell biological methods

2.6.1 Indirect immunofluorescence

Studies of subcellular protein localization were performed via indirect immunofluorescence. For this assay, coverslips to be used were washed with 3.6% HCl followed by dH_2O. For the adherent COS7 cells, these were aseptically cultivated on round coverslips in a 24-well plate until near confluency before being fixed and subjected to subsequent immuno-detection. As for *Dictyostelium*, exponentially growing cells (3 x 10^6 cells/ml) were harvested, washed twice with Soerensen buffer, and 1 x 10^6 cells were allowed to attach to the coverslips for 15 min, after which excess fluid was removed and the coverslips fixed in cold methanol for 10 min at –20°C followed by 30 min of air-drying. Alternatively, cells could be fixed with 3% paraformaldehyde (in PBS) for 15 min and then permeabilized for 1 min with 0.5% Triton-X 100 (in PBS) at RT and then washed with PBS followed by PBG. For the profilin null cells (pI/II-minus), they were fixed for 30 min in picric acid/paraformaldehyde solution (2% paraformaldehyde, 10 mM Pipes, 15% saturated picric acid, pH 6.0), and then washed several times with PBS-glycine and PBG.

After fixation, cells were incubated with undiluted hybridoma supernatants for at least 2 h before being washed with PBG, and then subjected to 1 h of incubation in the dark with FITC or Cy3 conjugated goat anti-mouse IgG secondary antibody (diluted 1:100-1:1000 in PBG). F-actin was labelled with either FITC-, TRITC-labelled phalloidin (diluted 1:100 in PBG) or a monoclonal antibody against *Dictyostelium* actin (Simpson *et al*., 1984). Improved F-actin labelling could be achieved by prolonged incubation of cells with phalloidin. Nuclei were stained with DAPI (4,6-diamidino-2-phenylindole, Sigma) diluted 1:1000 in PBG (0.5 µg/ml final concentration) for 1 h. After incubation with secondary antibody, cells were washed

several times with PBG, PBS and briefly with dH_2O before being embedded in gelvatol and kept at 4°C overnight until observation with epifluorescence or confocal laser scanning microscopy.

10 x PBS (for immunofluorescence, pH 7.4)
1.37 M NaCl
27 mM KCl
81 mM Na_2HPO_4
15 mM KH_2PO_4
-in dH_2O and autoclave

PBG
0.5% BSA
0.05% fish gelatine
-in 1 x PBS, sterilized by filtration

Gelvatol
20 g gelvatol 20-30 (polyvinylalcohol, MW 10,000) were stirred in 80 ml PBS for 16 h.
40 ml glycerol was then introduced and stirred for further 16 h.
Following centrifugation (12,000 g, 15 min, RT), 25 ng/ml anti-bleaching agent DABCO (Diazabicyclo (2,2,2) octane) was added to the supernatant. Aliquots were stored at –20°C.

2.6.2 Phagocytosis of yeast

Uptake of yeast particles by *D. discoideum* was examined via indirect immunofluorescence. In this assay, 300 µl of cells at a density of 2 x 10^6 cells/ml were incubated with an equal amount of Baker's yeasts (cultivated in 1% sucrose solution at 30°C) on coverslips for about 30 min, after which they were methanol-fixed and subsequently labelled with a monoclonal antibody specific for profilin II (174-336-8) and processed as described above (2.6.1). Observations were made with the aid of an Axiophot microscope (Zeiss).

2.6.3 *Yersinia* infection of COS7 cells

Changes of the actin cytoskeleton were studied via infection of COS7 cells by two strains of *Yersinia enterocolitica*, namely WA-P (wild type) and WA-C (virulence plasmid cured strain as control) with the aid of indirect immunofluorescence and confocal laser scanning microscopy (CLSM). For the infection studies, overnight cultures of both strains of bacteria, cultivated with agitation at 27°C in LB medium supplemented with 50 µg/ml Nalidixic acid, were each diluted 1:10 in fresh LB medium and grown for an additional 2 h at 37°C (the temperature shift from 27°C to 37°C allowed induction of the secretion of *Yersinia* outer proteins or Yops). Bacteria were then diluted to an OD_{600} value of 0.3 and 15 µl of bacteria

were introduced to the mammalian cells per coverslip per well. Prior to bacterial infection, growth media of cells were replaced with DMEM supplemented with 10% fetal calf serum but without penicillin/streptomycin solution. Following centrifugation (400 g, 5 min, RT) to synchronize infection, a time course experiment of infection from 0-2 h was carried out at 37°C. Basically 3 approaches were employed here for the infection studies. COS7 cells cultured on coverslips in a 24-well plate were infected with either WA-P or WA-C and uninfected cells were used as negative controls. After various time-points of infection, the cells were washed twice with 1 x PBS and fixed with 3% paraformaldehyde/PBS solution and processed for immuno-detection as described (2.6.1) with a panel of antibodies against various cytoskeletal proteins. Alternatively, COS7 cells on coverslips in 4-well plates (Nunc) were transiently transfected (2.4.18) with EGFP-actin (Choidas *et al*., 1998), EGFP-cofilin or EGFP-profilin (kindly provided by Dr. Walter Witke, EMBL, Rome, Italy) and then infected with either strain of bacteria for various time-points, after which the cells were fixed with 3% paraformaldehyde, washed and directly embedded for subsequent analyses by microscopy (the GFP fluorescence was not affected by the fixation).

Real-time observations of infection of EGFP-actin transfected COS7 cells with either WA-P or WA-C were made with the aid of CLSM in the attempt to examine rapid and transient modifications of the actin cytoskeleton. For this assay, cells were cultivated and transfected in 4-well Lab-Tek chamber slides (Nunc, cat. no. 136420) with borosilicate glass bottoms (0.13-0.17 mm thick) highly suited for *in situ* fluorescence microscopy. Following introduction of bacteria to the transfected cells, chamber slides were spun down and immediately analyzed.

2.6.4 Confocal laser scanning microscopy (CLSM)

The infected cells expressing different EGFP-cytoskeletal fusion proteins after undergoing fixation were examined via CLSM. This microscopic technique was also used to study the *in vivo* dynamic remodelling of the actin cytoskeleton during infection of EGFP-actin transfected mammalian cells. For these purposes, a 100x oil immersion objective (PL APO 100x 1.40-0.7) was used for observation of cells under the laser wavelength of 488 nm (FITC) with the help of an inverted confocal microscope (Leica TCS NT, TCS: True Confocal Scanner) operated with an argon laser. For double-labelled cells, both types of fluorescence were measured separately but at the same time, and the signals were layered onto each other using the programme “Merge“. The crude images obtained were further processed by a Power Macintosh (8500/180) using the computer programmes NIH Image 1.60 and Adobe Photoshop 5.0.

2.6.5 Growth curves of *D. discoideum* mutants

The growth rates of wild-type (AX2) and various mutant strains of *D. discoideum* were studied by cultivation of the strains at 21°C either on SM-*K. aerogenes* plates (Williams and Newell, 1976) or axenically in liquid medium (Claviez *et al*., 1982; Sussman, 1987) shaken at 150 rpm. Colony diameter or cell density was plotted against time with the aid of the computer programme Sigma Plot 2.01.

2.6.6 Development of *D. discoideum* mutants

The abilities of wild-type and various mutant strains to generate fruiting bodies were compared by cultivating the strains on SM-*K. aerogenes* plates at 21°C for at least 2 days. Observations were made with a stereomicroscope (Leica) and images captured using the computer software Bilddatenbank system (Leica) and further processed with the programme Adobe Photoshop 5.0.

3 RESULTS

3.1 Analyses of the point-mutated profilins in *D. discoideum*

3.1.1 The W3N and K114E point-mutated profilins

According to Bjoerkegren *et al.* (1993), mutation of the well conserved tryptophan at position three of human profilin to an asparagine (W3N) results in its loss of interaction with poly-(L)-proline stretches, thus the same amino acid exchange was made on *Dictyostelium* profilin. To abrogate the association between profilin and actin, the point mutation K114E was introduced into profilin II, since the lysine residue K115 of *Acanthamoeba* is a component of the actin-binding site of profilin and could be crosslinked to glutamic acid #364 of actin (Vandekerckhove *et al*., 1989; Schutt *et al*., 1993). Site-directed mutageneses of profilin II via PCR resulting in the substitution of the tryptophan residue #3 by an asparagine (W3N) or of the lysine residue in position 114 by glutamic acid (K114E) were performed by Iakowos Karakesisoglou (Lee *et al*., 2000). The point mutations W3N and K114E altering the poly-(L)-proline and actin-binding activities of profilin respectively were clearly indicated in Fig. 4 (section 1.4). The authenticity of the profilin mutants has been confirmed by sequencing, Southern, Northern and Western analyses. Transformants cultivated in HL-5 medium supplemented with 50-90 µg/ml hygromycin B were designated as DdW3N and DdK114E for *D. discoideum* profilin null cells (Haugwitz *et al*., 1994) which expressed W3N or K114E respectively.

3.1.2 Poly-(L)-proline binding properties of W3N and K114E

This unique feature was investigated by incubation of equal amounts of *Dictyostelium* total cell homogenates with poly-(L)-proline coupled agarose beads. The supernatants and pellets after centrifugation were analyzed by SDS-PAGE. Wild-type profilins I, II and the K114E profilin mutant were observed in the pellet fractions, in contrast to the W3N profilin mutant which was only detected in the supernatant fraction (Fig. 5). In this assay, while the K114E profilin mutant still retained its ability to associate with poly-(L)-proline, the substitution of tryptophan to asparagine on W3N profilin strongly reduced its affinity for poly-(L)-proline stretches.

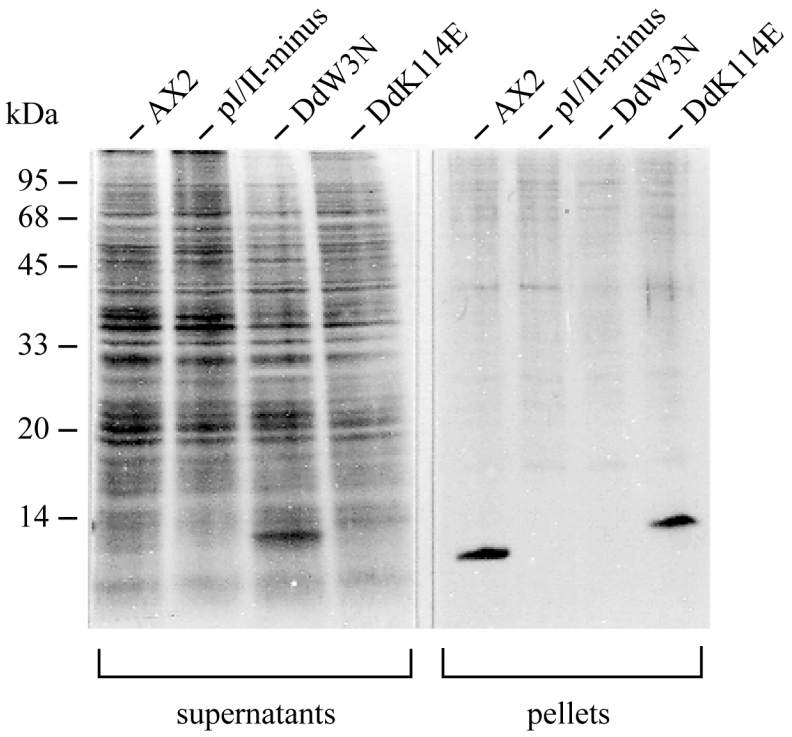

Fig. 5 Sedimentation assay with poly-(L)-proline beads
SDS-PAGE of supernatants (left) and pellets (right) from total cell homogenates after incubation with poly-(L)-proline beads showed that the point mutation W3N resulted in a complete loss of the polyproline-binding activity of profilin, whereas the K114E point-mutated profilin still retained its ability to bind poly-(L)-proline. The wild-type profilins from AX2 were used as a positive control for poly-(L)-proline binding.

3.1.3 Actin and PIP_2 binding characteristics of W3N and K114E

The interactions between the point mutated profilins (purified according to Lee *et al*., 2000) and rabbit skeletal muscle actin were investigated by fluorescence spectroscopy using pyrene-labelled G-actin. This approach is highly sensitive and the principle is based on an increase of up to 20-fold of fluorescence emission of pyrene-actin during the polymerization from G- to F-actin (Kouyama and Mihashi, 1981). Figure 6 distinctly demonstrates that a 1:1 ratio of wild-type profilin to rabbit G-actin was required to show the inhibitory effect of profilin on actin polymerization. A severe reduction in the affinity of the K114E for actin was observed, since it required a 3-fold excess of this mutated profilin compared to the wild-type profilin to display the same inhibitory effects. Actin-binding was slightly reduced in the W3N profilin mutant as a 1.5:1 ratio of W3N to actin was needed to match the inhibition of actin polymerization of wild-type profilin.

The influence of amino acid substitutions of profilin on its continued ability to bind phospholipids was also examined.

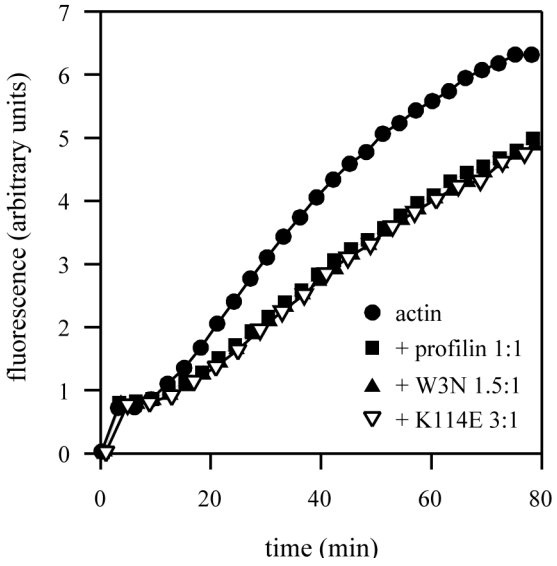

Fig. 6 Effects of wild-type and point-mutated profilin II on the polymerization of rabbit actin
The profilin/actin ratios were chosen in such a way that the inhibitory effects on polymerization were identical. Data indicate that actin binding is slightly reduced in W3N, but only a 3-fold amount of K114E over wild-type profilin II leads to a similar inhibition.

As illustrated in Figure 7A, PIP_2 interferred with the actin sequestering activity of wild-type profilin, indicating the capabilities of the *D. discoideum*'s profilins to interact with PIP_2 which competed with their affinities for G-actin. The inhibitory effect of PIP_2 on actin binding was also verified for the point mutated profilins, W3N and K114E (Fig. 7B), suggesting that the mutations did not significantly alter their binding to phospholipids.

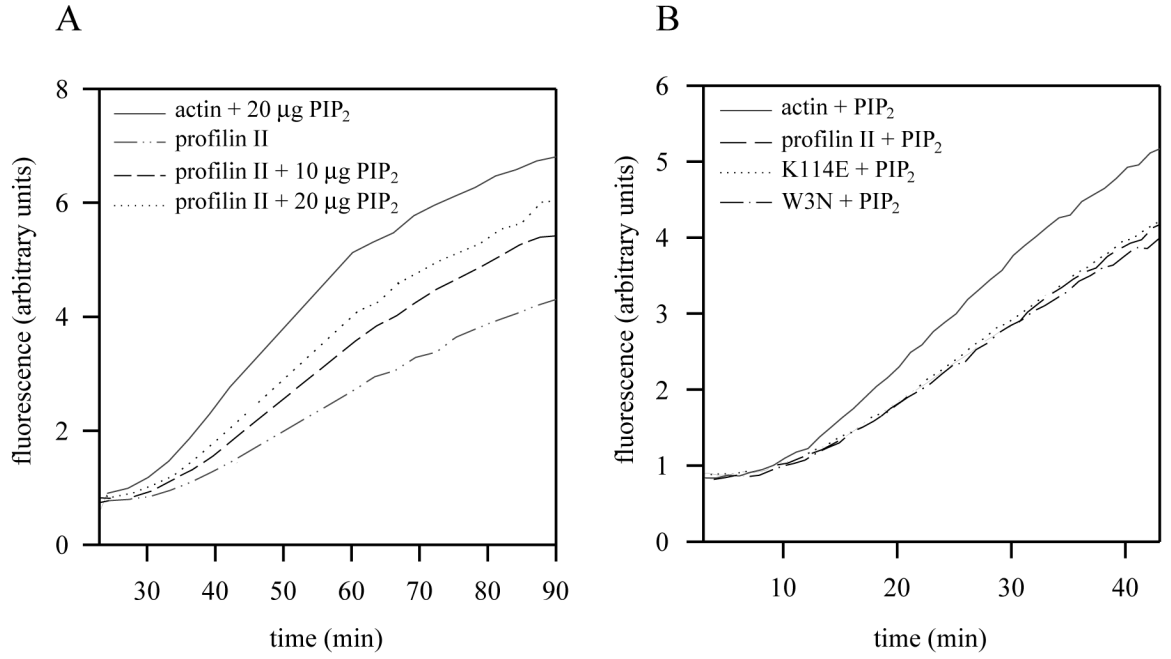

Fig. 7 Influence of varying amounts of PIP_2 on the actin-sequestering activity of wild-type and point-mutated profilins
(A) Polymerization of 3 µM rabbit actin was induced by 2 mM $MgCl_2$. Wild-type profilin II was used in a 1:1 ratio with actin in the presence of 0-20 µg PIP_2. (B) 3 µM rabbit actin were polymerized by induction with 2 mM $MgCl_2$. 1:1 ratio of profilin to actin, 1.5:1 ratio of W3N to actin and 3:1 ratio of K114E to actin were utilized in the fluorimetry measurements in the presence of 20 µg PIP_2. Data suggest that the point-mutated and wild-type profilins have similar affinity for phospholipids.

3.1.4 Cell morphology, cytokinesis and subcellular distribution of profilins

Cytokinesis, F-actin distribution and localization of profilins were investigated in AX2, DdW3N and DdK114E cells. Figure 8 showed that the DdW3N and DdK114E cells were indistinguishable from wild-type. Contrary to profilin deficient cells which are flattened, multinucleate and up to ten times larger than wild-type (Haugwitz *et al*., 1994; Karakesisoglou *et al*., 1996), DdW3N and DdK114E cells display normal cell morphology with 1-2 nuclei per cell typical for *D*. *discoideum* (Fig. 8A).

The uniform accumulation of F-actin around the edge of the profilin-minus cells forming a broad rim (Haugwitz *et al*., 1994; Karakesisoglou *et al*., 1996) was non-existent in DdW3N and DdK114E. Like the wild-type, only the leading edges of pseudopods of the mutant strains were stained with an antibody specific for *D. discoideum* actin (Simpson *et al.*, 1984). No obvious difference in F-actin distribution between DdW3N and DdK114E cells was detected.

As for the subcellular distribution of profilin, both DdW3N and DdK114E cells exhibited uniform cytoplasmic localization of profilin, similar to that of wild-type cells (Fig. 8B). However, non-homogenous populations of DdW3N and DdK114E cells with different levels of profilin expression were obtained. This can be observed in numerous other expression experiments as well. To have comparable cell populations in all studies, the strains were repeatedly recloned and used only for a limited period.

3.1.5 Development of DdW3N and DdK114E

In contrast to the profilin-minus cells which are unable to form fruiting bodies (Haugwitz *et al*., 1994), this developmental defect was restored in DdW3N and DdK114E cells due to the expressions of W3N and K114E point-mutated profilins respectively. Fig. 9 clearly showed that DdW3N and DdK114E cells were capable of producing fruiting bodies indistinguishable from that of wild-type cells.

Significantly, the rescue property of W3N profilin appeared to depend on its cellular concentration. By reducing hygromycin B concentration from 50 to 5 µg/ml, and finally under no selection pressure on a *Klebsiella* lawn, DdW3N clones were isolated which had lost their abilities to form fruiting bodies and thus assumed the aberrant phenotype of the profilin deficient cells. While these strains were incapable of generating fruiting bodies and exhibited diminished growth rates similar to that of the profilin-minus cells, they were still found to contain W3N profilin though at a reduced concentration similar to that of the K114E profilin in the DdK114E rescued cells (unpublished observation). Hence it is evident that an overexpression of W3N profilin is mandatory to restoring the fruiting phenotype of DdW3N.

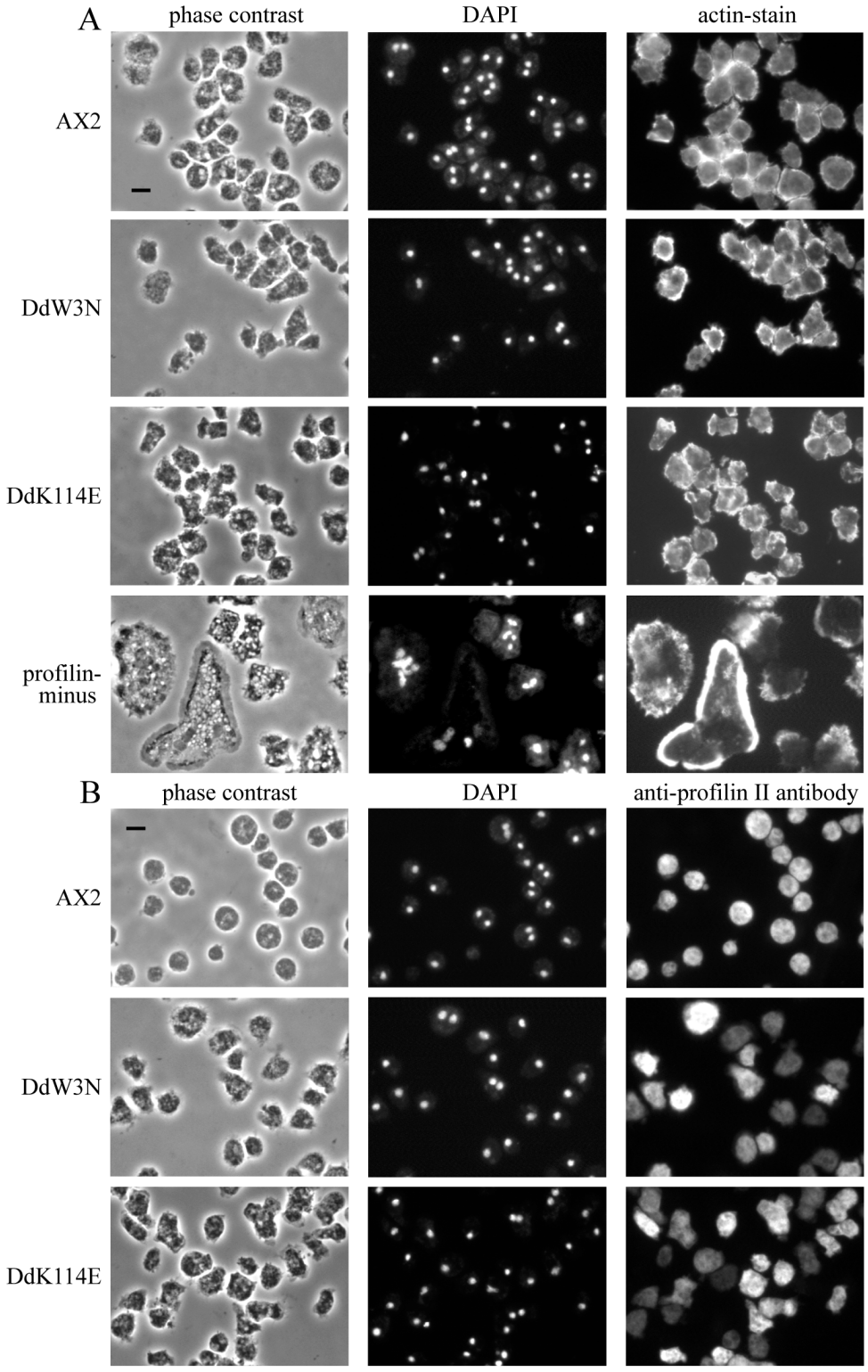

Fig. 8 Immunofluorescence labelling of actin and profilins in AX2, DdW3N and DdK114E
(A) In contrast to the large, multinucleated profilin-minus cells, the transformants DdW3N and DdK114E showed like the wild-type AX2 normal uni- or binucleated cells (DAPI). Staining for actin showed clearly the predominant localization of actin at the leading edge of pseudopods. The characteristic rim of F-actin accumulation around the edge of profilin-minus cells was not observed in the rescued strains. (B) Subcellular distribution of profilin II in AX2, DdW3N and DdK114E investigated with the aid of a monoclonal antibody specific for profilin II. Uniform cytoplasmic distribution of profilin was observed in the transformants, similar to that of AX2. Scale bars represent 10 μm.

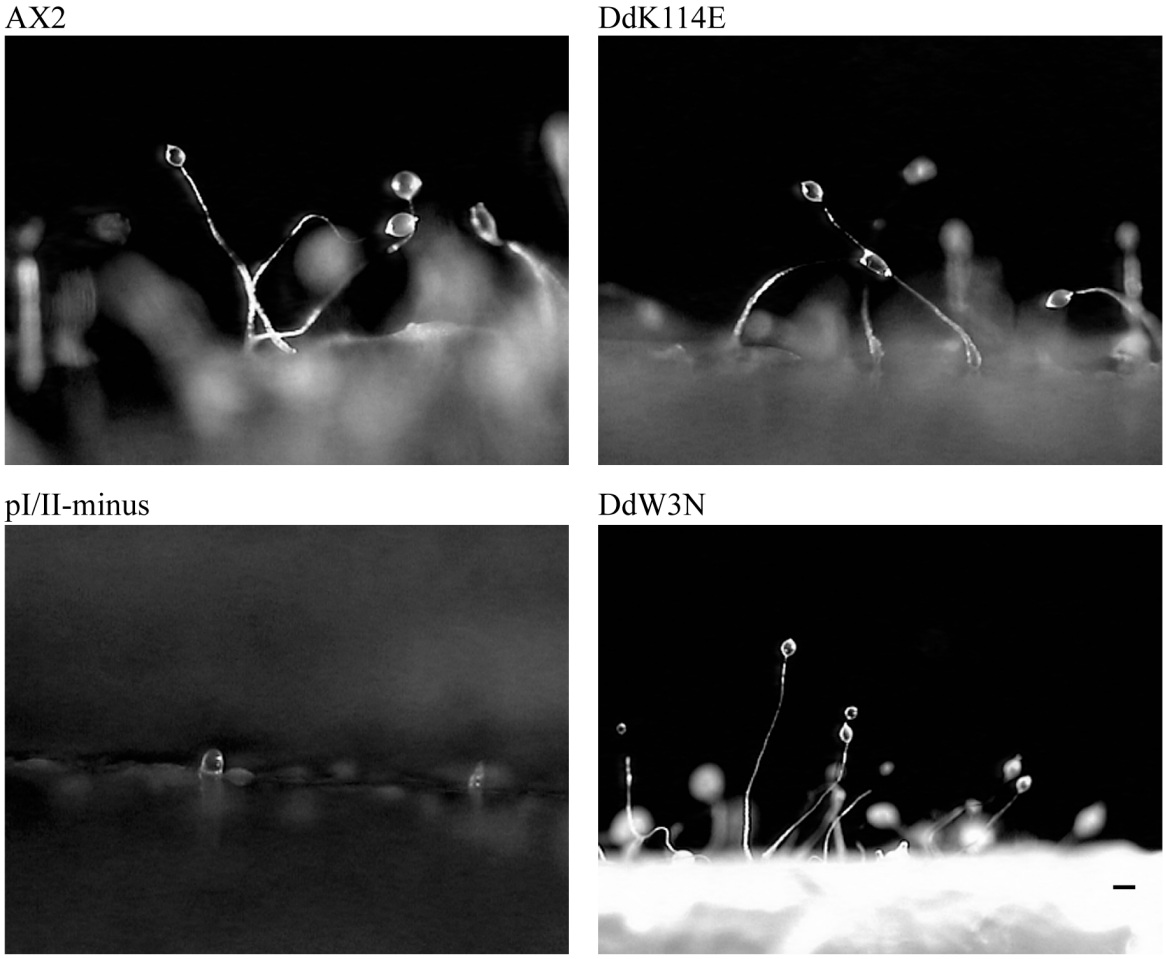

Fig. 9 Developmental stages of AX2, pI/II-minus, DdW3N and DdK114E.
The data showed the restoration of the abilities of the transformants DdW3N and DdK114E to form fruiting bodies similar to that of the wild-type AX2. Without profilins, as seen in the pI/II-minus cells, development of fruiting bodies is inhibited and only finger-like protrusions were observed. Scale bar represents 100 µm.

3.1.6 Profilin localization at phagocytic cups

Uptake of particles during phagocytosis requires a finely tuned programme of protein recruitment to phagocytic cups. The question of whether fully functional actin or poly-(L)-proline binding sites are necessary for the involvement of profilin in phagocytic cup formation is being addressed here. AX2, DdW3N and DdK114E cells were mixed with equivalent amounts of yeasts, fixed, and then subjected to conventional immunostaining using an antibody specific for profilin II. In all three cell types, prominent profilin staining was observed at the rims of developing phagocytic cups in close proximity to yeast particles (Fig. 10). These data indicate that the point-mutated profilins are recruited as efficiently as the wild-type profilin in the formation of phagocytic cups, even though actin-binding is strongly reduced in K114E and poly-(L)-proline binding is essentially absent in W3N.

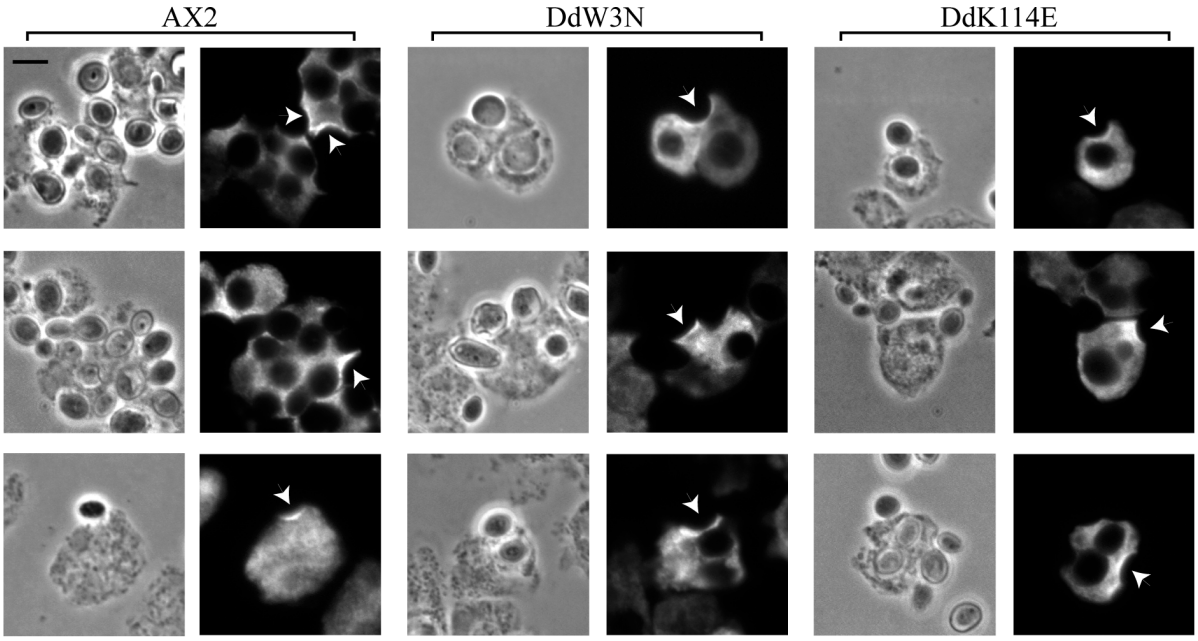

Fig. 10 Comparative studies of profilin localization during phagocytosis of yeast particles by AX2, DdW3N and DdK114E
In all three strains, profilin was accumulated at the edges of phagocytic cups (arrowheads), indicating that the point mutations have no effects on the distribution of profilin in the phagocytic cups in the course of yeast phagocytosis. Scale bar represents 5 μm.

3.2 Analyses of profilin in *D. discoideum* via GFP fusion

3.2.1 Generation of profilin-GFP vector construct and *Dictyostelium* transformants

In order to have a clearer understanding of its *in vivo* role, profilin II from *Dictyostelium* was fused to the N-terminus of a blue-shifted variant of GFP (excitation maximum at 433 nm and emission maximum at 475 nm; Heim and Tsien, 1996) separated by a linker sequence of 100 amino acid (aa) residues. Previous experiments (unpublished observations) have determined the necessity of a long linker sequence between profilin and the N-terminus of GFP for fully functional activities of the fusion protein as compared to the native profilin, in terms of the abilities to bind poly-(L)-proline and to rescue the developmental defects of the profilin null cells (Haugwitz *et al*., 1994). Past efforts made in the fusion of profilin and GFP via a 10 aa- (SGSAEFKKLK) and a 14 aa- (VAGSSGSAEFKKLK) linkers have resulted in fusion proteins which were unable to interact with poly-(L)-proline and transformants have lost their abilities to develop into fruiting bodies (data not shown).

The segment 4 of the six 100 aa-residue repetitive segments of the rod domain of the 120 kDa gelation factor (ABP-120) from *D. discoideum* was used as the linker between profilin and

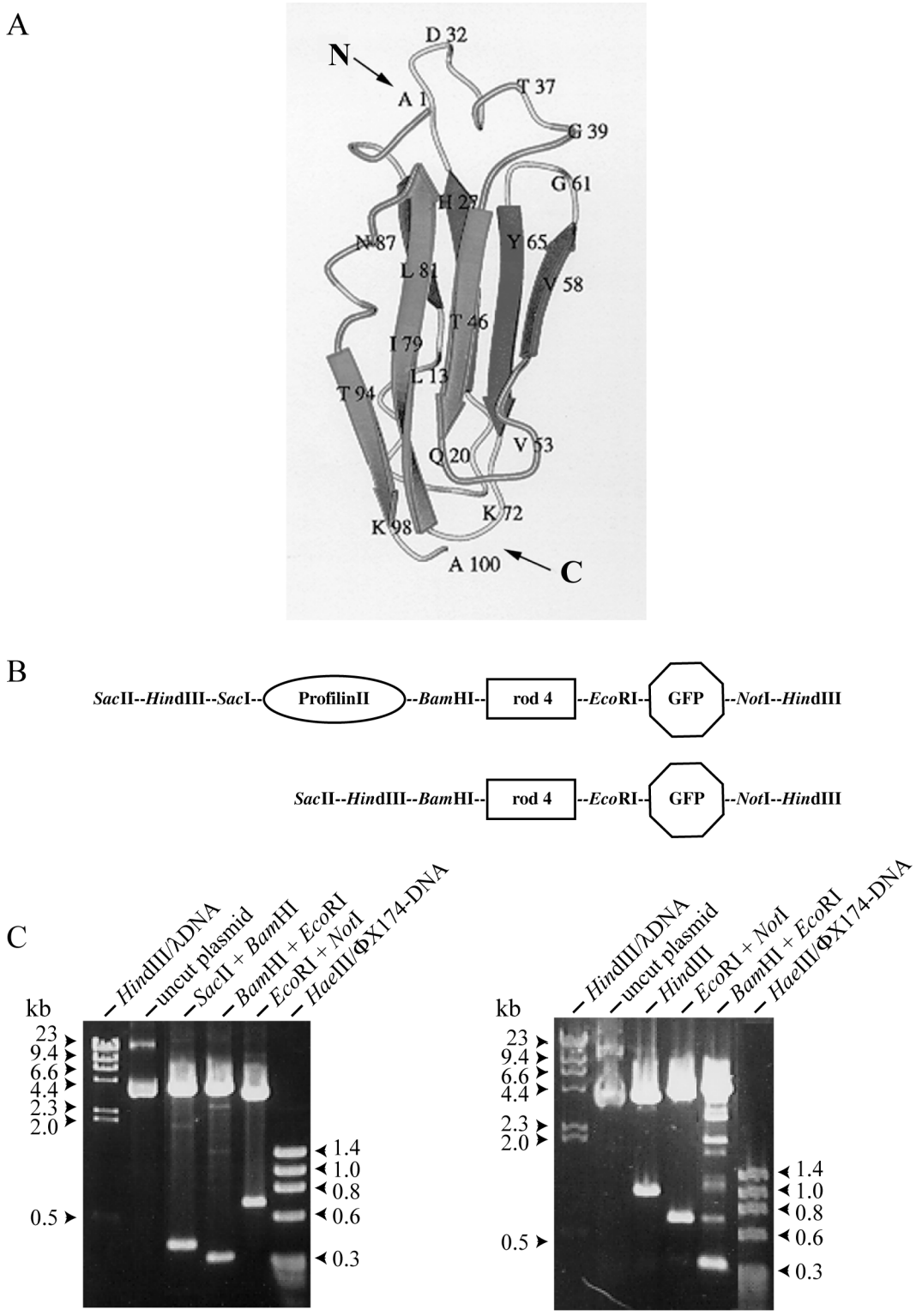

Fig. 11 Profilin II-GFP construct

(A) Ribbon drawing of rod4 (Fucini *et al*., 1997), the 100 aa-residue segment 4 of the rod domain of *D. discoideum* ABP-120, which was used as the linker between profilin II and GFP.

(B) Schematic diagram of the profilin-GFP construct and as a control, only the rod4 linker fused to the N-terminus of GFP. (C) Restriction analyses showing distinct inserts of the expected sizes of 0.4 kb for profilin II (*Sac*II + *Bam*HI), 0.3 kb for rod4 (*Bam*HI + *Eco*RI) and 0.7 kb for GFP (*Eco*RI + *Not*I) for the profilin II-rod4-GFP construct (left panel). For the control rod4-GFP construct (right panel), restriction digests showed DNA inserts of the expected sizes of 1.0 kb for the complete rod4-GFP (*Hin*dIII), 0.7 kb for GFP (*Eco*RI + *Not*I) and 0.3 kb for rod4 (*Bam*HI + *Eco*RI).

GFP. Due to its availability and its recently known 3-D structure (Fucini *et al*., 1997), consisting of seven ß-sheets arranged in an immunoglobulin-like (Ig) fold with the N- and C-terminals at the opposite end of each other, the rod4 was selected as a linker (Fig. 11A). The profilin II-rod4-GFP was constructed as described in Materials and Methods (section 2.4.17). As a control, a rod4-GFP construct with only the linker fused to the GFP was made as well. Both fusion constructs are depicted in a schematic diagram (Fig. 11B). In restriction analyses, DNA bands of expected sizes for profilin II (~0.4 kb), rod4 (0.3 kb) and GFP (~0.7 kb) were obtained (Fig. 11C). The two fusion constructs were individually introduced into profilin deficient *D. discoideum* cells (2.4.14) and transformants exhibiting green fluorescence were cloned (2.4.15) and cultivated in HL-5 medium supplemented with 5 µg/ml blasticidin.

3.2.2 Western analysis of the GFP fusion proteins

Immunoblotting performed on total cell homogenates of the *Dictyostelium* transformants using monoclonal antibodies specific for either profilin II (174-336-8) or GFP (264-236-2) confirmed the expected size of the profilin II-rod4-GFP fusion protein of about 55 kDa (~15 kDa for profilin II, ~12 kDa for rod4 linker and 28 kDa for GFP) (Fig. 12A & 12B). As for the cells transformed with rod4-GFP, a band of the predicted size of about 40 kDa was obtained with the aid of an antibody specific for GFP (Fig. 12B). The wild-type AX2 and the profilin null cells (pI/II-minus) were used as positive and negative controls for profilin expression respectively. Equal amounts of cell homogenates were subjected to SDS-PAGE (Fig. 12C).

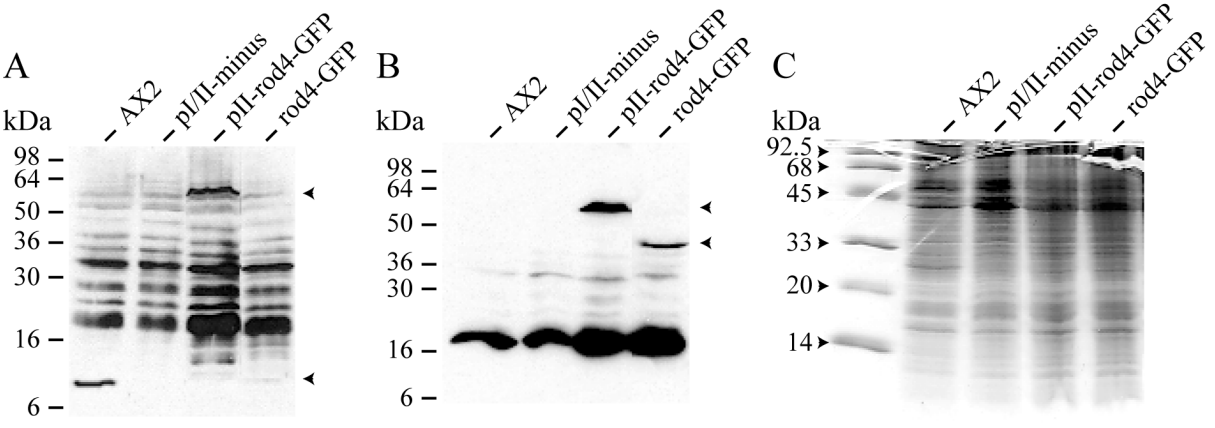

Fig. 12 Western analysis of the profilin II-GFP fusion protein
With the aid of monoclonal antibodies specific for either (A) profilin II (174-336-8) or (B) GFP (264-236-2), a band of the appropriate size of about 55 kDa for the profilin II-rod4-GFP fusion protein was observed (see arrowheads). As for the control rod4-GFP fusion protein, a band of the expected size of about 40 kDa was obtained (B; see arrowhead) with an anti-GFP antibody (1:20 dilution in PBG). AX2 and pI/II-minus cells were used as positive and negative controls for profilin expression respectively, whereby a band of around 15 kDa was detected for the native profilin II in AX2 (A; see arrowhead). (C) Equivalent amounts of total cell homogenates were electrophoresed on a SDS-polyacrylamide gel (15% acrylamide).

3.2.3 Development of the profilin-GFP *Dictyostelium* transformant

Contrary to the profilin null cells which are unable to develop fruiting bodies, this aberrant phenotype was partially rescued in the profilin-GFP transformed cells due to the expression of the fusion protein. These transformants were capable of generating fruiting bodies which almost resembled those of the wild-type cells (Fig. 13). As for the rod4-GFP transformed cells, they still were not able to rescue the developmental defect of the profilin null cells, and only "finger" stage of development was observed (data not shown). Henceforth, only the *Dictyostelium* cells transformed with profilin-GFP were further analyzed.

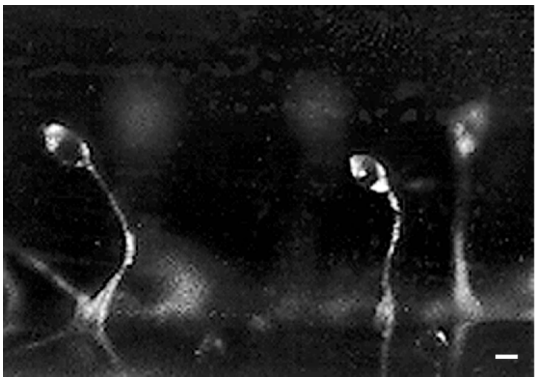

Fig. 13 Development of the profilin II-GFP transformed *D. discoideum* cells
In contrast to the profilin null cells which are unable to generate fruiting bodies (see Fig. 9), cells transformed with profilin-GFP restored their abilities to form fruiting bodies which partially resembled those of the wild-type AX2 (see Fig. 9). Scale bar represents 100 µm.

3.2.4 Growth rate of profilin-GFP cells

In contrast to the pI/II-minus cells, profilin null cells transformed with profilin-GFP could be cultivated in shaking suspensions (Fig. 14).

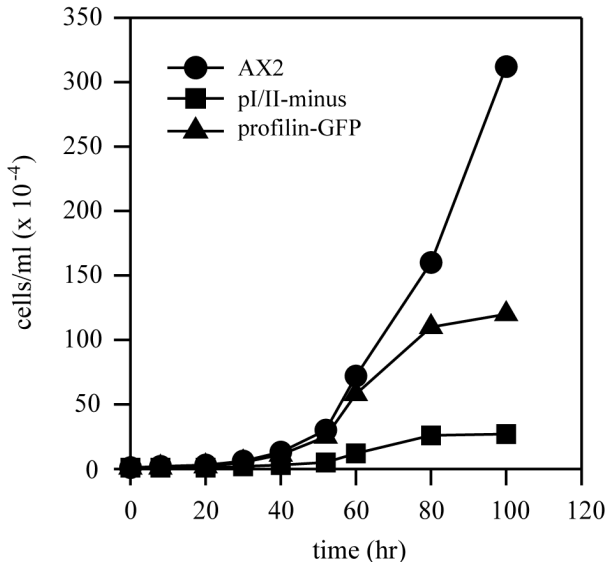

Fig. 14 Growth curve of the profilin-GFP *D. discoideum* transformants.
Unlike the profilin null cells (pI/II-minus), the profilin-GFP transformants could be cultivated in shaking suspensions whereby their growth rates resembled that of the wild-type AX2 within the first two days. Thereafter, a gradual decrease in the growth rate of the transformants was observed, until a plateau was reached by the fourth day, whereby the growth rate of the transformants now resembled that of the pI/II-minus cells.

As compared to the wild-type AX2 cells, the profilin-GFP transformants grew initially at almost the same rate during the first 2 days, however, their growth slowed down gradually until a plateau was reached by the fourth day. Thus these transformants were able to grow like the wild-type cells only for a short period within the first 2 days, after which their growth rates approached that of the profilin null cells.

3.2.5 Interaction between poly-(L)-proline and profilin-GFP

The affinity of the profilin-GFP fusion protein for poly-(L)-proline stretches was examined by sedimentation with poly-(L)-proline coupled agarose beads as described in Materials and Methods (section 2.5.11). As shown in Figure 15, the profilin-GFP fusion protein has lost its ability to bind to poly-(L)-proline since immunoblot analysis on total cell homogenates using a monoclonal antibody specific for profilin II (174-336-8) detected an appropriately sized band of the fusion protein of about 55 kDa only in the supernatant fraction (Fig. 15A). AX2 was used as a positive control whereby the native profilin was able to bind poly-(L)-proline beads and a band of about 15 kDa was detected in the pellet fraction as observed in both immunoblot (Fig. 15A) and SDS-polyacrylamide gel (Fig. 15B).

However, the poly-(L)-proline binding ability of the fusion protein appeared to be restored to a small extent after passage of the total cellular proteins through an anion-exchange monoQ column and protein fractions eluted with a linear NaCl gradient. Two eluted fractions containing the fusion protein, namely fractions #28 and #31, were allowed to incubate with poly-(L)-proline beads for some hours and then sedimented. Western analyses with the aid of monoclonal antibodies specific for either profilin II (Fig. 15C) or GFP (Fig. 15D) showed the presence of minute quantities of the fusion protein in the pellet fractions, though much larger amounts of profilin-GFP were still found in the supernatants.

3.2.6 Interaction between profilin-GFP and actin

Generally, the interaction between profilin and actin could be studied by a highly sensitive fluorescence spectroscopic method using pyrene-labelled G-actin (Kouyama and Mihashi, 1981). This approach will require at least a 1:1 ratio of wild-type profilin to actin or about 3 μM of proteins. However, a difficulty to obtain a large amount of the profilin-GFP transformed cells was encountered as these cells could only grow within a short timespan (see 3.2.4, Fig. 14), thus it has not been possible to obtain sufficient amounts of the fusion protein for kinetic analyses.

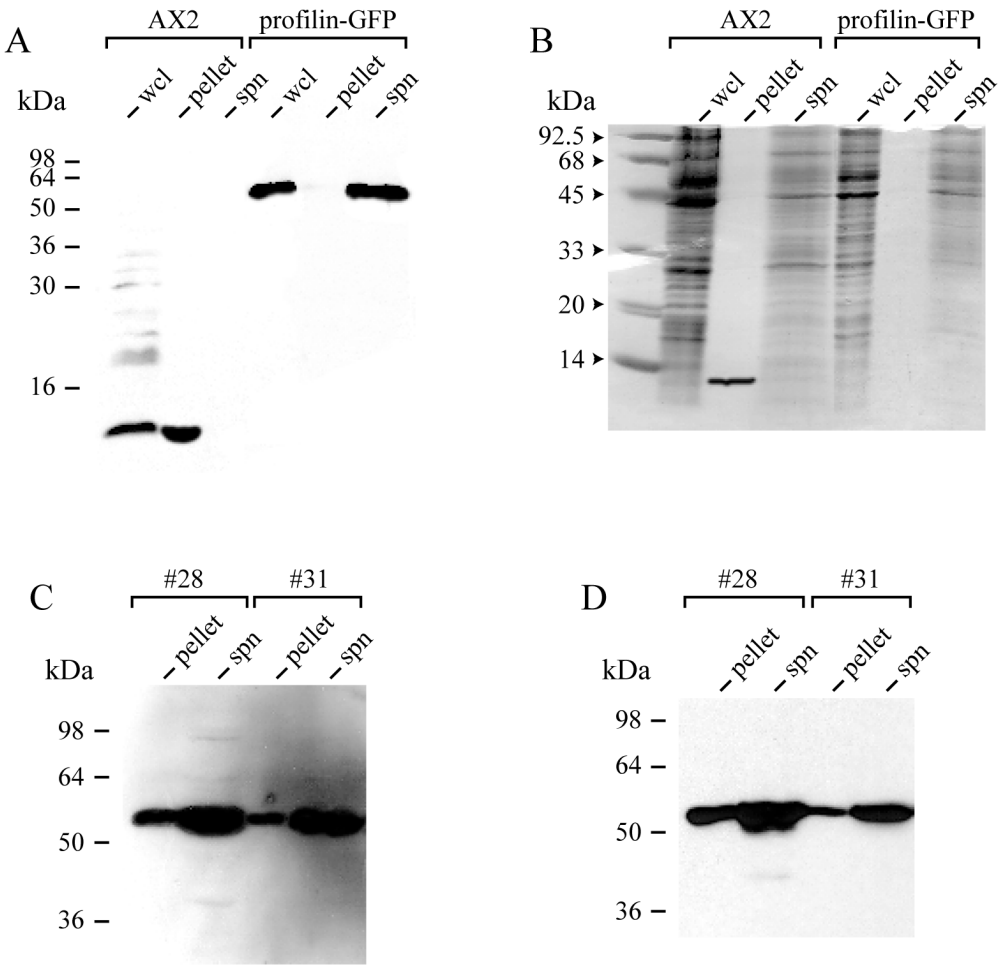

Fig. 15 Affinity of the profilin-GFP fusion protein for poly-(L)-proline
(A) Immunoblot analysis using an anti-profilin II monoclonal antibody (174-336-8) on whole cell lysates (wcl) after sedimentation with poly-(L)-proline agarose beads revealed a 55 kDa band of the fusion protein only in the supernatant (spn) fraction, suggesting that profilin-GFP was unable to bind poly-(L)-proline. AX2 was used as a positive control for poly-(L)-proline binding whereby a band of about 15 kDa for profilin II was detected in the pellet fraction. (B) SDS-PAGE was performed on whole cell lysates (wcl), pellet and supernatant (spn) fractions after sedimentation with poly-(L)-proline beads from AX2 and the profilin-GFP *Dictyostelium* transformants. In the AX2 positive control, a band of about 15 kDa for profilin II was obtained in the pellet fraction of the Coomassie Blue-stained gel. The poly-(L)-proline binding ability of profilin-GFP was also assayed after semi-purification via a monoQ anion-exchange column and proteins eluted with a linear NaCl gradient (0-400 mM). 2 eluted fractions namely, #28 and #31 were incubated with poly-(L)-proline beads, sedimented and analyzed via Western assay. Using monoclonal antibodies specific for profilin II (C) and GFP (D), most of the profilin-GFP fusion protein was present in the supernatants, however small amounts of the fusion protein were also found in the pellets. Thus, partial purification of the fusion protein appears to improve its poly-(L)-proline binding ability.

Profilin has been known to form a tight profilin-actin complex or profilactin *in vivo* which is involved in the elongation of actin filaments at the barbed ends only (Tilney *et al*., 1983; Pollard and Cooper, 1984; Kaiser *et al*., 1986). This property of profilin being able to associate with actin as profilactin complex is the basis on which the interaction between actin and profilin-GFP was being investigated as described in Materials and Methods (section 2.5.13). Normally, the profilactin complex would be bound by an anion exchange column and could be eluted with a 0-400 mM linear NaCl gradient between 10-14 mS. From a small quantity of lysed cells, the total cellular proteins were first semi-purified through an anion-exchange monoQ column and subsequently, two of the eluted fractions, one containing only profilin-GFP and the second consisting of both the fusion protein and actin, were separately fractionated by size via gel filtration chromatography using the FPLC system and a highly sensitive SMART system. Their elution profiles, detected by Western analysis with an antibody specific for the fusion protein, were then compared and if the fusion protein is able to bind to actin, this larger complex will be eluted earlier.

Like the wild-type *D. discoideum* profilins (Haugwitz *et al*., 1991), the profilin-GFP fusion protein was detected in the soluble fraction of total cell homogenate by immunoblot analysis (Fig. 16A). Following anion exchange chromatography, Western analyses were carried out with monoclonal antibodies specific for *Dictyostelium* actin (Simpson *et al*., 1984), GFP and profilin II (Fig. 16B). Actin, a 42 kDa protein, was detected mainly in fractions #27 and #28. With both anti-profilin and anti-GFP antibodies, the 55 kDa profilin-GFP fusion protein was found in the eluted fractions #27-31. The fractions #28 containing both actin and the fusion protein (A+FP) and #31 consisting of only the fusion protein (FP) were then separately subjected to gel filtration chromatography. After FPLC and with the aid of a GFP-specific antibody, the bulk of the fusion protein was found to be eluted between fractions #26-28 for both A+FP and FP fractions. However, the fusion protein could already be detected in much earlier fractions starting from #21 for the A+FP fraction only (Fig. 16C). Similarly, following gel filtration with the SMART system, immunoblot analyses using an anti-GFP antibody showed that the fusion protein was eluted mainly between fractions #20-23 for both the A+FP and FP fractions and a shift to an earlier elution of the fusion protein beginning at fraction #17 was observed for the A+FP fraction only (Fig. 16D). Data from both the FPLC and the SMART systems consistently showed earlier elutions of the fusion protein when both actin and the fusion protein were present together, strongly suggesting the affinity of profilin-GFP for actin thus forming larger complexes which could be eluted earlier by size sieving.

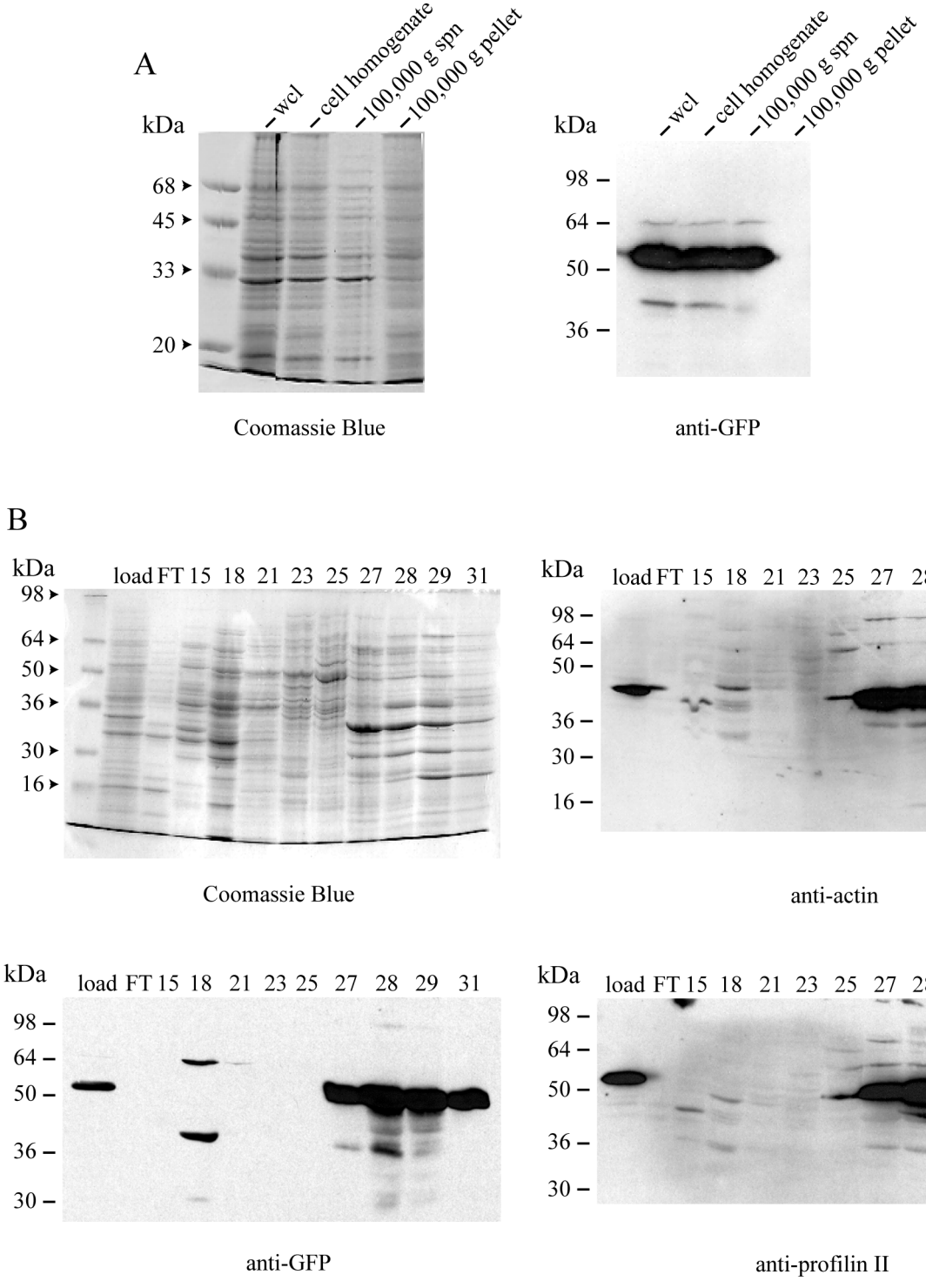

Fig. 16 (A & B) Immunoblot analyses of profilin-GFP before and after anion-exchange chromatography
(A) Western analysis of the profilin-GFP *D. discoideum* transformants using an anti-GFP antibody revealed distinctly a 55 kDa band of the fusion protein in the whole cell lysate (wcl), the cell homogenate after lysis of cells with nuclepore filters, and in the soluble 100,000 g supernatant (spn) fraction. (B) Anion-exchange chromatography was performed on the soluble cellular fraction using a monoQ column and proteins eluted with a linear NaCl gradient (0-400 mM). An anti-actin antibody detected a band of about 42 kDa in the eluted fractions #27 and #28. Immunoblot analyses using antibodies specific for either profilin II or GFP showed a predominant band of about 55 kDa for the fusion protein in the fractions #27-31. The fractions #28 which contained both actin and the fusion protein and #31 containing only the fusion protein were later subjected to gel filtration chromatography.

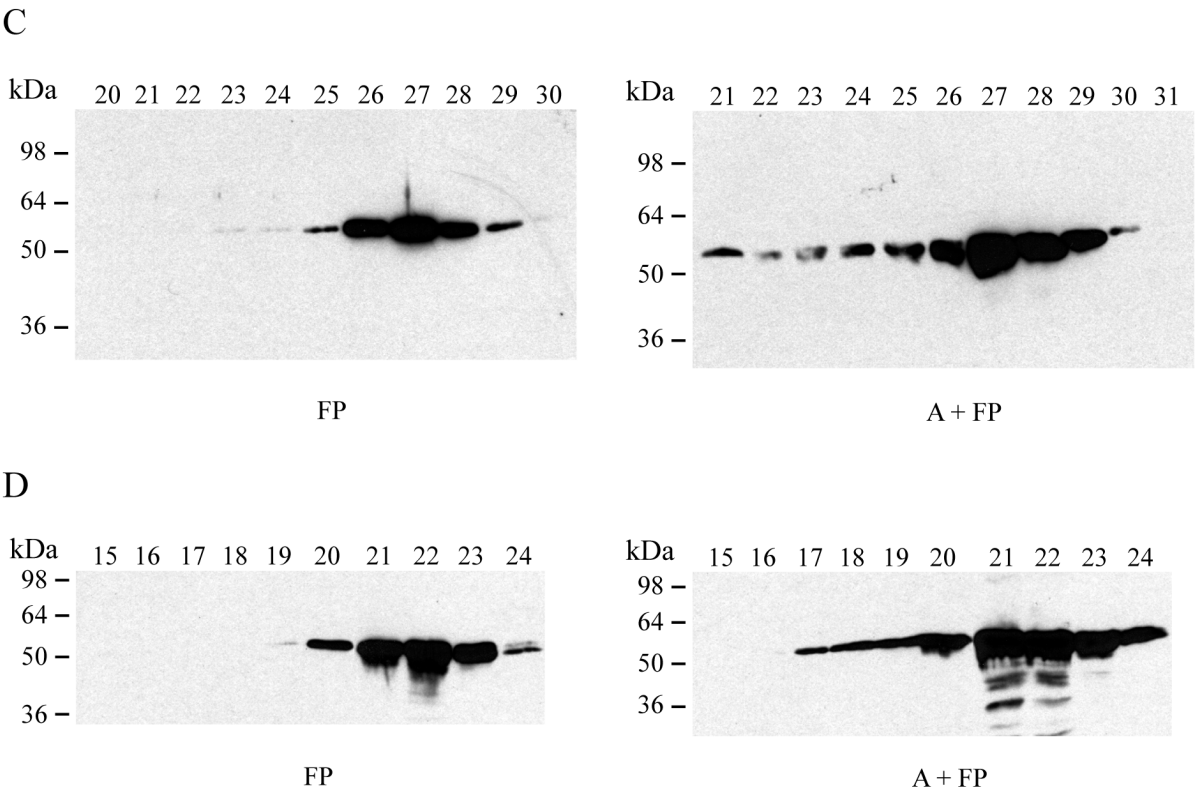

Fig. 16 (C & D) Affinity of profilin-GFP for actin
Two monoQ fractions namely, #28 containing both actin and the profilin-GFP fusion protein (A + FP) and #31 consisting of only the fusion protein (FP) were separately subjected to gel filtration chromatography using both the FPLC (C) and the SMART (D) systems. (C) After FPLC, immunoblot analysis with an anti-GFP antibody detected a 55 kDa band of the fusion protein predominantly in the eluted fractions #25-29 for the FP fraction, and in #21-29 for the A + FP fraction. (D) Western analysis of the eluted fractions with an anti-GFP antibody after gel filtration chromatography using the SMART system, showed the presence of most of the fusion protein in fractions #20-24 for the FP fraction, and in #17-24 for the A + FP fraction. Thus gel filtration chromatography with both the FPLC and SMART systems showed an earlier elution of the profilin-GFP fusion protein in the presence of actin, strongly suggesting interaction between the fusion protein and actin resulting in the formation of larger complexes which could be eluted earlier.

3.2.7 Cell morphology and subcellular distribution of profilin-GFP

As compared to the profilin null cells, pI/II-minus (Haugwitz *et al*., 1994), which are multinucleate, very much bigger than wild-type cells and have accumulations of broad rims of F-actin around their edges (see Fig. 8A), the profilin deficient cells transformed with the profilin-GFP construct were observed to resemble the wild-type AX2 cells. After cell fixation with 3% paraformaldehyde and labelling of the nuclei and F-actin with DAPI and TRITC-phalloidin respectively, these profilin-GFP transformed cells were embedded directly for fluorescence microscopy. The transformants showed normal cell morphology with 1-2 nuclei per cell and the broad accumulations of F-actin were no longer present, instead F-actin staining was found only at the leading edges of pseudopods of these cells (Fig. 17A). Similar to the profilin localization in AX2 (see Fig. 8B), fluorescence from the profilin-GFP fusion protein was observed to be distributed evenly throughout the cytoplasm (Fig. 17A).

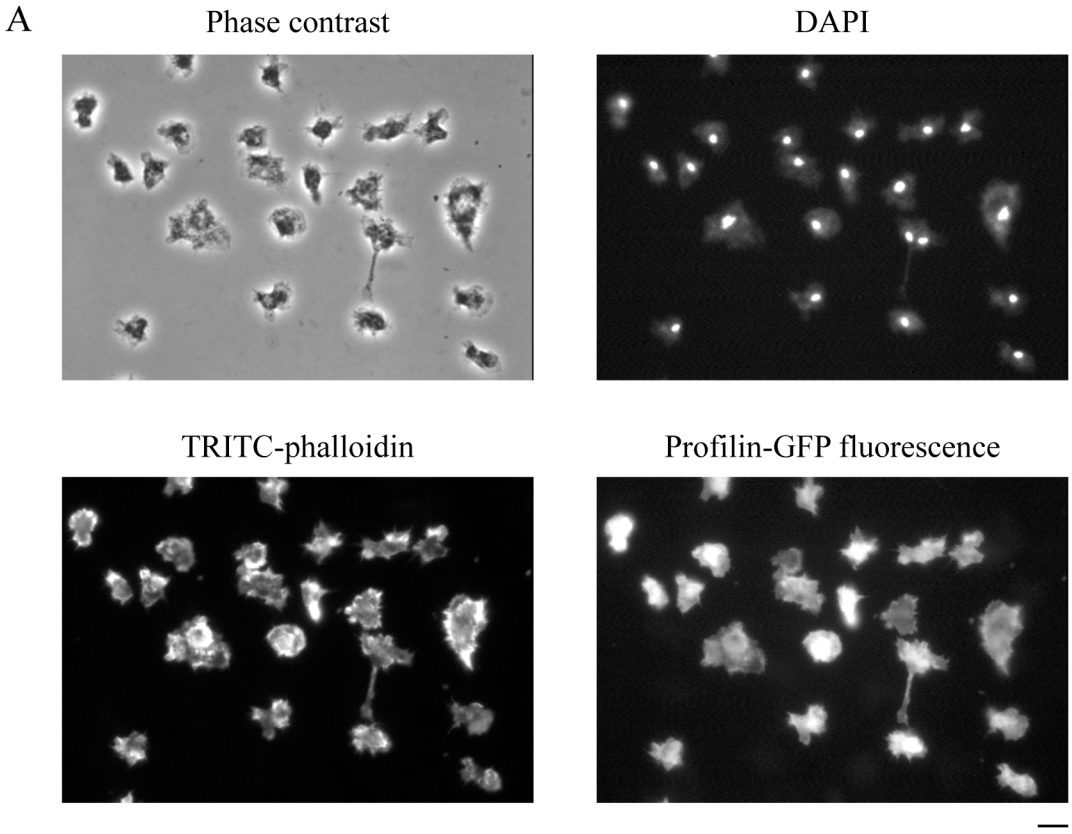

Fig. 17 Subcellular distribution of profilin II-GFP
(A) In the profilin null cells transformed with profilin-GFP, profilin was observed to have an overall cytoplasmic localization. Transformants exhibit normal number of 1-2 nuclei per cell as shown by the DAPI staining. F-actin labelling with TRITC-phalloidin showed concentration of actin at the leading edges of pseudopodia, similar to that of the wild-type AX2 cells.
(B) During phagocytosis of yeast particles, profilin-GFP was found to accumulate at the rims of phagocytic cups. Scale bars represent 10 μm.

The localization of profilin-GFP during phagocytosis of yeast particles was also analyzed to determine if the fusion protein behaved similarly as the wild-type profilin. Profilin-GFP transformed cells were mixed with an equal amount of Baker's yeasts, methanol-fixed and then subjected to fluorescence microscopy. As compared to AX2 (see Fig. 10), the profilin-GFP fusion protein was also observed at the edges of developing phagocytic cups in close contact with yeast particles (Fig. 17B). This result suggests that the profilin-GFP fusion protein is recruited as efficiently as the wild-type profilin in phagocytic cups and could thus be used further in *in vivo* studies of actin-based cellular processes.

3.2.8 *In vivo* distribution of the profilin-GFP fusion protein

The confocal microscopy studies of the *in vivo* dynamics of profilin in *D. discoideum* cells transformed with profilin-GFP were performed in collaboration with Timo Zimmermann (Zoological Institute, LMU, Munich). The specificity of the localization of the fusion protein has been confirmed by ratio measurements whereby the fluorescent signal of profilin-GFP was ratioed over an uniformly distributed cytoplasmic marker as described (Yumura and Fukui, 1998). Profilin was found to be associated with highly active regions of the cells in actin-based cellular processes. As shown in Fig. 18, the fusion protein was predominantly localized at the cell cortex (A) and additionally, in the process of macropinocytosis, the fusion protein was observed to accumulate at the actin-rich macropinocytotic crowns (B).

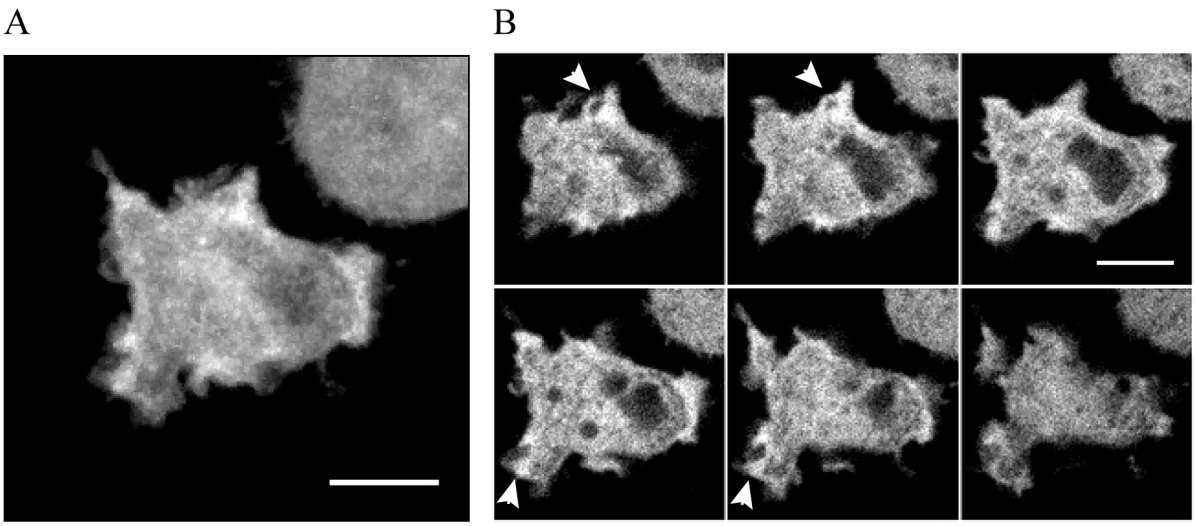

Fig. 18 Localization of profilin-GFP to highly dynamic regions of cells
(A) Confocal study of a single section of a *D. discoideum* cell (0.6 µm thickness) transformed with profilin II-GFP showed the distinct accumulation of profilin at the highly active regions of the cell cortex. (B) Selected sections of the same cell showed again the cortical distribution of the fusion protein and in addition, during macropinocytosis, the fusion protein was clearly detected at the macropinocytotic crowns (arrowheads). Scale bars represent 5 µm. Pictures are kindly provided by Timo Zimmermann (Zoological Institute, LMU, Munich).

In the aggregation stage, the fusion protein was detected transiently at the leading edges of elongated cells moving in an aggregation stream (Fig. 19A). During pseudopodial extension, there is a transient distribution of profilin-GFP at the cell front, suggesting that profilin might be involved in protrusion of pseudopodia (Fig. 19B).

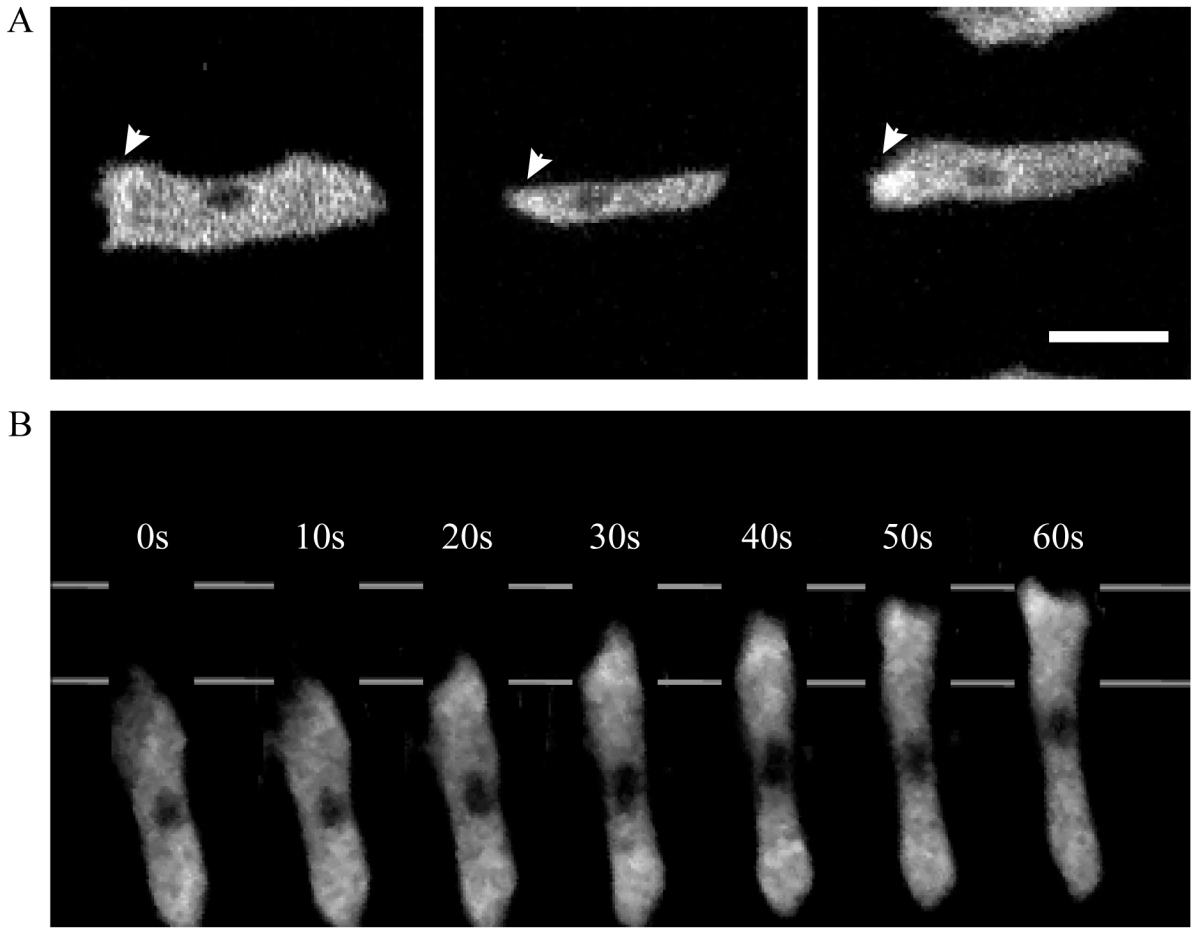

Fig. 19 Distribution of profilin II-GFP in locomoting cells
(A) Confocal images (courtesy of Timo Zimmermann) of a single section of three individual cells in an aggregation stream which have been transformed with profilin II-GFP revealed transient localization of the fusion protein at the cell fronts (arrowheads). (B) A time sequence of a cell showing transient profilin distribution at the cell front during pseudopodial extension. Scale bar represents 10 μm.

3.3 Studies of severin in *D. discoideum* via GFP fusion

3.3.1 Generation of severin-GFP *Dictyostelium* transformants

Severin, the major Ca^{2+}-dependent F-actin fragmenting and capping protein of *D. discoideum*, has been well characterized *in vitro* (Eichinger *et al*., 1991; Eichinger and Schleicher, 1992). A novel approach has been used here to examine its *in vivo* redistribution and roles by fusion with a red-shifted GFP mutant and then transforming *Dictyostelium* cells which were subsequently analyzed at high spatial and temporal resolutions using confocal microscopy.

Dictyostelium severin was fused via a 10 aa linker to the N-terminal of S65T GFP according to Materials and Methods (section 2.4.16). The flexible linker sequence consists of mainly small and basic amino acid residues and the severin-GFP construct is shown in a schematic diagram (Fig. 20). The severin-GFP recombinant plasmid was then transformed into AX2 and HG1132 severin null (André *et al*., 1989) *D. discoideum* cells as described (section 2.4.14). The transformants were cloned (section 2.4.15) and could be cultivated in shaking suspensions in AX medium supplemented with 10 µg/ml geneticin. They were designated as AX2-T for the severin-GFP transformed wild-type cells, and HG1132-T for the severin null cells transformed with the fusion construct.

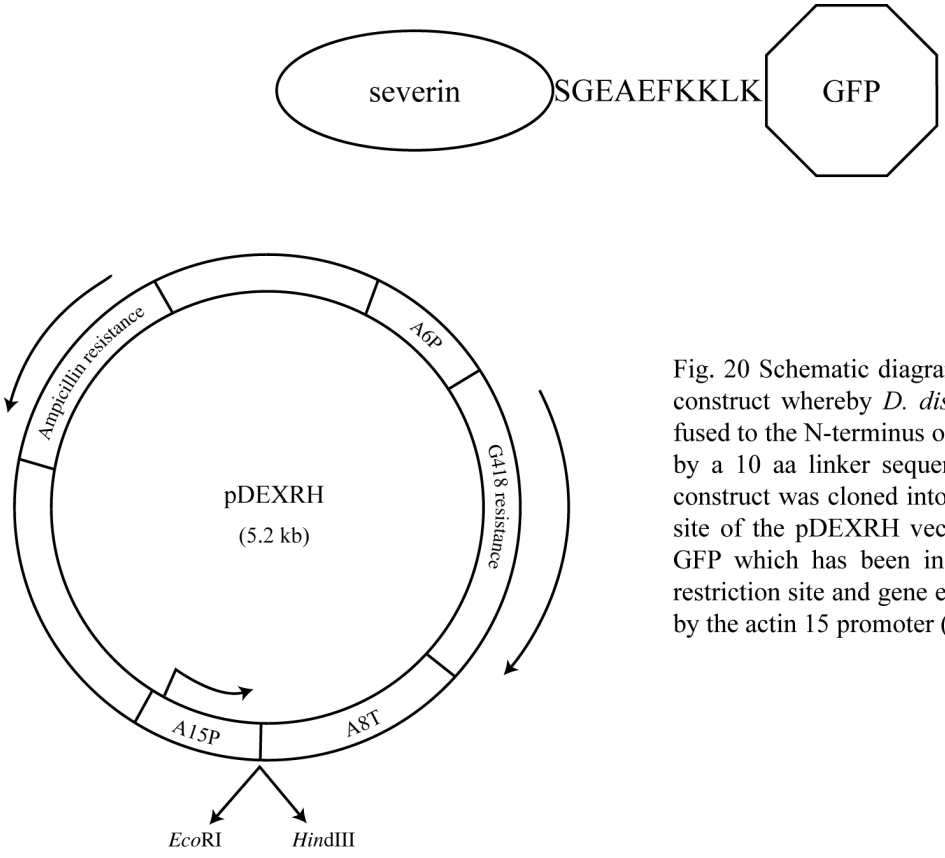

Fig. 20 Schematic diagram of the severin-GFP construct whereby *D. discoideum* severin was fused to the N-terminus of S65T GFP separated by a 10 aa linker sequence (top). The fusion construct was cloned into the *Eco*RI restriction site of the pDEXRH vector in frame with the GFP which has been inserted in the *Hin*dIII restriction site and gene expression is regulated by the actin 15 promoter (A15P) (left).

3.3.2 Immunoblot analysis of the severin-GFP fusion protein

Equal amounts of total cell homogenates were subjected to SDS-PAGE (Fig. 21A) after which immunoblot analysis was performed with a monoclonal antibody targeted at the N-terminal of severin (102-425-1). AX2 and the HG1132 severin null cells were used as positive and negative controls for severin expression respectively. For both the AX2-T and HG1132-T transformants, a prominent band of the expected size of about 70 kDa for the severin-GFP fusion protein was observed in each case (Fig. 21B). For AX2-T, an additional band of 40 kDa corresponding to the native severin protein was also detected. In comparison, the native severin and the severin-GFP fusion proteins appeared to be present in equivalent quantities in the AX2-T *Dictyostelium* transformant (Fig. 21B).

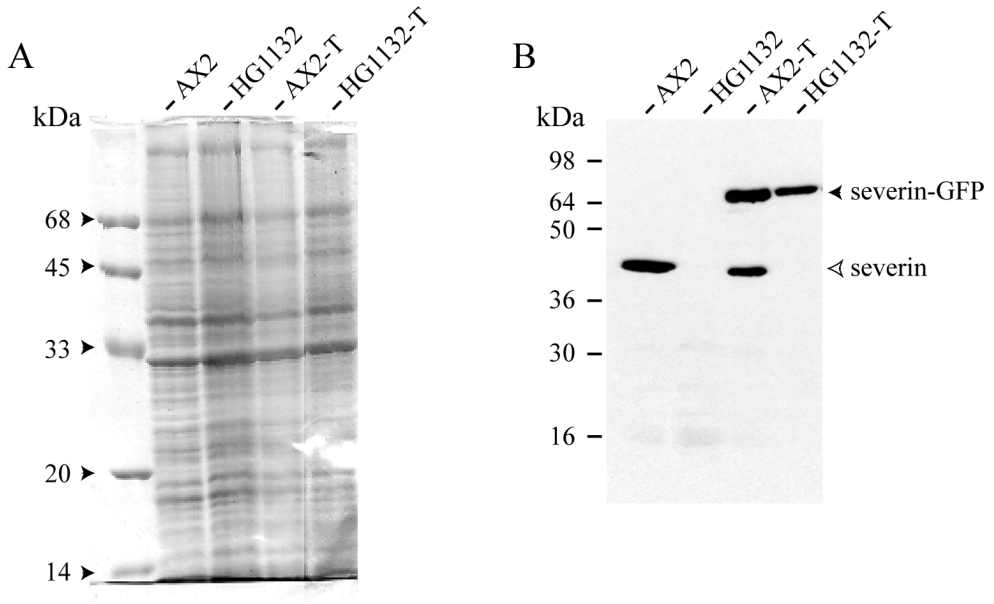

Fig. 21 Immunoblot analysis of the severin-GFP fusion protein
(A) Equal amounts of total cell homogenates were subjected to SDS-PAGE. (B) With the aid of an anti-severin monoclonal antibody (102-425-1), a band of the expected size of 70 kDa for the fusion protein was obtained in both the AX2 wild-type (AX2-T) and the severin null (HG1132-T) *D. discoideum* transformants (see filled arrowhead). In the case of AX2-T, an additional band of about 40 kDa corresponding to the native severin was also observed (see unfilled arrowhead). AX2 and severin null cells (HG1132) were used as positive and negative controls for severin expression respectively.

3.3.3 Partial purification of the severin-GFP fusion protein

The severin-GFP fusion protein was partially purified from the HG1132-T *Dictyostelium* transformant lacking the native severin as described in Materials and Methods (section 2.5.8). Soluble extract from 10 l of cells was first subjected to an anion-exchange column whereby the fusion protein, as analyzed by immunoblotting, did not bind to the resin (Fig. 22A). The flow-through was then passed over a phosphocellulose cation-exchange column and under the

conditions using MEDABP (pH 6.5) as running buffer (see Materials and Methods, section 2.5.8), the fusion protein was again found in the flow-through (Fig. 22A). To reduce the sample volume, ammonium sulphate precipitation was carried out on this flow-through and Western analysis with a severin-specific antibody showed that the fusion protein was precipitated between 50-80% of saturation (Fig. 22B).

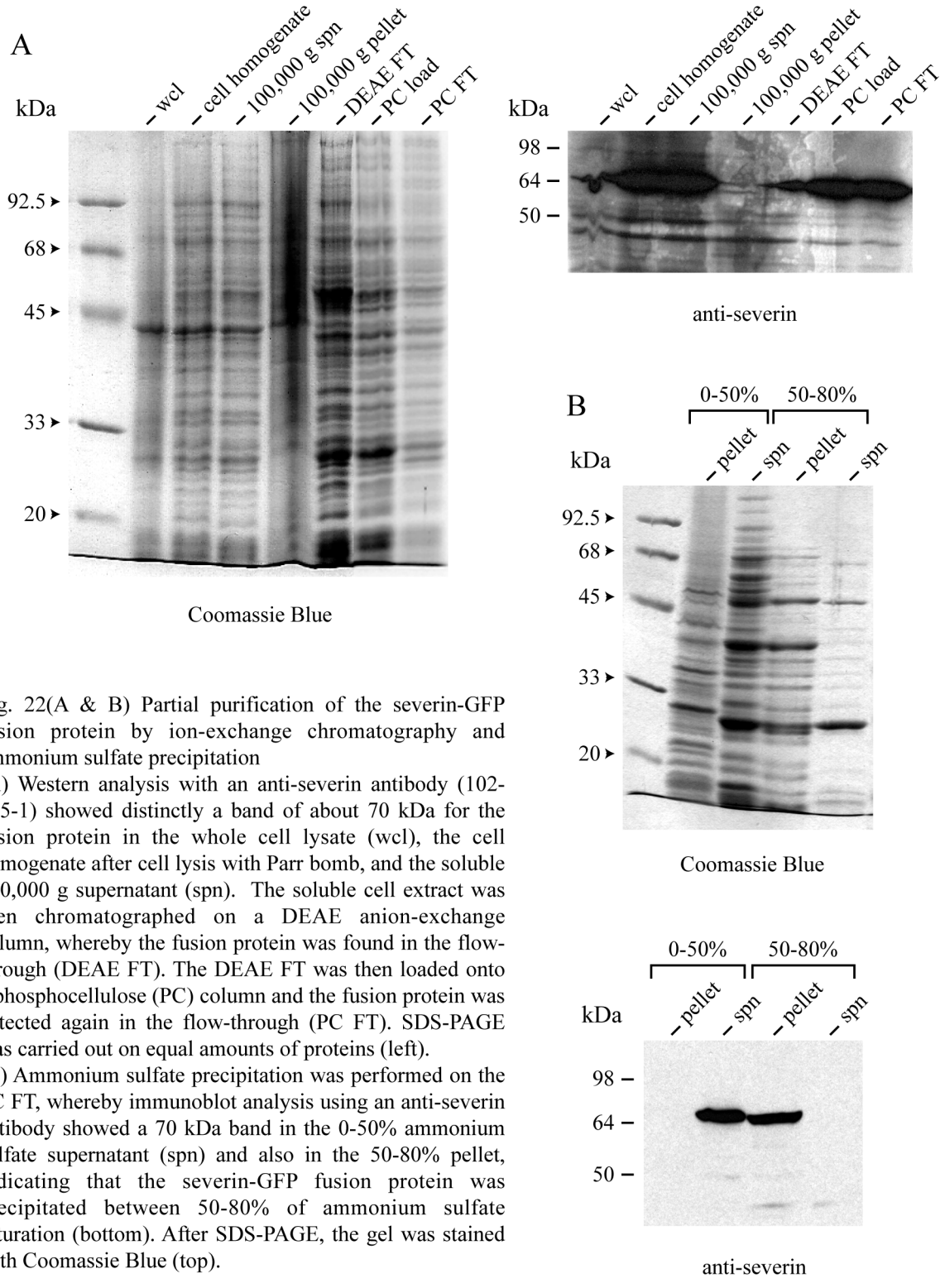

Fig. 22(A & B) Partial purification of the severin-GFP fusion protein by ion-exchange chromatography and ammonium sulfate precipitation

(A) Western analysis with an anti-severin antibody (102-425-1) showed distinctly a band of about 70 kDa for the fusion protein in the whole cell lysate (wcl), the cell homogenate after cell lysis with Parr bomb, and the soluble 100,000 g supernatant (spn). The soluble cell extract was then chromatographed on a DEAE anion-exchange column, whereby the fusion protein was found in the flow-through (DEAE FT). The DEAE FT was then loaded onto a phosphocellulose (PC) column and the fusion protein was detected again in the flow-through (PC FT). SDS-PAGE was carried out on equal amounts of proteins (left).

(B) Ammonium sulfate precipitation was performed on the PC FT, whereby immunoblot analysis using an anti-severin antibody showed a 70 kDa band in the 0-50% ammonium sulfate supernatant (spn) and also in the 50-80% pellet, indicating that the severin-GFP fusion protein was precipitated between 50-80% of ammonium sulfate saturation (bottom). After SDS-PAGE, the gel was stained with Coomassie Blue (top).

After dissolution of the pellet in a small volume of column buffer, the green-colored sample was subjected to gel filtration chromatography and the eluted fractions were subsequently analyzed by immunoblotting to detect fractions containing the fusion protein (Fig. 22C). Finally, these active fractions were pooled together and chromatographed on a hydroxylapatite column whereby the severin-GFP fusion protein was eluted with potassium phosphate. On the Coomassie gel, other proteins were still present, with a possible band of the fusion protein detected at about 70 kDa in fractions #67 and #68. With the aid of a severin-specific antibody, prominent bands of the expected size were observed in fractions #67 and #68 (Fig. 22D). The partially purified fraction #68 was later used for *in vitro* activity assays.

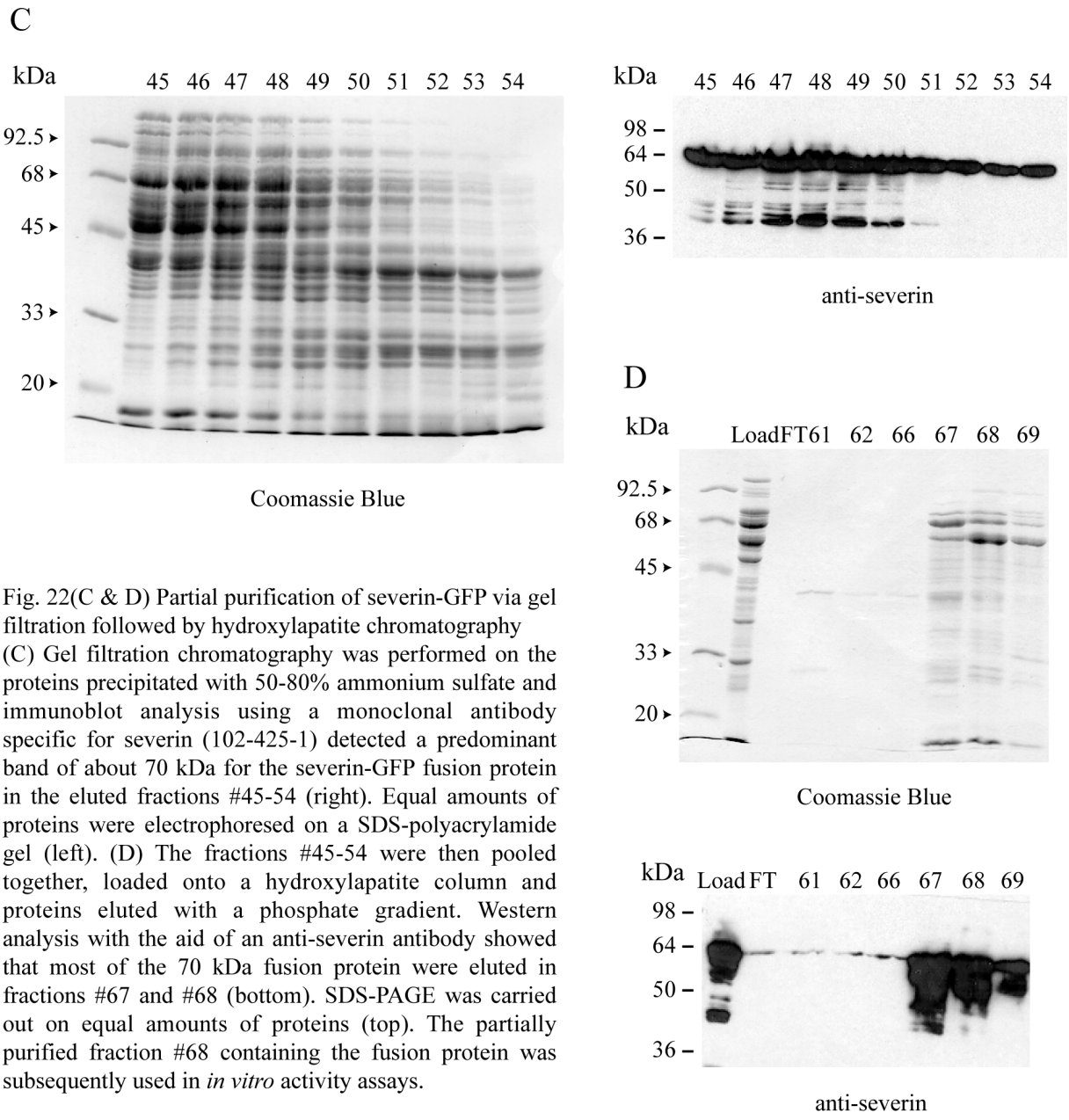

Fig. 22(C & D) Partial purification of severin-GFP via gel filtration followed by hydroxylapatite chromatography
(C) Gel filtration chromatography was performed on the proteins precipitated with 50-80% ammonium sulfate and immunoblot analysis using a monoclonal antibody specific for severin (102-425-1) detected a predominant band of about 70 kDa for the severin-GFP fusion protein in the eluted fractions #45-54 (right). Equal amounts of proteins were electrophoresed on a SDS-polyacrylamide gel (left). (D) The fractions #45-54 were then pooled together, loaded onto a hydroxylapatite column and proteins eluted with a phosphate gradient. Western analysis with the aid of an anti-severin antibody showed that most of the 70 kDa fusion protein were eluted in fractions #67 and #68 (bottom). SDS-PAGE was carried out on equal amounts of proteins (top). The partially purified fraction #68 containing the fusion protein was subsequently used in *in vitro* activity assays.

The purification method for the severin-GFP fusion protein appeared to deviate slightly from that of severin (Yamamoto *et al*., 1982; Schleicher *et al*., 1984). Briefly, *Dictyostelium* severin can be purified by chromatographing the soluble cell extract firstly on an anion-exchange column, followed by a cation-exchange column whereby the severin-containing fractions eluted with a linear salt gradient were finally subjected to hydroxylapatite chromatography and pure severin could be eluted with a linear KCl gradient (0-400 mM KCl). In contrast to severin, the severin-GFP fusion protein did not bind to the cation-exchange resin and thus an extra step to separate the fusion protein by size was performed via gel filtration before chromatographing on a hydroxylapatite column. Another difference is that the fusion protein could only be eluted with a phosphate gradient (0-10 mM KH_2PO_4) in the presence of KCl since it could not be eluted using a linear KCl gradient.

3.3.4 Severing activity of the severin-GFP fusion protein

Two simple, yet elegant approaches have been used to determine the severing activity of the partially purified fusion protein. In the low shear falling-ball viscometry assay (section 2.5.9), severin-GFP was found to sever F-actin or to reduce the viscosity of F-actin gels only in the presence of Ca^{2+} (Fig. 23A). It was calculated that 250 ng/ml of the partially purified fusion protein is fully active. For the fluorescence measurements (section 2.5.10), in the absence of

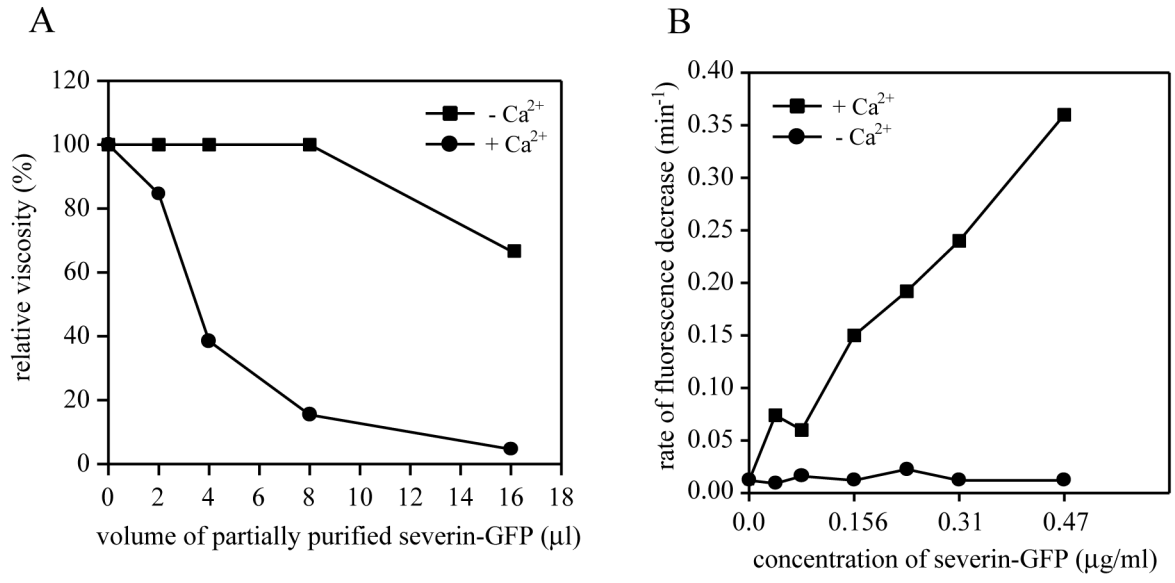

Fig. 23 *In vitro* severing activity of a partially purified fraction of severin-GFP
(A) Low shear falling-ball viscometry assay showed the Ca^{2+} dependence of severin-GFP for its F-actin fragmenting activity. Relative viscosity was plotted against increasing volume of the fusion protein.
(B) Data from fluorescence spectroscopy also indicated the absolute requirement of Ca^{2+} by the fusion protein for its actin severing activity. In the plot of the rate of fluorescence decrease versus amount of fusion protein used, the severing activity was found to increase linearly in direct proportion to the elevating concentrations of severin-GFP. In the absence of Ca^{2+}, the severing activity of the fusion protein is negligible.

Ca^{2+}, the severing activity or rate of decrease of the arbitrary relative fluorescence values was found to be negligible with increasing concentrations of the fusion protein. On the contrary, when Ca^{2+} was present, severin-GFP was shown to exhibit increased F-actin fragmenting activity with rising concentrations of the fusion protein (Fig. 23B). Thus far, an active severin-GFP fusion protein has been generated in the severin minus *D. discoideum* cells and could be used for the *in vivo* studies of the dynamics of actin-related processes.

3.3.5 Localization of severin-GFP during macropinocytosis

The HG1132-T *Dictyostelium* cells were used for the *in vivo* study of the distribution of the severin-GFP fusion protein in the course of uptake of liquid by the cells using confocal laser scanning microscopy (CLSM). This highly resolving microscopy technique is suitable for the direct visual examination of rapid and transient processes of live cells with the aid of GFP-fused proteins. CLSM is also useful for analysing fixed cells in immunofluorescence studies since it can resolve spatially the location of the protein of interest within a cell. Indirect immunofluorescence analysis of wild-type AX2 cells with a monoclonal antibody specific for severin showed only overall cytoplasmic staining (André *et al*., 1989). This disadvantage of immunofluorescence study could be overcome by the use of the sensitive CLSM.

During macropinocytosis, severin-GFP was located prominently at the macropinocytotic crown-like structures. In the time sequence shown from 0-75 seconds, rapid redistribution of the fusion protein was distinctly observed in the macropinocytotic crowns (Fig. 24).

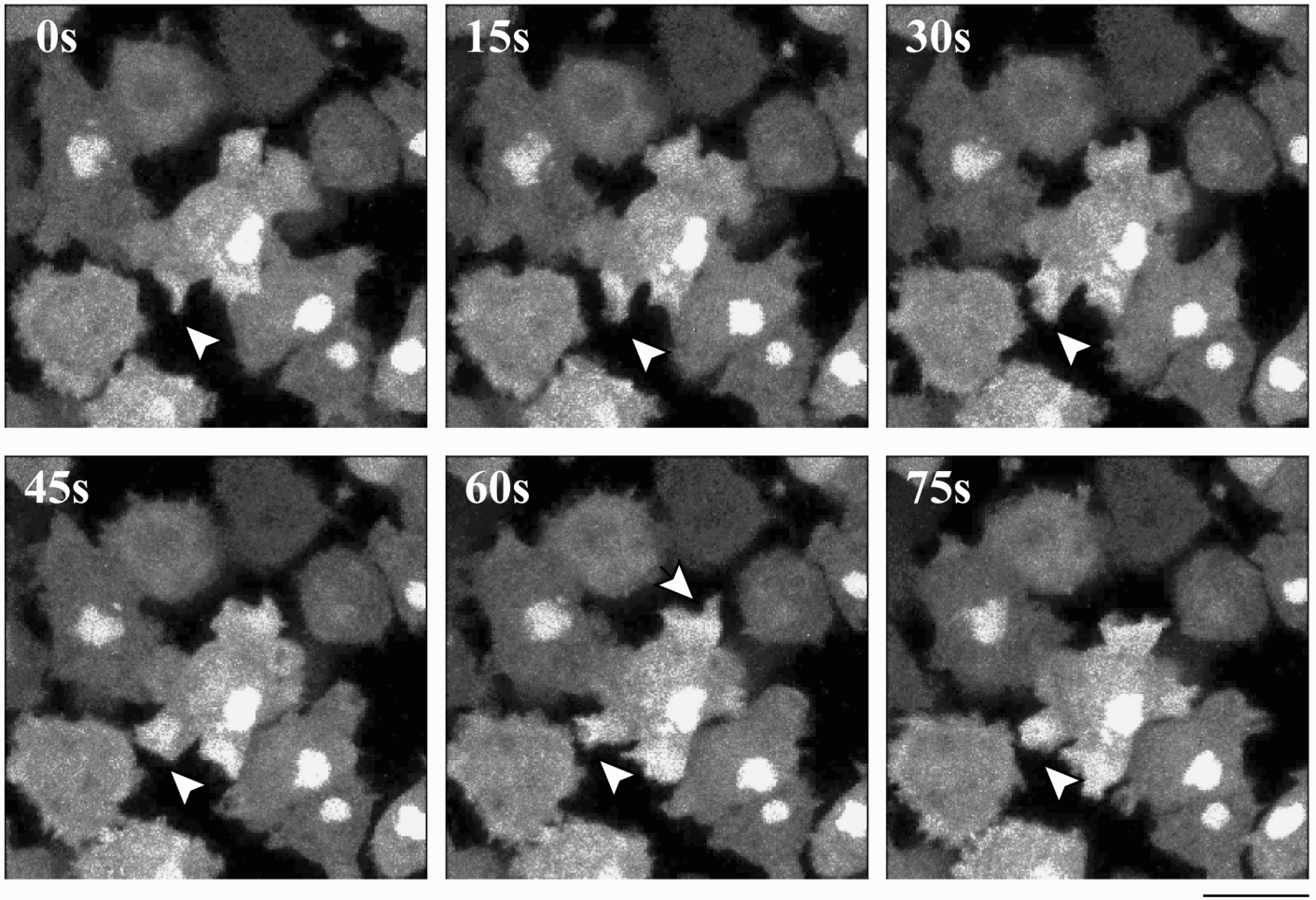

Fig. 24 Confocal images showing the distribution of severin-GFP during macropinocytosis in *D. discoideum*
CLSM study of severin null cells transformed with severin-GFP (HG1132-T) revealed distinct accumulations of the fusion protein in macropinocytotic crown-like structures in the process of uptake of liquid. The time sequence from 0-75 s showed rapid redistribution of the fusion protein in these macropinocytotic crowns (arrowheads). The nuclear stainings are artefacts probably due to the presence of a partial nuclear localization signal sequence in the linker sequence of the severin-GFP fusion protein. Scale bar represents 10 µm.

3.4 *Yersinia* infection and the actin cytoskeleton

3.4.1 Indirect immunofluorescence analyses of selected cytoskeletal proteins during *Yersinia enterocolitica* infection

The mammalian cell-line, COS7, was used in infection studies with either the *Yersinia enterocolitica* wild-type strain (WA-P) or the strain cured of the Yop secretion plasmid (WA-C) (Heesemann, 1987) in time course experiments whereby infected cells were fixed after various time points of infection and subjected to conventional immunostaining with monoclonal antibodies specific for human vinculin (V-9131), talin (T-3287), and also with an anti-ß-COP monoclonal antibody (E5A3) (Pepperkok *et al*., 1993; Mohrs *et al*., 2000). Uninfected cells labelled with these antibodies were used as negative controls.

Vinculin and talin, found in a wide variety of tissues and cell types, are cytoskeletal proteins which are able to interact with each other (Gilmore *et al*., 1992; Lee *et al*., 1992; Gilmore and Burridge, 1996), associate with F-actin (Johnson and Craig, 1995; Hemmings *et al*., 1996) and are involved in cell-cell and cell-extracellular matrix adherens junctions. They are important for the assembly of stress fibres and focal adhesions and are part of a large complex of interacting proteins thought to be involved in anchoring F-actin to the membrane, thus generating a transmembrane connection between the extracellular matrix and the cytoskeleton at adhesion plaques or focal contacts (see review by Critchley, 2000).

The ß-COP protein (Duden *et al*., 1991), a non-clathrin-coated vesicle-associated coat protein, is one of seven subunits making up the hetero-oligomeric complex known as coatomer. Coatomer together with ADP-ribosylation factor or ARF (Serafini *et al*., 1991) make up the COP-I membrane coat of transport vesicles of the early secretory pathway. Thus the mammalian ß-COP is essential for biosynthetic membrane transport from the endoplasmic reticulum (ER) to the Golgi complex (Pepperkok *et al*., 1993) which is further supported by data from the yeast homologs (Duden *et al*., 1994).

COS7 cells infected with either WA-P or WA-C were fixed after 15 min, 30 min and 1h of infection and subsequently labelled with anti-human vinculin, -talin and –ß-COP antibodies. For the anti-vinculin staining, infection with both strains of *Yersinia enterocolitica* showed similar vinculin staining at focal adhesions throughout the entire duration of infection like those of the uninfected cells (Fig. 25A). Labelling with an anti-talin antibody revealed no discernable differences between the uninfected cells and cells infected with either strain of bacteria. Similar talin staining of focal contacts was observed up to 1h of infection with either

WA-P or WA-C as seen in the case for the uninfected cells (Fig. 25B). Immuno-detection with an anti-ß-COP antibody showed comparable labellings of the ER-Golgi network for both uninfected and WA-P- or WA-C-infected cells throughout the course of infection (Fig. 25C).

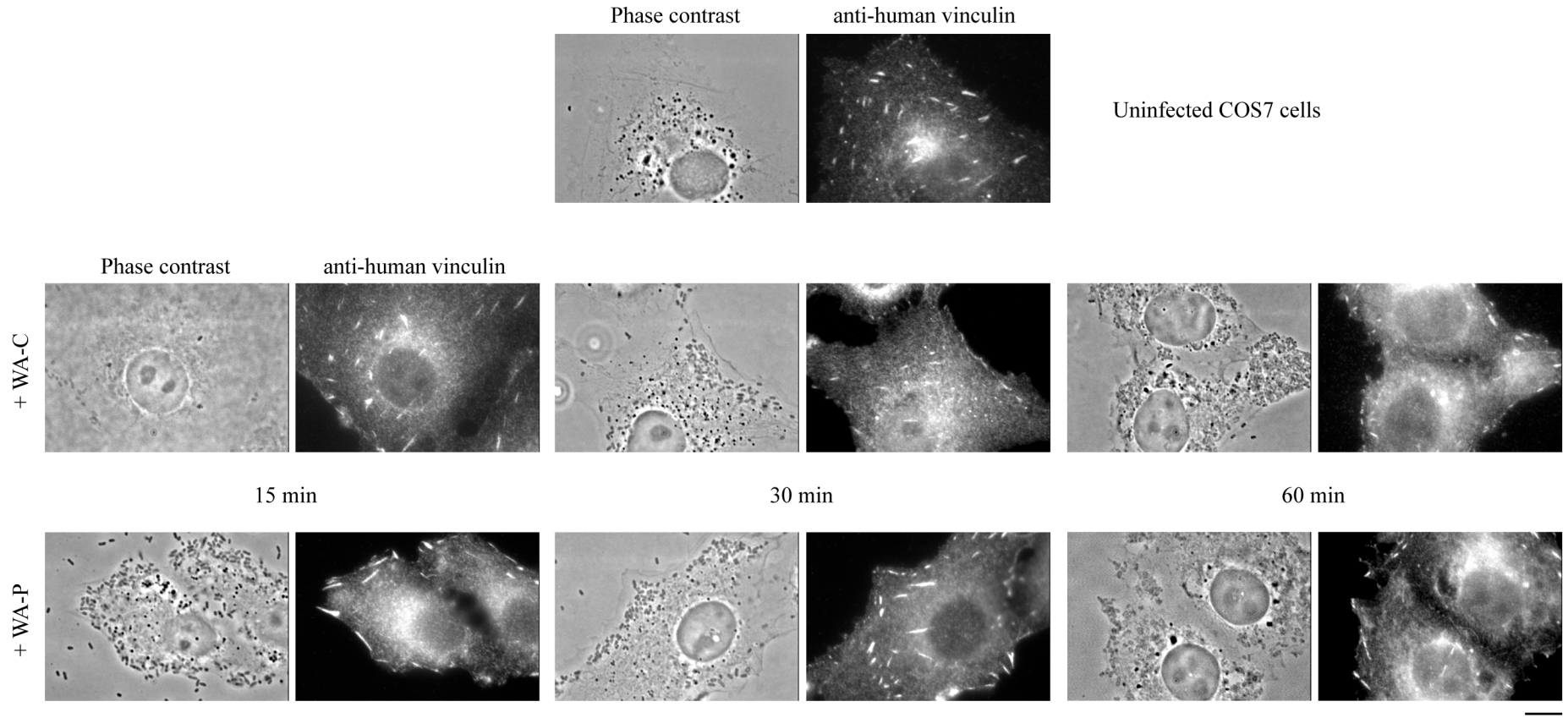

Fig. 25(A) Anti-human vinculin stainings of COS7 cells after infection for 15, 30 and 60 minutes with a *Yersinia enterocolitica* wild-type strain (WA-P) and a Yop-secretion minus strain (WA-C). Uninfected mammalian cells were used as negative controls. Data showed similar vinculin labellings for both the uninfected and WA-C or WA-P infected cells throughout the time course of infection. Scale bar represents 10 µm.

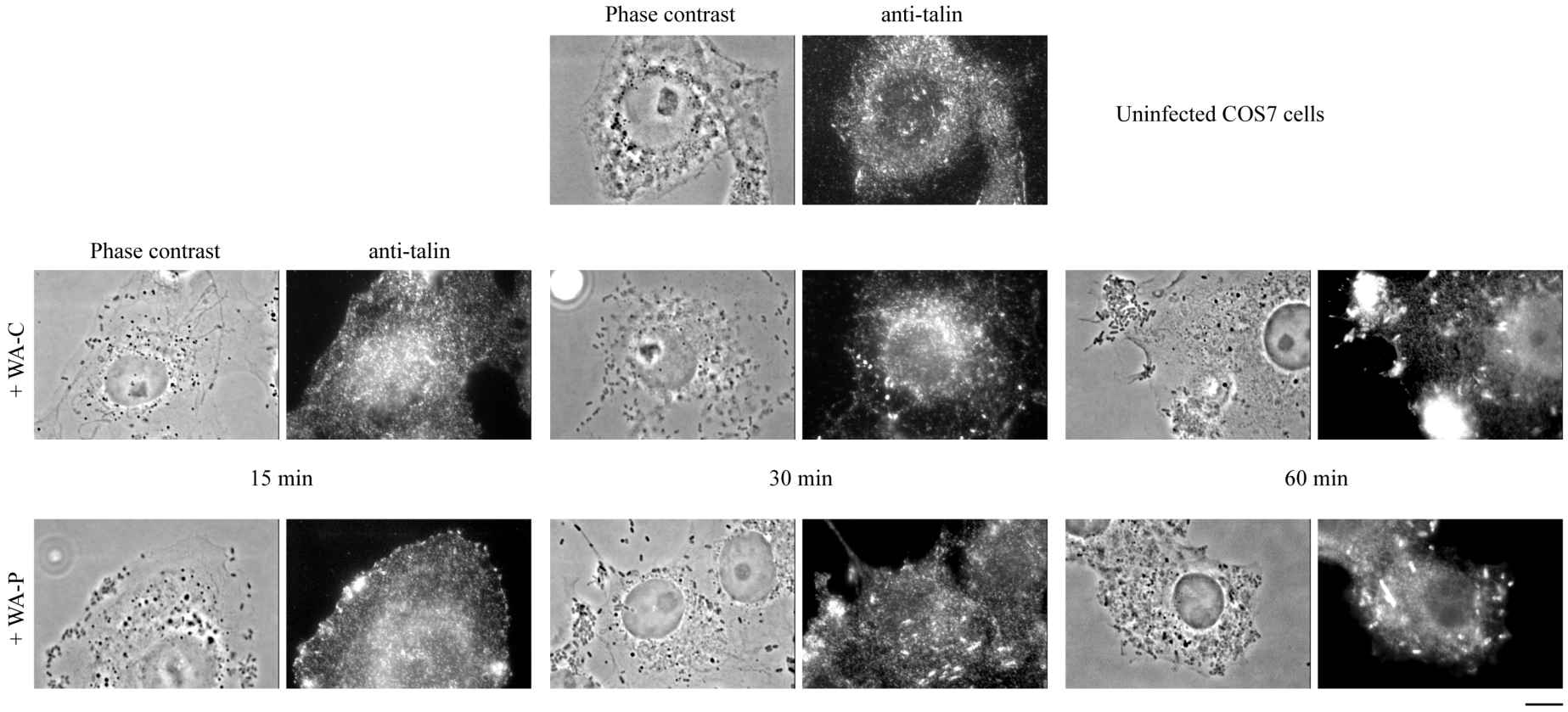

Fig. 25(B) Anti-talin labellings of COS7 cells after infection with either a *Yersinia enterocolitica* wild-type strain (WA-P) or a Yop-secretion minus strain (WA-C) for 15, 30 and 60 minutes. In comparison with the uninfected cells as negative controls, the cells infected with either WA-P or WA-C exhibited similar talin stainings during the course of infection. Scale bar represents 10 µm.

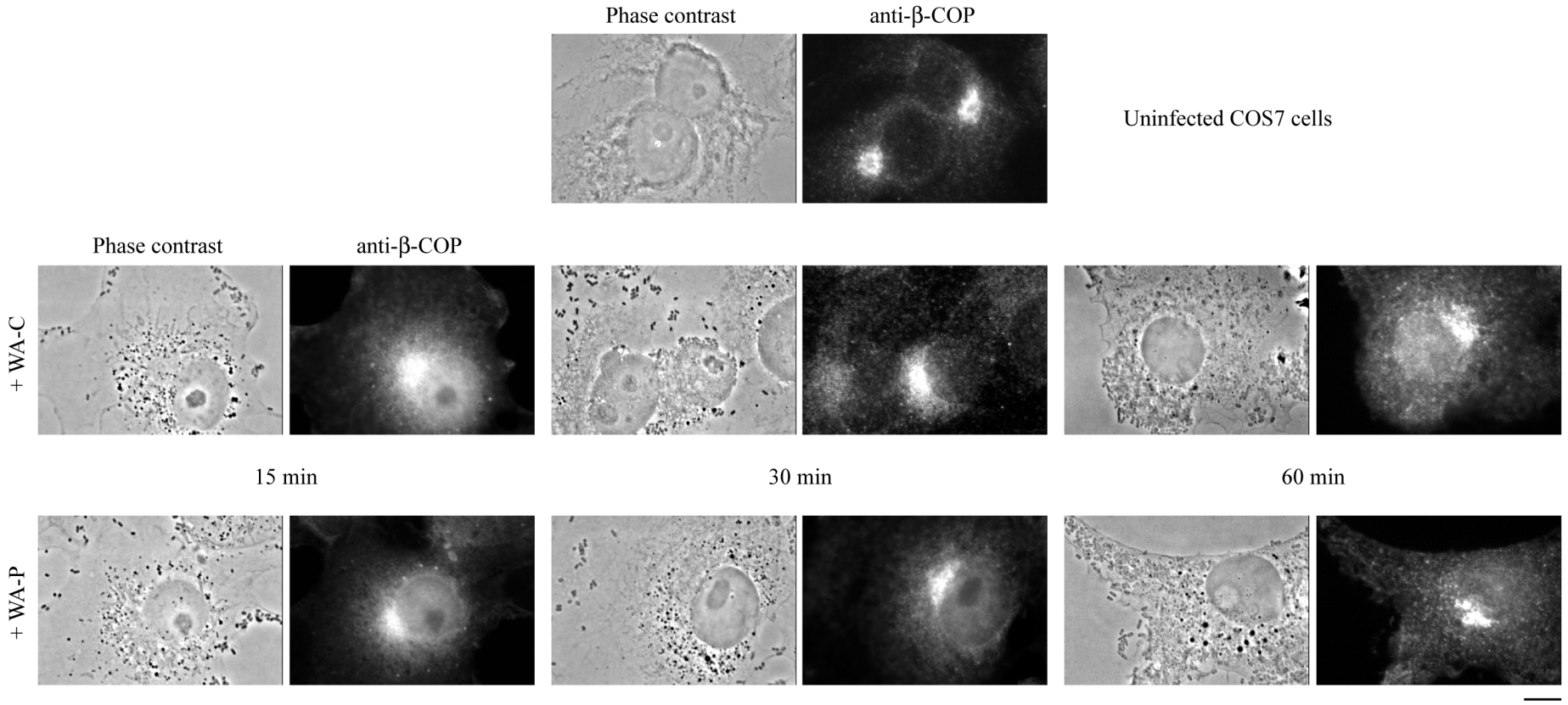

Fig. 25(C) Anti-β-COP stainings of COS7 cells after infection for 15, 30 and 60 minutes with either WA-P or WA-C revealed prominent Golgi labellings similar to that of the uninfected cells which were used as negative controls. No obvious difference in Golgi stainings was observed between the WA-P or WA-C infected cells throughout the time course of infection. Scale bar represents 10 μm.

3.4.2 Studies of selected GFP-fused cytoskeletal proteins during *Yersinia* infection

Infection studies were also performed on COS7 cells transiently transfected with GFP-actin (Choidas *et al*., 1998), GFP-cofilin or GFP-profilin II (both fusion constructs kindly provided by Dr. Walter Witke, EMBL, Rome, Italy). This approach has two main advantages in that artefacts generated via indirect immunofluorescence labelling could be circumvented, and most importantly, GFP-fused cytoskeletal proteins could be directly monitored with the aid of the highly sensitive CLSM to examine with high resolution any rapid and transient remodelling of the dynamic cytoskeleton.

Uninfected cells transfected individually with the three different GFP fusion constructs were used as negative controls. COS7 cells transfected separately with GFP-actin, -cofilin or –profilin II were infected with either WA-P or WA-C in a time course experiment from 0-2 h. Infected cells were fixed with paraformaldehyde after 15 min, 30 min, 1 h and 2 h of infection and directly embedded for confocal microscopy. Alternatively, *in situ* infection of the transfected cells was monitored in real time using CLSM as described in Materials and Methods (sections 2.6.3 & 2.6.4).

The authenticity of the GFP-actin labelling was confirmed by phalloidin staining of F-actin. For both uninfected and infected cells, actin labelling was observed to be comparable with either phalloidin (Fig. 26) or GFP-actin (Fig. 27). Infection of GFP-actin transfected cells with WA-C up to 2 h showed actin staining similar to that of the uninfected cells, whereby actin was predominantly distributed at the cell cortex (Fig. 27). Cytoplasmic staining contributed by monomeric actin was also observed.

In contrast, after about 30 min of infection with WA-P, cells began to lose actin staining and actin patches were observed. The actin cytoskeleton was disrupted and reorganized to allow rounding up of cells after 2 h of infection with WA-P as compared to infection with WA-C whereby the cells remained flattened after 2 h (Fig. 27).

Cofilin, a 21 kDa actin-binding protein found in all eukaryotes examined so far, represents the cofilin family of actin regulating proteins. It is a phosphoinositide-sensitive actin-binding protein (Yonezawa *et al*., 1990; Aizawa *et al*., 1995) which can reversibly regulate actin polymerization and depolymerization in a pH-dependent manner (Yonezawa *et al*., 1985; Hawkins *et al*., 1993). Cofilin forms intranuclear and/or cytoplasmic actin-cofilin rods in cultured cells exposed to various extracellular stimuli (Nishida *et al*., 1987).

Uninfected COS7 (TRITC-phalloidin)

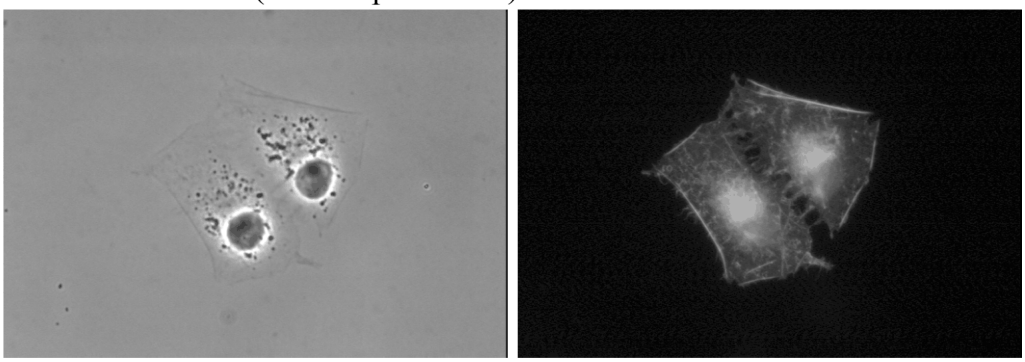

COS7 + WA-C

15’

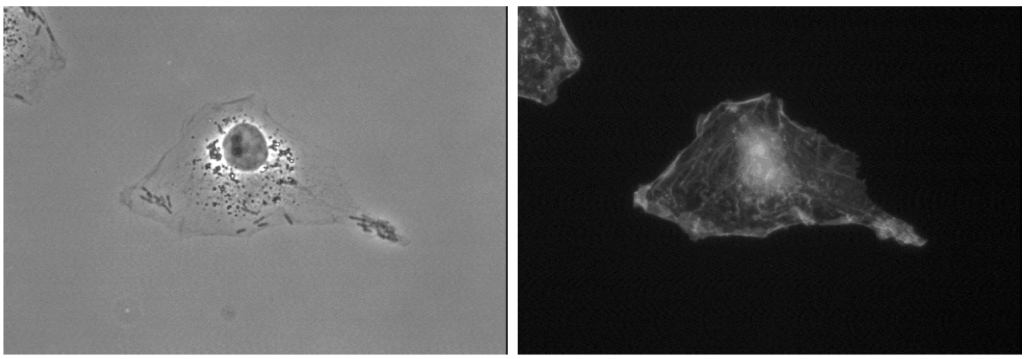

30’

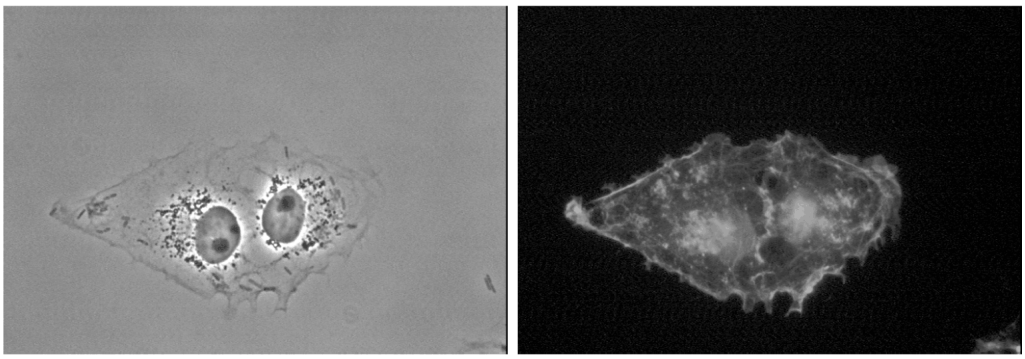

COS7 + WA-P

15’

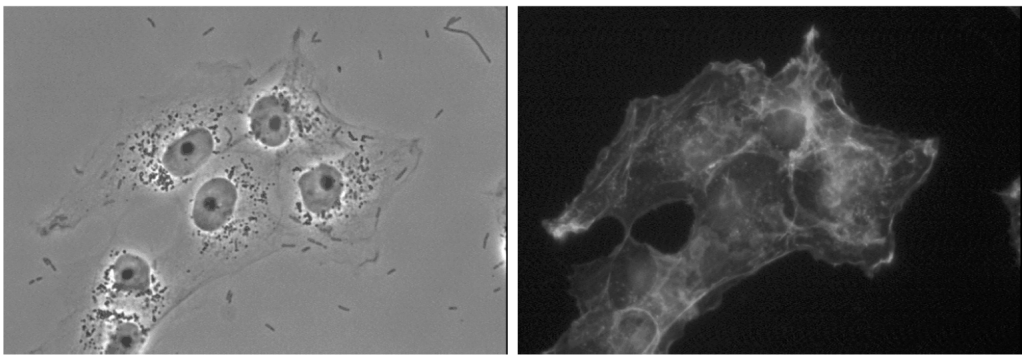

30’

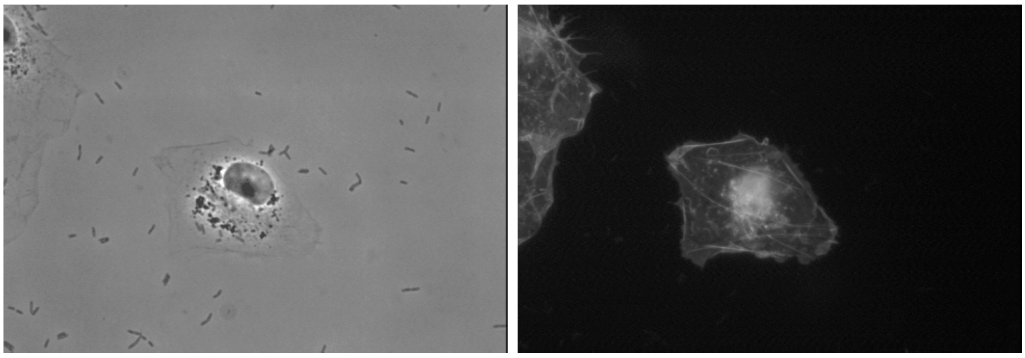

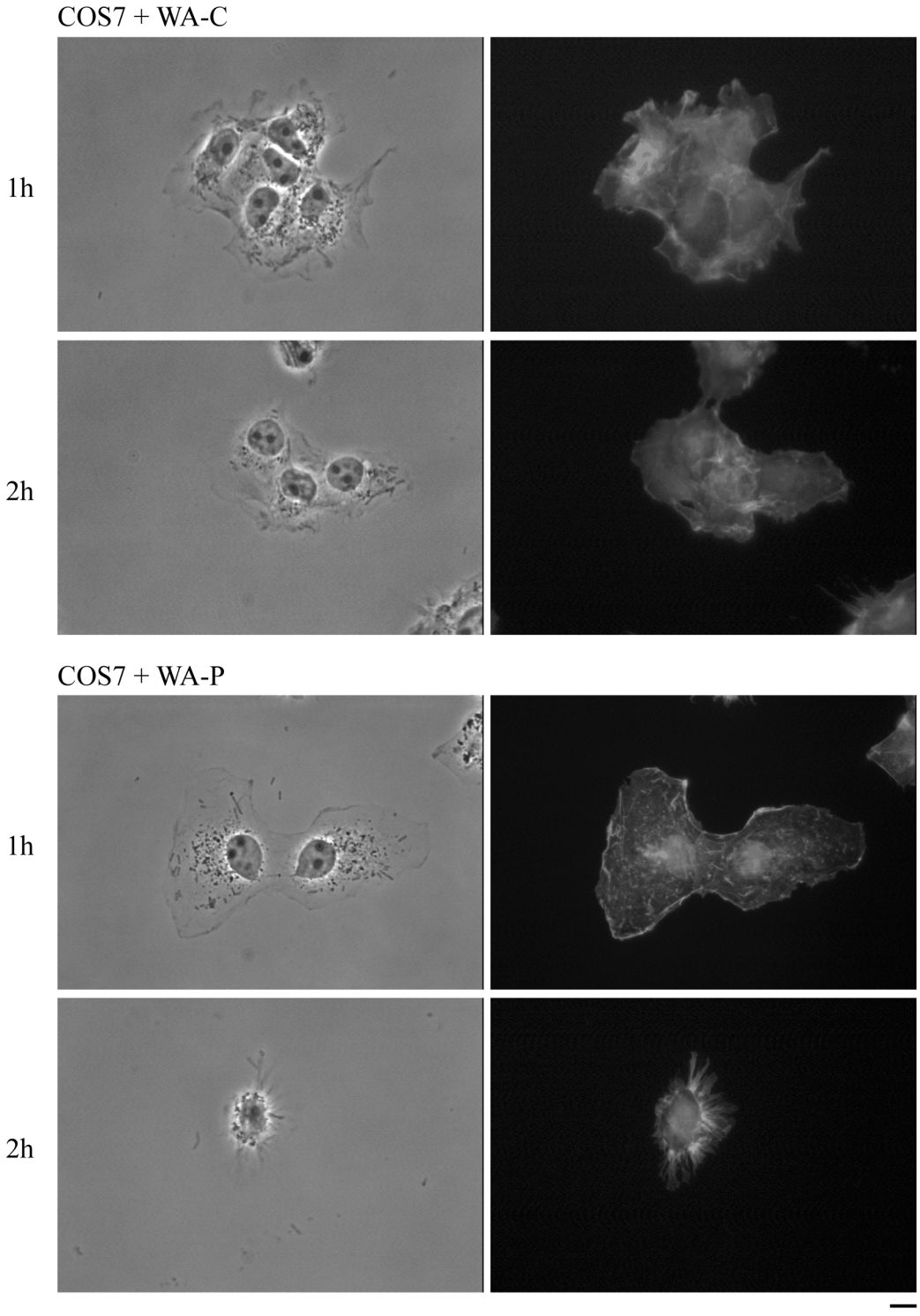

Fig. 26 Phalloidin staining of F-actin in COS7 cells
Paraformaldehyde-fixed cells were labelled with TRITC-phalloidin after 15, 30, 60 and 120 min of infection with either a *Y. enterocolitica* wild-type strain (WA-P) or a Yop secretion-minus strain (WA-C). Uninfected cells were used as negative controls. After about 1h of infection with WA-P, dissembly of the microfilaments was observed and the cells rounded up after 2h of infection with WA-P compared to that with WA-C, whereby the cells still retained actin staining throughout the time course of infection. Left, phase contrast; right, fluorescent images. Scale bar represents 10 µm.

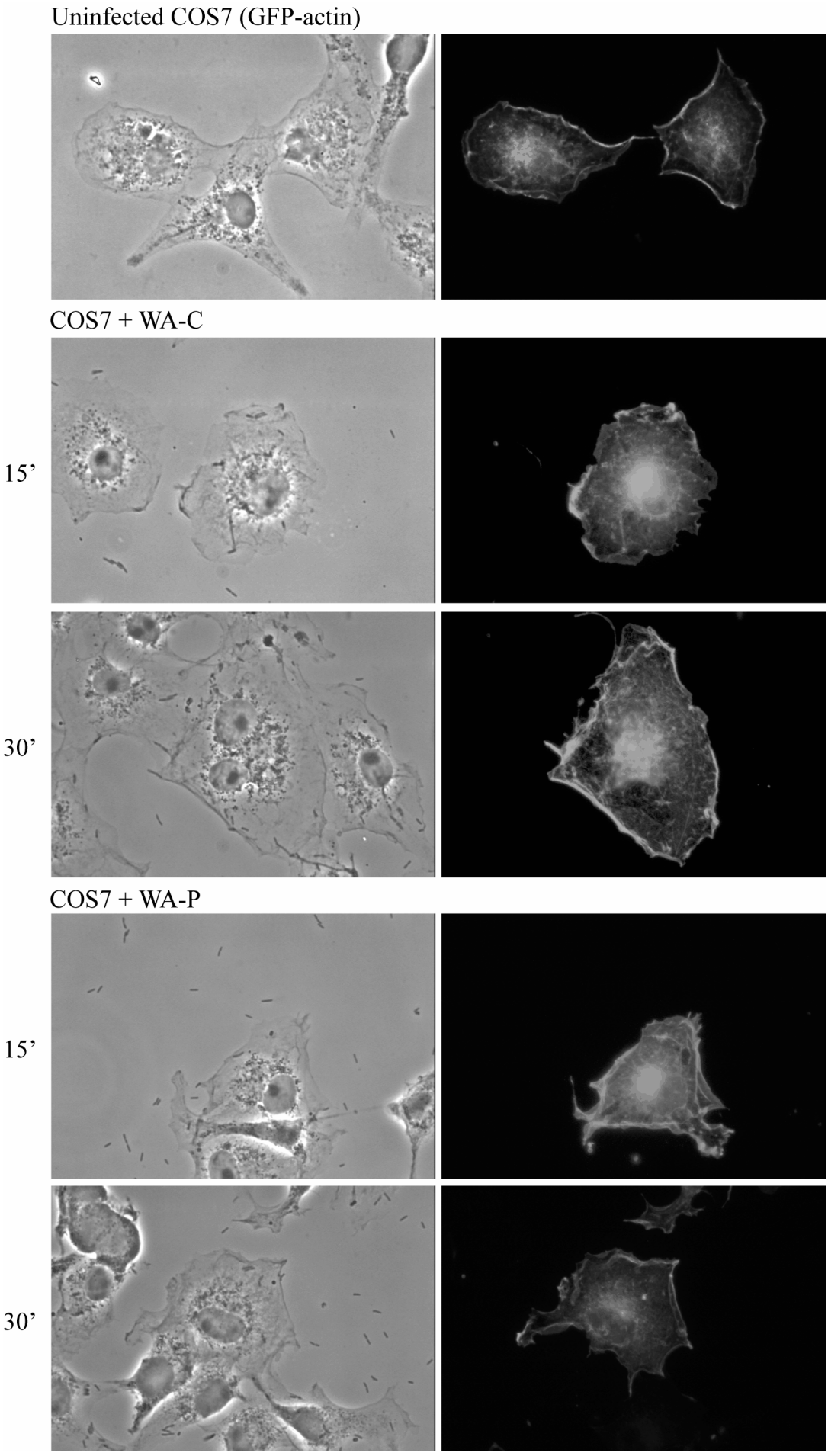
Uninfected COS7 (GFP-actin)
COS7 + WA-C
15’
30’
COS7 + WA-P
15’
30’

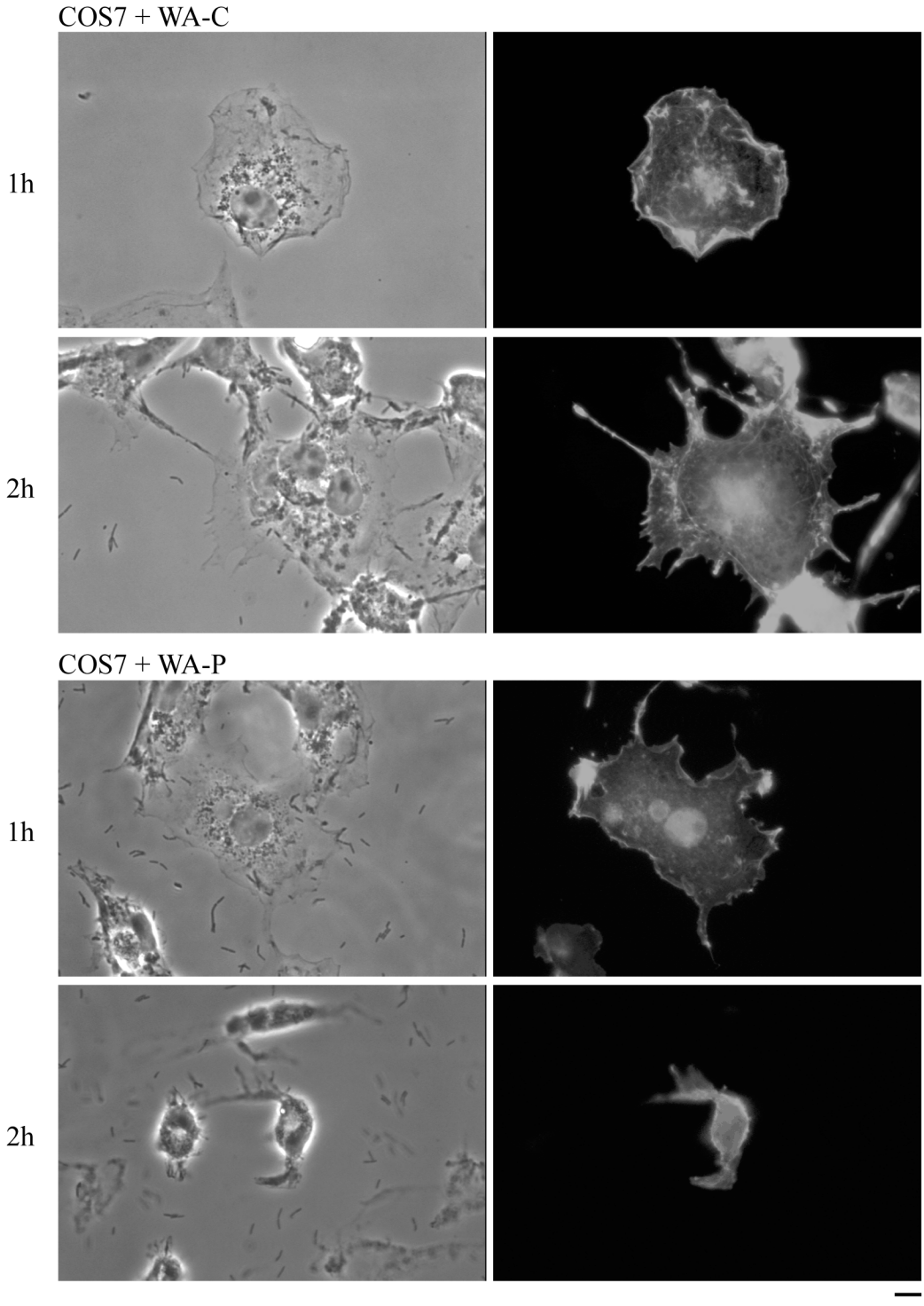

Fig. 27 Actin staining of COS7 cells using GFP-actin
Cells transiently transfected with GFP-actin were infected with either WA-P or WA-C over a period of 2h and then fixed with paraformaldehyde. Uninfected cells transfected with GFP-actin were used as negative controls. Similar actin stainings were observed with both TRITC-phalloidin and GFP-actin. The WA-C infected cells exhibited comparable cortical actin labellings to that of the uninfected cells up to 2h of infection. On the contrary, after about 30 min of infection with WA-P, cells started to lose actin staining and diffuse actin patches were seen whereby after 2h of infection, the actin cytoskeleton was reorganized to allow rounding up of cells in contrast to the flattened WA-C infected cells. Left, phase contrast; right, fluorescent images. Scale bar represents 10 μm.

Similar to the uninfected cells, GFP-cofilin labelling of the actin-cofilin rods was observed in cells infected with WA-C throughout the entire duration of infection (Fig. 28). Infection with WA-P, on the contrary, showed that after 1 h of infection, there was a decrease in the length of the actin-cofilin rods (Fig. 28), suggesting the actin disaggregating ability of Yops which prevents formation of long actin-cofilin rods.

Profilin-GFP transfected cells showed overall cytoplasmic labelling for both uninfected and WA-C- or WA-P-infected cells over a 2 h-period of infection (Fig. 29). Data imply that the Yops do not have any major effect on the distribution of the GFP-profilin fusion protein.

Confocal microscopy analyses of GFP-actin transfected cells were performed either via cell fixation after bacterial infection or during real time infection. Both approaches showed similar results whereby F-actin structures resembling phagocytic cups were observed at bacterial attachment sites for cells infected with either WA-P (Fig. 30A) or WA-C (Fig. 30B) after 30 min. The data suggest that the mammalian cells react already upon adhesion of *Yersinia enterocolitica*.

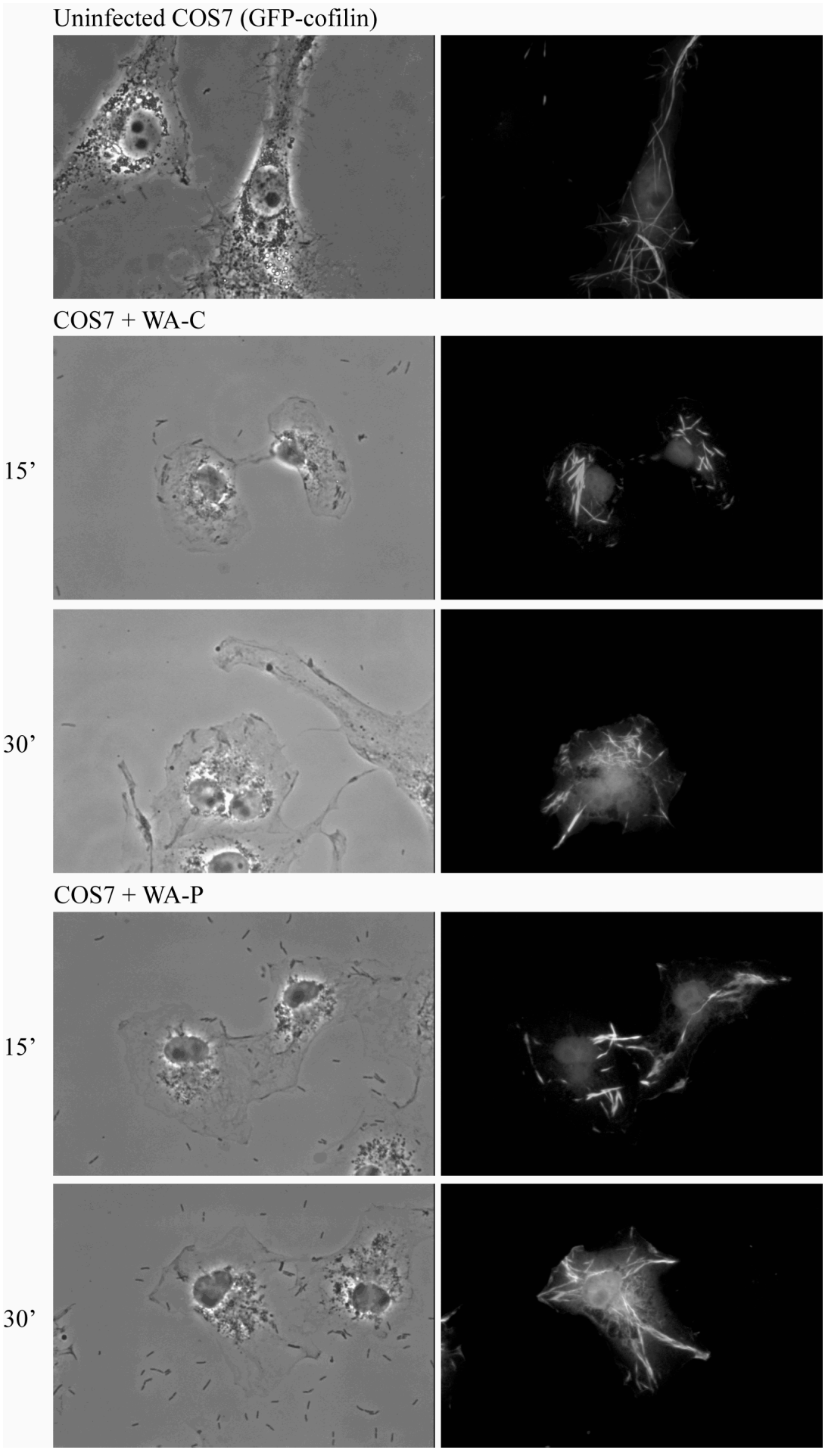
Uninfected COS7 (GFP-cofilin)
COS7 + WA-C
15’
30’
COS7 + WA-P
15’
30’

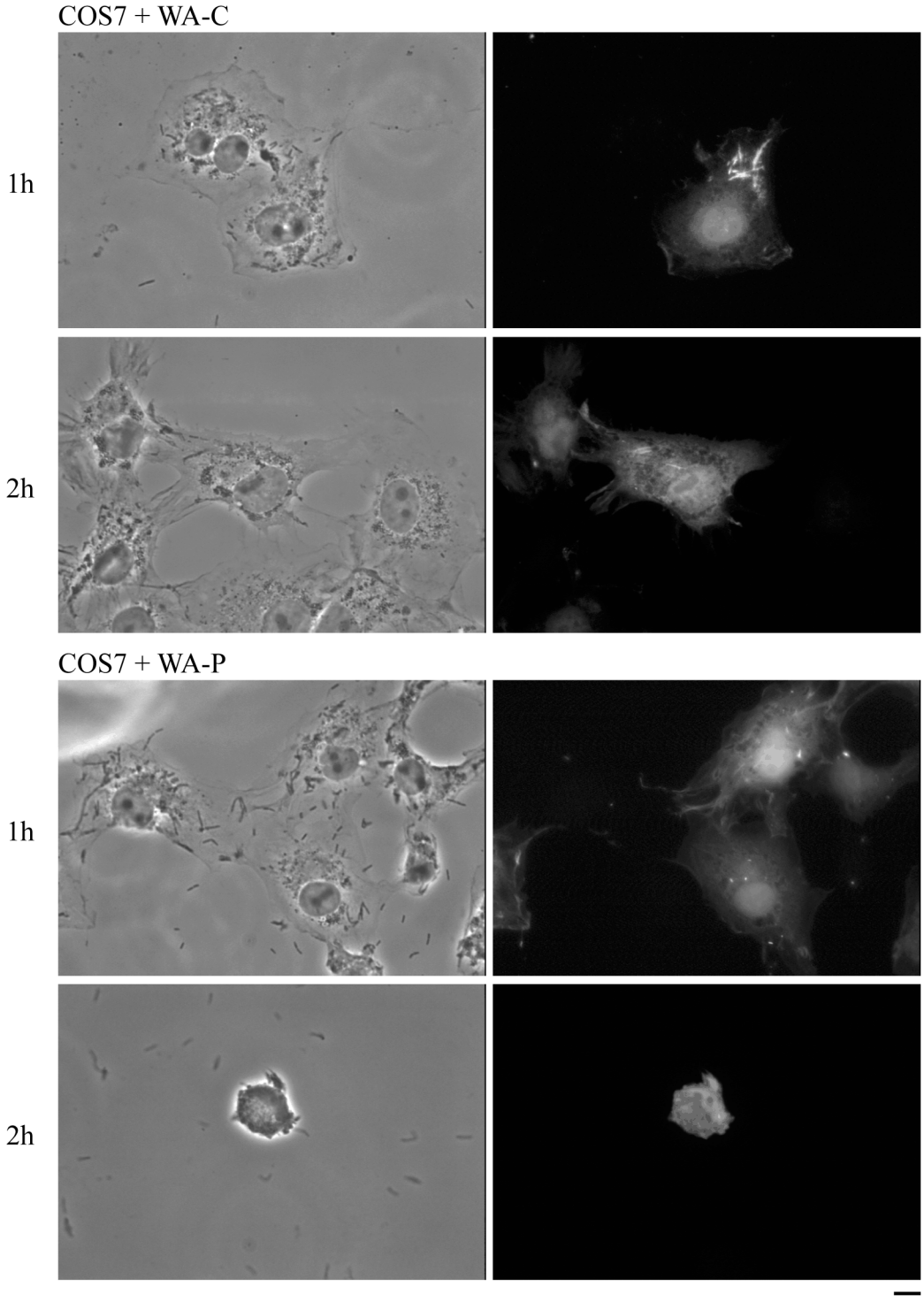

Fig. 28 Labelling of actin-cofilin rods using GFP-cofilin
COS7 cells transiently transfected with GFP-cofilin were infected with either WA-P or WA-C for periods of 15, 30, 60 and 120 min. Uninfected cells which were transfected also with GFP-cofilin were employed as negative controls. The extranuclear actin-cofilin rod stainings for the WA-C infected cells were found to be similar to that of the uninfected cells throughout the time course of infection. On the other hand, after 1h of infection with WA-P, a decrease in the length of actin-cofilin rods was observed, suggesting that the actin disruption activity of Yops might prevent formation of long rods. Left, phase contrast; right, fluorescent images. Scale bar represents 10 μm.

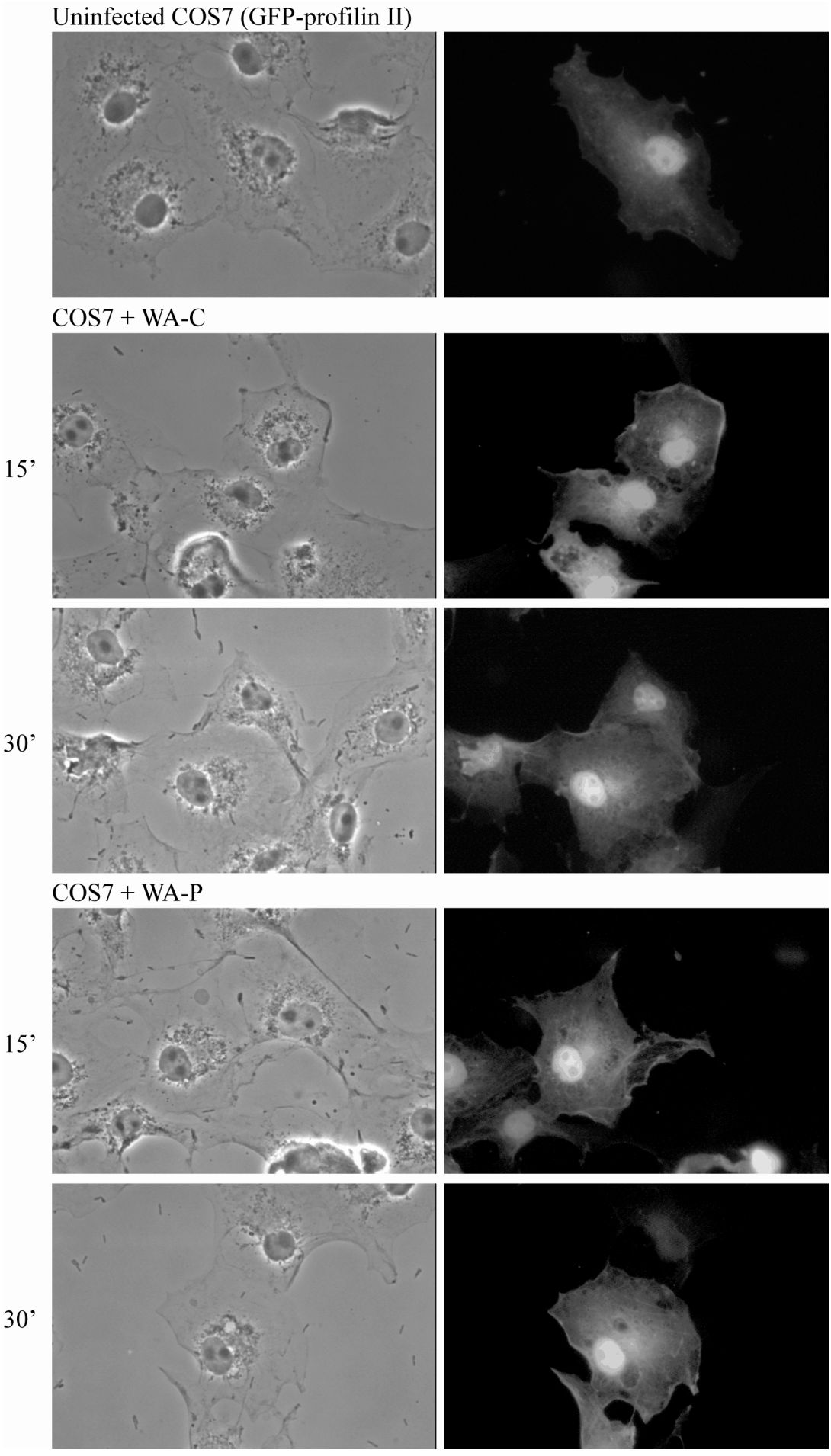
Uninfected COS7 (GFP-profilin II)
COS7 + WA-C
15’
30’
COS7 + WA-P
15’
30’

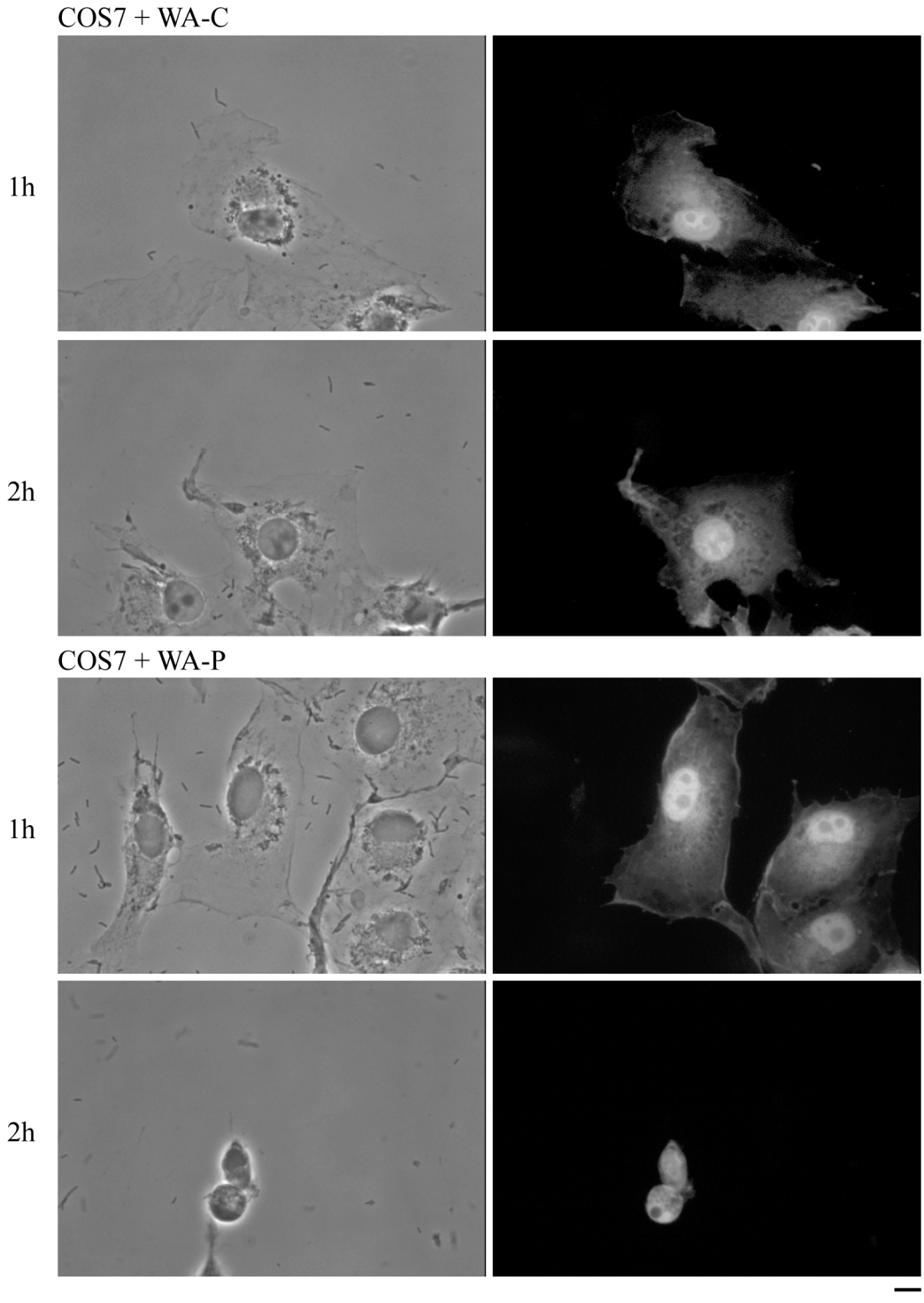

Fig. 29 Profilin staining with the aid of GFP-profilin
COS7 cells transfected with GFP-profilin II were infected with either WA-P or WA-C over a time course of 2h after which they were fixed with paraformaldehyde and subjected to confocal microscopy study. Uninfected cells were employed as negative controls. Like the uninfected cells, both the WA-P and WA-C infected cells exhibited overall cytoplasmic labelling of profilin throughout the entire course of infection, suggesting that the Yops may not play a significant role on the subcellular distribution of profilin. Left, phase contrast; right, fluorescent images. Scale bar represents 10 μm.

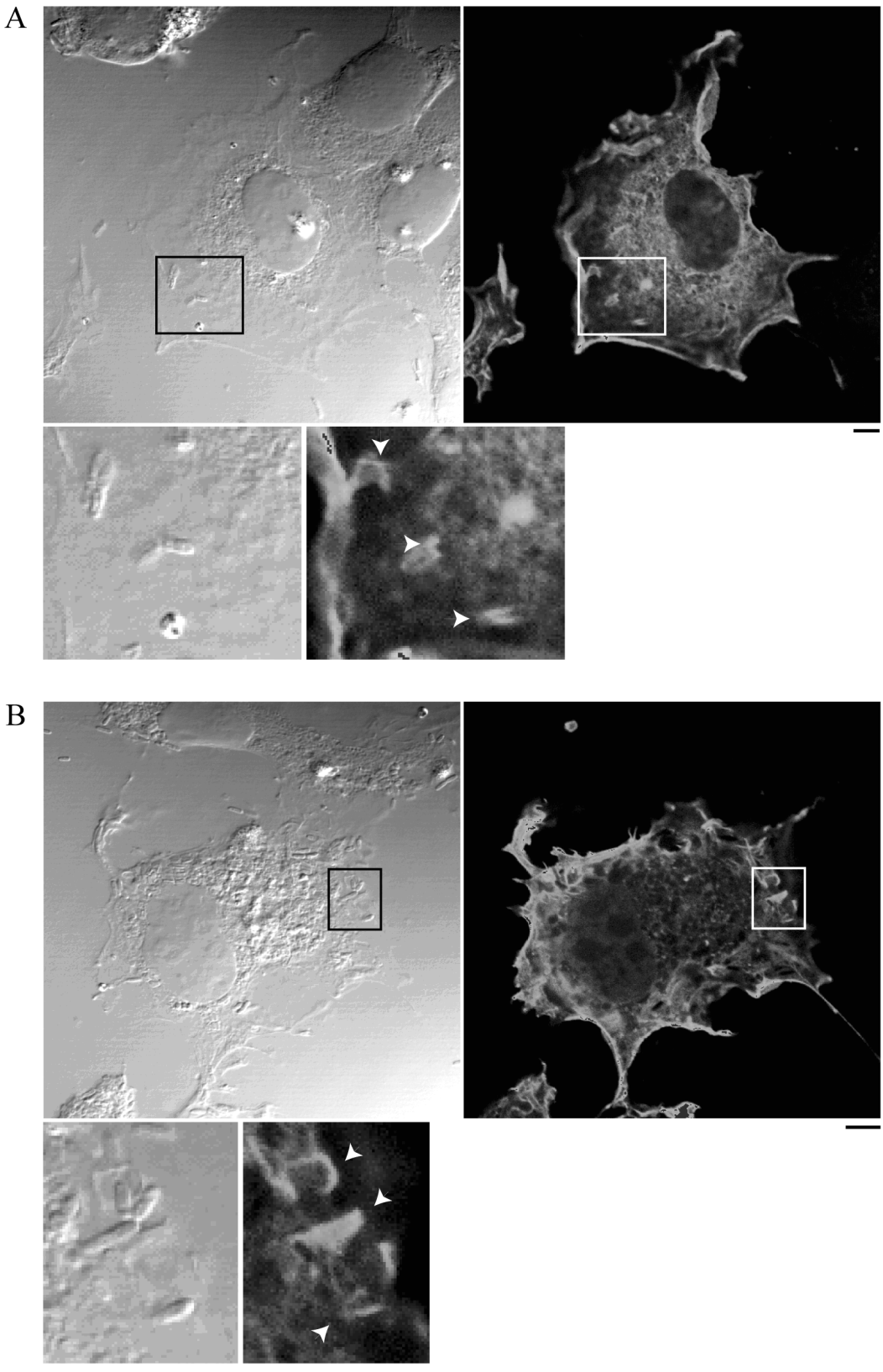

Fig. 30 Response of the actin cytoskeleton to *Y. enterocolitica* infection
COS7 cells transfected with GFP-actin were either infected with (A) the wild-type *Yersinia* species (WA-P), or (B) the Yop secretion-minus strain (WA-C). The enlarged confocal images revealed F-actin structures which resemble phagocytic cups (arrowheads) at sites of bacterial adherence (see DIC images; left and fluorescent images; right) for both the WA-P and WA-C infected cells after 30 min. These data imply that the mammalian cells respond already upon adherence of *Y. enterocolitica*. Scale bars represent 10 μm.

4 DISCUSSION

4.1 The point-mutated profilins, W3N and K114E

The *in vivo* roles of profilin with regard to its poly-(L)-proline binding and actin-binding activities were investigated. Point mutations performed on the poly-(L)-proline or actin-binding sites of profilin II allowed the characterization of the significance of these two properties of profilin in the maintenance of normal cellular physiology via expression of these altered profilins in the profilin null *D. discoideum* cells. Their abilities to rescue the aberrant phenotype of the profilin null cells were examined. Two highly conserved residues W3 and K114 of the profilin II isoform of *D. discoideum* were selected for site-directed mutagenesis by PCR. The data suggest a) that a functional poly-(L)-proline binding activity is more important for suppression of the mutant phenotype than the G-actin binding activity of profilin, and b) that the enrichment of profilin in highly active phagocytic cups might be independent of either poly-(L)-proline or actin-binding activities.

4.1.1 *In vitro* analyses of W3N and K114E

The actin, poly-(L)-proline and PIP_2 binding characteristics of W3N and K114E were investigated. A sedimentation assay revealed that the W3N profilin had indeed lost its capability to bind to a poly-(L)-proline matrix, contrary to the wild-type and K114E profilins. Although the poly-(L)-proline binding site is structurally distinct from the actin-binding domain, fluorescence spectroscopy measurements using pyrene-labelled actin monomers revealed a mild decrease in the affinity of W3N profilin for G-actin. In fact, a 1.5-fold excess of W3N, in contrast to wild-type profilin, was essential to achieve comparable actin polymerization kinetics. According to Bjoerkegren *et al*. (1993) and Haarer *et al.* (1993), mutagenized profilins which had lost their affinities to poly-(L)-proline stretches were not accompanied by any changes in their affinities for actin. This slight negative influence of a single mutation in the poly-(L)-proline binding site on actin-binding was detected most likely due to the high sensitivity of the methodology being used here. However, controversial data from Bjoerkegren-Sjoegren *et al*. (1997) showed that their two profilin mutants with reduced affinities for poly-(L)-proline also exhibited decreased affinities for actin, suggesting that structural alterations in the poly-(L)-proline binding site of profilin can have an effect on the distantly located actin-binding region and that the poly-(L)-proline binding activity of profilin may play an important regulatory role of the actin cytoskeleton.

The K114E point-mutated profilin differed from W3N in that only its actin-binding activity was severely affected. The affinity of K114E profilin for G-actin was drastically reduced as fluorescence spectroscopy measurements revealed that a 3-fold excess of K114E was obligatory to obtain similar kinetic behaviour as with wild-type profilin. While these data support the evidence that the conserved lysine #114 is indispensable for strong actin binding, they also show that this point mutation is insufficient to deplete entirely the affinity of profilin for actin, providing additional support for the existence of extensive contacts between profilin and actin (Schutt *et al*., 1993). To explore further the biochemical properties of the point-mutated profilins, their abilities to interact with PIP_2 were tested. Our data suggested that as with the wild-type profilin, the binding of W3N and K114E profilins to phospholipids was unaltered, which agreed with previous data (Haarer *et al*., 1993; Sohn *et al*., 1995), indicating that the amino acid residues W3 and K114 are not essential for phospholipid binding.

4.1.2 Rescue of the profilin null phenotype by W3N and K114E

The aberrant phenotype of the profilin null cells (Haugwitz *et al*., 1994) was overcome by the expression of either W3N or K114E. DdW3N and DdK114E transformant cells exhibited normal cell morphology with the usual number of 1-2 nuclei per cell and the characteristic broad rim of F-actin accumulation around the edge of the profilin null cells was absent in these transformants. In addition, DdW3N and DdK114E, unlike the profilin null mutant, were able to develop into fruiting bodies resembling those of the wild-type cells. However, an overexpression of W3N profilin seemed essential for the restoration of the fruiting phenotype of DdW3N. Decrease in the level of expression of W3N to that of K114E resulted in impairment of the ability of DdW3N to generate fruiting bodies, suggesting the poly-(L)-proline binding activity of profilin is more significant than its actin-binding activity, since the K114E profilin which still has an intact poly-(L)-proline binding site is capable of rescuing the developmental defect of the profilin null cells.

4.1.3 Profilin localization at phagocytic cups

The point-mutated profilins, W3N and K114E, are recruited as efficiently as the wild-type profilin to the phagocytic cups, although actin-binding is strongly reduced in K114E and poly-(L)-proline binding is virtually absent in W3N. Phagocytosis in *Dictyostelium* is strikingly similar to that in mammalian leukocytes (Howard and Watts, 1994), with the *Dictyostelium* cells displaying similar actin-based cytoskeletal reorganization as the neutrophils. In *Dictyostelium*, the morphological fine structure of pseudopods developed in

response to phagocytic signal resembles that of macrophages (Reaven and Axline, 1973; Hartwig and Shevlin, 1986; Cox *et al*., 1995), with the materialization of a phagocytic cup at the site of particle adherence. Various actin associated proteins have been shown to exhibit distinct localization in the phagocytic cups. According to Maniak *et al*. (1995), *Dictyostelium* coronin is evidently located at the phagocytic cups. With the aid of coronin-GFP, it was observed that in the established cup, the complete area in contact with the yeast particle is enriched in the fusion protein. Other proteins known in *D. discoideum* to colocalize with actin at phagocytic cups are myosin IB (Fukui *et al*., 1989), a 30 kDa actin-bundling protein (Furukawa and Fechheimer, 1994) and the actin-binding protein, ABP-120 (Cox *et al*., 1996). In mammalian cells, myosin II (Stendahl *et al*., 1980; Valerius *et al*., 1981) and subsequently myosin I (Allen and Aderem, 1995) have both been shown to assemble with F-actin at developing phagosomes of macrophages.

Furthermore, Watanabe *et al*. (1997) found that a protein essential for cytokinesis namely p140mDia, a mammalian homolog of *Drosophila* diaphanous (Castrillon and Wasserman, 1994) which belongs to a family of formin-related proteins, exhibited binding to RhoA and profilin. The family of formin-related proteins possesses repetitive polyproline stretches, and includes Bni1p of *Saccharomyces cerevisiae* (Imamura *et al.*, 1997), mouse formin (Woychik *et al.*, 1990), *Drosophila* cappuccino (Emmons *et al.*, 1995), fus1p of *Schizosaccharomyces pombe* (Petersen *et al.*, 1995) and FigA of *Aspergillus nidulans* (Marhoul and Adams, 1995). It was observed that in cultured Swiss 3T3 fibroblasts p140mDia, profilin and RhoA are recruited in a Rho-dependent manner around phagocytic cups induced by fibronectin-coated beads, suggesting the evolutionary conserved localization and role of specific actin-binding proteins in phagocytosis.

In this study, although the W3N and K114E point-mutated profilins, like the wild-type profilin, are observed at the edge of developing phagocytic cups, it is difficult to determine if the process of phagocytosis is still fully functional. It could well be that these cells are capable of forming phagocytic cups around yeast particles but are incapable of membrane fusion and hence pinching off of phagosomes may be defective, perhaps due to the reduced affinity of the mutated profilins for actin underlying the phagocytic cups. Thus the use of profilin-GFP fusion should facilitate our understanding of the complex mechanism of phagocytosis.

4.1.4 Significance of the poly-(L)-proline binding property of profilin

The ability of the W3N profilin to restore the profilin null phenotype is dependent on its cellular concentration as an overexpression of this point-mutated profilin is essential for its

rescue capability. In comparison, the K114E profilin with a strongly reduced affinity for actin, but still harbouring an intact poly-(L)-proline binding activity, was found to be able to overcome the developmental defect of the profilin null mutant. These data suggest that the poly-(L)-proline binding activity of profilin is more important than its actin-binding property in the maintenance of normal cell physiology. Even though an interaction between W3N profilin and poly-(L)-proline stretches is non-detectable in this study, most likely there exists a reduced affinity of W3N profilin mutant for its unknown *D. discoideum* proline-rich proteins. The presence of excessive amounts of W3N profilin in DdW3N can therefore restore the interaction between profilin and its targets, thereby allowing the transformed cells to overcome the profilin null defects. K114E rescues the mutant phenotype at lower concentrations because it harbours a fully functional poly-(L)-proline binding site.

Data from other studies support this interpretation. According to Ostrander *et al*. (1999), poly-(L)-proline binding is an essential function of human profilin in yeast since it was found that an overexpression of the aberrant human profilin gene is absolutely necessary for normal cell growth. Other experiments performed on yeast profilin, which had severe loss in its ability to bind *in vitro* poly-(L)-proline stretches as a result of a deletion of three amino acids from the C-terminal end, did not implicate the significance of poly-(L)-proline binding activity of profilin to the maintenance of normal cellular physiology (Haarer *et al*., 1993). On closer examination, it was observed that in sedimentation assays, this truncated yeast profilin still showed low affinity for the poly-(L)-proline matrix. Furthermore, yeast profilin mutants lacking six to eight amino acids from the C-terminal are not able to rescue the profilin null mutant, in spite of the fact that these mutants can still bind actin (Haarer *et al*., 1993), suggesting that actin-binding is insufficient for normal profilin function. Data from pollen profilin mutant with two-fold higher affinity for poly-(L)-proline as compared to the native pollen profilin also showed the importance of the poly-(L)-proline binding role of profilin (Gibbon *et al*., 1998).

As compared to W3N, the affinity of *D. discoideum* profilin II for actin was much reduced in K114E, the suppression of the profilin-minus phenotype however, required much more W3N than K114E suggesting a great importance of the poly-(L)-proline binding activity of profilins. These findings also shed light onto the experiments done with bovine profilin in *Dictyostelium* (Schlueter *et al*., 1998). Wild-type and a mutated (F59A) profilin from bovine were able to partially rescue the aberrant phenotype of profilin-minus *Dictyostelium* mutants. But taking into consideration that the affinity between F59A profilin and actin was reduced even by an order of magnitude, one has to assume that the still intact poly-(L)-proline binding

site of F59A plays a considerable role during suppression of the phenotype. The *in vivo* significance of this functional domain is also reflected in the same study in which the distinct distribution of F59A in fibroblasts clearly suggests a binding of the mutated profilin to targets other than actin (Schlueter *et al*., 1998).

4.2 Study of *D. discoideum* profilin via GFP fusion

The exact roles of profilins and the regulation of their activities *in vivo* are poorly understood despite extensive studies (Carlier and Pantaloni, 1997; Schlueter *et al*., 1997). The profilin isoform II from *D. discoideum* was fused to the N-terminal of GFP separated by a 100-aa linker and the fusion protein subsequently characterized for its suitability for use in *in vivo* real-time examination of its involvement in the dynamic actin-related processes.

4.2.1 Partial rescue properties of the profilin-GFP fusion protein

A novel profilin II-GFP fusion protein of about 55 kDa has been generated in the profilin null *D. discoideum* mutant and the ability of the fusion protein to rescue the aberrant phenotype of the profilin null cells was investigated. In contrast to the profilin-minus cells whose capability to develop fruiting bodies was lost and only "finger" stage of development was observed, the profilin-GFP transformants were once again able to develop long stalks with sporangia at their tips. However, these fruiting bodies have a slightly different appearance as compared to those of the wild-type. The expression of the profilin-GFP fusion protein also helped to overcome the cytokinesis defect of the profilin null cells in shaking suspensions. The profilin-minus cells cannot grow in shaking cultures but are able to grow on surfaces as they accomplish cell division by traction-mediated cytofission (Zang *et al*., 1997), a myosin II-independent process (De Lozanne and Spudich, 1987; Knecht and Loomis, 1987; Pollenz *et al*., 1992; Neujahr *et al*., 1997). Intriguingly, the profilin-GFP transformants were found to exhibit an initial growth rate similar to that of the wild-type cells in shaking cultures only within the first two days. Thereafter, these cells appeared to reach a stationary phase and assumed a growth rate of the profilin null cells. Hence the profilin-GFP transformed cells are able to grow only within a short period of time even though these cells still harbour the expression vector and the fusion protein is still expressed.

In addition, normal cell morphology was restored in the profilin-GFP transformants. These transformants, unlike the profilin null cells which are multinucleate and up to ten times larger than wild-type cells (Haugwitz *et al*., 1994), possess the usual number of 1-2 nuclei per cell. The characteristic broad rim of F-actin accumulation around the edge of the profilin null cells

was also absent in these profilin-GFP transformants. Instead actin was found to be distributed at the leading edges of these cells as in the wild-type cells. Furthermore, the profilin-GFP fusion protein was observed to have an overall cytoplasmic localization similar to that of the native profilins in the wild-type cells.

4.2.2 *In vitro* analyses of the profilin-GFP fusion protein

The unique property of profilin's ability to bind poly-(L)-proline stretches (Bjoerkegren *et al*., 1993; Haarer *et al*., 1993; Metzler *et al*., 1993; Schutt *et al*., 1993; Archer *et al*., 1994; Kaiser and Pollard, 1996) was also investigated for the profilin-GFP fusion protein. In contrast to the wild-type profilins which were able to be sedimented with poly-(L)-proline coupled agarose beads, the profilin-GFP fusion protein has lost its ability to associate with poly-(L)-proline. However, an initial purification of this fusion protein by anion-exchange chromatography appeared to restore the ability of profilin-GFP, albeit to a small extent, to bind poly-(L)-proline coated beads. The possibility of competition binding between native profilins and the profilin-GFP fusion protein for the poly-(L)-proline sequences could be ruled out since the *D. discoideum* mutant lacking both profilin isoforms (Haugwitz *et al*., 1994) was used for transformation with the fusion construct. Likely explanations are that the initial purification step could have removed some of the unknown *D. discoideum* proline-rich cellular ligands, thus improving the ability of the fusion protein to interact with poly-(L)-proline coupled beads. The chromatography step could perhaps also lead to minor structural changes of the fusion protein via interference with its folding, hence slightly increasing its affinity for poly-(L)-proline. The loss of the ability of the fusion protein to associate with poly-(L)-proline could be due to the fact that both the amino- and carboxy-termini of profilin are implicated in ligand binding and interaction with poly-(L)-proline stretches. Mutations or deletions in these regions have confirmed their importance for poly-(L)-proline binding (Bjoerkegren *et al*., 1993; Metzler *et al*., 1994; Kaiser and Pollard, 1996), thus the fusion of GFP at the C-terminal end of profilin might decrease the interaction between the fusion protein and poly-(L)-proline.
The affinity of the fusion protein for actin was also examined. As a result of the much reduced association between the fusion protein and poly-(L)-proline, it was not possible to conveniently purify the fusion protein using a one-step poly-(L)-proline affinity chromatography (Tanaka and Shibata, 1985; Lindberg *et al*., 1988; Kaiser *et al*., 1989; Haarer *et al*., 1990; Metzler *et al*., 1993). In addition, due to the ability of the profilin-GFP transformants to be cultivated only within a limited period of time, it has not been possible to obtain large quantities of cells for protein purification. So, instead of using fluorescence

spectroscopy for kinetic measurements of the interaction between the fusion protein and actin (Kouyama and Mihashi, 1981), which will require at least a 1:1 ratio of wild-type profilin to actin, implying large amounts of the fusion protein would be necessary, the interaction between actin and the fusion protein was investigated by exploiting the ability of profilin to form stable profilin-actin complex or profilactin *in vivo* (Tilney *et al*., 1983; Pollard and Cooper, 1984; Kaiser *et al*., 1986). Gel chromatography revealed that the profilin-GFP fusion protein was eluted earlier in the presence of actin, suggesting that indeed there is interaction between the fusion protein and actin forming a larger complex which could be eluted earlier as compared to the elution pattern of the fusion protein alone. Of course, one could also argue that the different elution patterns of the fusion protein in the presence or absence of actin could be due to varied protein concentrations, whereby larger amounts of protein lead to a broader elution spectrum. However, preliminary data strongly suggest affinity between actin and the fusion protein. Further attempts to purify the fusion protein for kinetic studies of its effect on actin polymerization via the highly sensitive fluorescence spectroscopic method should help to clarify their interaction with each other. One probable purification method for the profilin-GFP fusion protein would be the use of a bovine pancreatic DNase I column since the monomeric actin-binding protein DNase I is able to form a tight 1:1 complex with monomeric actin (Mannherz *et al*., 1975; Nefsky and Bretscher, 1989). Hence it would be possible to isolate monomeric actin-binding proteins which have affinity for the actin-DNase I complex. This feature has been exploited in the purification of villin on immobilized DNase I from a cell extract harbouring both actin and villin (Bretscher and Weber, 1980). The use of actin-DNase I affinity purification of the profilin-GFP fusion protein should also provide hints on its actin-binding ability.

4.2.3 Profilin-GFP, a functional construct?

Previous experience from our lab has stressed the neccessity of a linker sequence separating profilin and the N-terminal of GFP in order to have a functional fusion protein with respect to its ability to bind poly-(L)-proline and whose expression in the profilin null *D. discoideum* helped to restore the fruiting phenotype. Fusion proteins containing a linker sequence of either 10-aa or 14-aa between profilin II and the N-terminal end of GFP have been made, but these were unable to bind poly-(L)-proline and could not restore the aberrant phenotype of the profilin null cells. Since the GFP is larger than profilin, steric hindrance caused by the GFP moiety might reduce the affinity of these fusion proteins for poly-(L)-proline stretches. The fusion of GFP to profilin might also lead to an alteration of its three-dimensional folding

which could interfere with the accessibility of the poly-(L)-proline binding site for its ligands, thus decreasing or even abolishing binding to poly-(L)-proline. Moreover, the much reduced affinity of these fusion proteins for the unknown *D. discoideum* proline-rich cellular ligands might also impair the development of fruiting bodies as the use of the W3N point-mutated profilin, with reduced affinity for poly-(L)-proline, has shown the importance of its poly-(L)-proline binding activity in the maintenance of normal cellular physiology (Lee *et al*., 2000). According to Geese *et al*. (2000), their GFP-profilin I constructs with GFP fused at either the N- or C-terminal end of profilin I did not work and they attributed it to steric interference caused by the large GFP. However, they found that an active fusion protein was generated when GFP was fused to the C-terminal end of profilin II via a 20-aa linker (Geese *et al*., 2000). Minor structural differences between profilin I and II (Lambrechts *et al*., 1997) might clarify the reason for the loss of functional activities of the GFP-profilin I fusion proteins since the poly-(L)-proline binding site on profilin II assumes an extended structure and thus it is not so easily masked by the fusion with GFP as compared to the smaller poly-(L)-proline binding site on profilin I (Nodelman *et al*., 1999). Hence, a longer linker between profilin and GFP might improve the ligand binding property of this fusion protein.

In this study, a new profilin-GFP construct has been made in which profilin II was fused to the N-terminal end of GFP via a 100-aa linker sequence. Due to its known 3-D structure (Fucini *et al*., 1997) whereby the N- and C-termini are at the direct opposite end of each other, this long linker is selected for the fusion of profilin to GFP, so that the larger GFP moiety is separated far away from the small profilin to avoid steric hindrance. Also, the 3-D folding of this fusion protein consisting a long linker might likely be in a conformation whereby all the functional sites on profilin are still accessible for ligand binding. But this profilin-GFP fusion protein was found to have a much reduced affinity for poly-(L)-proline. Thus the fusion of GFP to profilin seemed to interfere with the poly-(L)-proline binding activity of profilin and this is not surprising as both the N- and C-termini of profilin have been implicated in interaction with poly-(L)-proline stretches (Bjoerkegren *et al*., 1993; Metzler *et al*., 1994; Kaiser and Pollard, 1996). In particular, the C-terminal end of profilin has been shown to be quite sensitive to manipulations and the extreme C-terminal end of profilin has been suggested to be essential for poly-(L)-proline binding (Kaiser and Pollard, 1996). In spite of this, the human profilin isoform II has recently been successfully fused to the N-terminal of GFP (Geese *et al*., 2000) and the fusion protein was still found to possess fully active *in vitro* ligand-binding properties and *in vivo* it has been shown to have an active role in bacterial motility in *Listeria*-infected cells.

The partial restoration of normal cell physiology and the result that the *Dictyostelium* profilin-GFP fusion protein is recruited as efficiently as the wild-type profilin in phagocytic cup formation suggest this fusion protein as a feasible tool for studying profilin dynamics in living *D. discoideum* cells.

4.2.4 *Dictyostelium* profilin is involved in highly dynamic cellular processes

Confocal microscopy data from live *D. discoideum* cells transformed with profilin II-GFP showed that profilin is associated with the highly dynamic actin-related cellular processes. The fusion protein was found to have a predominant distribution at the cell cortex and was also transiently detected in macropinocytotic crowns, the leading edges of aggregating cells and the cell fronts during pseudopodial extension. These data were supported by a previous study of the distribution of fluorescent profilin in live *Acanthamoeba* cells which were syringe-loaded with rhodamine-labelled profilin II (Kaiser *et al*., 1999). In these loaded cells, profilin is uniformly distributed in the cytoplasm but is excluded from organelles, which include the nucleus, mitochondria, vacuoles and large vesicles. In addition, the fluorescent profilin was detected transiently near the plasma membrane at a site of macropinocytosis and it is also enriched in the lamellapodia of migrating cells (Kaiser *et al*., 1999). Similar distribution of fluorescent profilin has been observed in living vertebrate cells (Tarachandani and Wang, 1996) and plant cells (Vidali and Hepler, 1997). As for fixed cells, anti-profilin antibodies have been known to label the cytoplasm of amoebas (Tseng *et al*., 1984), plant cells (Vidali and Hepler, 1997) and vertebrate cells (Buss *et al*., 1992; Watanabe *et al*., 1997). The *D. discoideum* profilin II-GFP fusion protein was found to be excluded from nuclei similar to that observed in *Acanthamoeba* (Kaiser *et al*., 1999). However, profilin staining in nuclei has been previously reported (Mayboroda *et al*., 1997; Schlueter *et al*., 1998).

According to Geese *et al*. (2000), they have created a novel human profilin II-GFP fusion protein which was found to localize to focal contacts and the front of protruding lamellapodia in cultured vertebrate cells. Apparently, profilins seem to be involved in the regulation of the actin cytoskeleton as they have been localized to highly dynamic regions of migrating amoebas (Kaiser *et al*., 1999) and spreading cultured cells (Buss *et al*., 1992; Mayboroda *et al*., 1997; Geese *et al*., 2000). In addition, the distribution of GFP-VASP in spreading lamellapodia of cultured vertebrate cells (Rottner *et al*., 1999) might suggest an important role of the interaction between profilin and its proline-rich VASP ligand in the remodeling of the dynamic actin network.

4.3 Study of *D. discoideum* severin via GFP fusion

Severin, the Ca^{2+}-dependent F-actin fragmenting and capping protein from *D. discoideum*, was fused to the N-terminal end of GFP via a 10-aa linker sequence and the resultant fusion protein was characterized both *in vitro* and *in vivo*. The fusion of GFP to severin should allow direct observation and a better understanding of severin's involvement in the dynamic actin-associated cellular events occurring in real-time.

4.3.1 Severin-GFP is a functional fusion construct

Dictyostelium severin has been successfully fused to the N-terminus of a red-shifted variant of GFP separated by a 10-aa linker of the sequence SGEAEFKKLK which belongs to the sequence of the vector (Faix *et al*., 1992). Severin null transformed cells expressing the fusion protein showed an overall cytoplasmic distribution similar to that obtained by antibody labelling of native severin in vegetative cells (Brock and Pardee, 1988; André *et al*., 1989). In contrast, a nuclear label was also observed in these severin-GFP expressing cells which is most likely an artefact and could be probably explained by the linker sequence of the fusion protein whereby part of its sequence KKLK partially resembles the nuclear targeting signal PKKKRKV of SV40 (Kalderon *et al*., 1984).

A novel severin-GFP fusion protein of about 70 kDa has been generated in a *D. discoideum* mutant strain lacking the native severin protein. In order to determine its activity and suitability for use in real-time observation of severin dynamics in various cellular processes, the fusion protein has been purified to a partial extent from the *D. discoideum* transformants which lacked native severin, and analyzed *in vitro* for its severing activity. The purification procedure of severin-GFP follows that of native severin (Yamamoto *et al*., 1982; Schleicher *et al*., 1984) with slight variations. In contrast to native severin, the fusion protein does not have affinity for the cation-exchange resin anymore, so an additional step to separate the fusion protein by size via gel filtration was carried out before performing the hydroxylapatite chromatography. A second major difference is that the fusion protein could only be eluted with a phosphate gradient instead of a KCl gradient as in the case for severin.

Both experimental methods, low shear falling-ball viscometry and fluorescence spectroscopy measurements, showed that the severin-GFP fusion protein was able to fragment F-actin or reduce the viscosity of F-actin gels only in the presence of micromolar Ca^{2+}. Without Ca^{2+}, the severing activity of the fusion protein was found to be non-existent similar to that of native severin, thus distinguishing the viscosity decreasing effect of the fusion protein from that of the Cap32/34 F-actin capping protein (Hartmann *et al*., 1989; Eddy *et al*., 1996) by its

Ca^{2+} dependence. For the determination of the F-actin severing activity of the fusion protein by fluorescence spectroscopy, the actin filaments are usually precapped at their barbed ends for example with DS151, the capping domain of *D. discoideum* severin (Eichinger *et al*., 1991), to differentiate the F-actin severing activity of the fusion protein from its capping activity since severin is known to possess both activities which are able to reduce the viscosity of F-actin gels, whereby severin exerts its capping activity by preventing elongation of actin filaments at the barbed ends. When the barbed ends of microfilaments are precapped and the actin concentration is diluted to below its critical concentration at the pointed ends (Wegner and Isenberg, 1983), the presence of severing activity would raise the number of pointed ends, leading to a dramatic increase in the rate of actin depolymerization. In this study, the filament-severing activity of the severin-GFP fusion protein has not been properly measured, however, whether it caps or severs F-actin, the fusion protein harbours activity only when Ca^{2+} is present, indicating that severin-GFP is indeed an active fusion protein and could be used for further *in vivo* studies.

4.3.2 *In vivo* studies of severin dynamics

Despite severin being a highly active protein *in vitro*, the severin null *D. discoideum* mutant does not have any observable phenotypic difference from that of the wild-type cells (André *et al*., 1989) suggesting that severin is not essential for growth, cell motility or development. This is not so surprising, as knock-out mutants for some of the F-actin cross-linking proteins such as α-actinin, ABP120, Cortexillins I and II have shown only subtle changes for the single knock-out mutants while the double mutants have severe defects in either cytokinesis or development (Schleicher *et al*., 1988; Brink *et al*., 1990; Witke *et al*., 1992; Cox *et al*., 1995; Faix *et al*., 1996; Fisher *et al*., 1997; Rivero *et al*., 1998), leading to the suggestion of the redundancy of the cytoskeletal activities whereby the loss of a single actin-binding protein could probably be functionally compensated by other proteins (Witke *et al*., 1992). Besides severin, *D. discoideum* also harbours other F-actin fragmenting and capping proteins with viscosity decreasing activities like protovillin (Hofmann *et al*., 1993), villidin (unpublished data), the heterodimeric Cap32/34 capping protein (Schleicher *et al*., 1984; Hartmann *et al*., 1989) and probably some other unknown proteins which might have an overlapping role with severin. Thus the study of severin's involvement in various actin-related cellular processes via severin-GFP should improve our understanding of the behaviour of other functionally-related proteins.

The *in vivo* studies were made in collaboration with Timo Zimmermann (Zoological Institute, LMU, Munich). Confocal microscopy investigations of the severin-GFP fusion protein revealed transient accumulation of severin in macropinocytotic crowns, phagocytic cups, membrane ruffles and at the leading edge of motile cells. Severin is also enriched at the cell fronts of elongated cells moving towards a cyclic AMP (cAMP) source during chemotaxis and it too is localized at cell-cell contacts of aggregating cells at the cell fronts in the process of directed motion. Severin appears to be excluded from the process of pseudopodial extension, but was found to be associated with the forward movement of the cell body into the newly-formed pseudopod. In higher vertebrate cells, a *Xenopus* homolog of coronin or Xcoronin has been isolated and found also to have an overall cytoplasmic distribution with accumulations at the membrane ruffles. During cell spreading, Xcoronin was observed to be concentrated at the leading edges of lamellipodia (Mishima and Nishida, 1999). In the process of macropinocytosis, severin was observed to accumulate around the forming vesicle, whereby upon vesicle closure, severin became concentrated at the region distal to the vesicle and the label round the vesicle disappeared entirely within 30-40s during internalization. Various actin-binding proteins have been known to be involved in macropinocytosis, including coronin (Maniak *et al*., 1995; Hacker *et al*., 1997), myosin IB (Novak *et al*., 1995; Jung *et al*., 1996b), RacF1 GTPase (Rivero *et al*., 1999) and RasS GTPase (Chubb *et al*., 2000). Similar to RacF1 (Rivero *et al*., 1999), the duration of the severin label around the vesicle appears to be shorter than that of coronin (Hacker *et al*., 1997) and actin (Nolta *et al*., 1994; Adessi *et al*., 1995) which could be detected for up to 1 min around the vesicle.

In the course of phagocytosing yeast, a weak label of severin-GFP has been observed around the forming phagosome, which vanished within 30s after vesicle closure, suggesting an early involvement of severin in phagosome generation. This is in agreement with data obtained by antibody staining whereby cells feeding on a bacterial lawn formed phagocytic vesicles surrounded by a severin-rich cell cortex (Brock and Pardee, 1988). Other cytoskeletal proteins from *Dictyostelium* implicated to play a role in phagocytosis include coronin (Maniak *et al*., 1995), myosin IB (Fukui *et al*., 1989), a 30 kDa actin-bundling protein (Furukawa and Fechheimer, 1994), ABP120 (Cox *et al*., 1996) and RasS GTPase (Chubb *et al*., 2000). In vegetative cells, severin-GFP was observed to have an uniform cytoplasmic distribution as confirmed by antibody labelling (Brock and Pardee, 1988; André *et al*., 1989). Antibody staining for severin in aggregating cells showed also an uniform cytoplasmic labelling (Brock and Pardee, 1988; André *et al*., 1989), which is in marked contrast to the *in vivo* data. The highly resolving confocal studies revealed that during early aggregation phase, the fusion

protein was concentrated at the leading edge of these polarized moving cells. Similarly, cells moving towards a chemotatic source also displayed prominent severin localization at the cell fronts as observed for the coronin-GFP fusion protein (Gerisch *et al*., 1995). Together with the observation that severin is not directly involved in pseudopod extension, but rather in the movement of the cell body into the newly generated pseudopod, these data suggest that severin is involved in the establishment of a new cell front. In addition, cells in aggregation streams showed concentration of severin at the front of each cell, at the site of its contact with the preceding cell, similar to that observed with a GFP-actin fusion protein (Westphal *et al*., 1997). Myosin I has also been shown to localize to the leading edges of migrating *Dictyostelium* amoebae (Fukui *et al*., 1989) and similar distributions of other myosin I isozymes are detected in pseudopods of locomoting leukocytes and macrophages (Stendahl *et al*., 1980; Valerius *et al*., 1981).

Thus far, in randomly motile vegetative cells, severin has been observed not to be involved in the early step of pseudopod extension by a stationary cell body, as opposed to cell motion, whereby the forward movement of the cell body induces an accumulation of severin at the cell front. Supported also by antibody studies (Brock and Pardee, 1988), the localization of severin at the continuously restructuring edges, regions whereby extensive actin cytoskeletal rearrangement occurs, be it at macropinocytotic crowns, phagocytic cups, membrane ruffles or leading edges of locomoting cells, indicates an *in vivo* role for severin in the remodelling of existing F-actin structures which agrees with its *in vitro* actin fragmenting activity. Furthermore, recent data from the study of the small GTPase RacF1, whereby it has been found to be excluded from pseudopods during protrusion but reconstitutes itself to the cortex upon ceasure of the pseudopod extension (Rivero *et al*., 1999), showed similar behaviour to severin, suggesting redistribution of some cytoskeletal proteins after pseudopod extension. The parallel expressions of GFP-actin or some other GFP-labelled actin-binding proteins, such as the F-actin-binding GFP-ABD from the gelation factor ABP120 (Pang *et al*., 1998), and severin-GFP together in the same cells should clarify further the interaction between severin and the actin cytoskeleton simultaneously and provide a better understanding of severin's role in the regulation of various actin-based processes.

4.4 *Y. enterocolitica* infection and the actin cytoskeleton

In the infection studies, the mammalian cells COS7 were infected with either *Y. enterocolitica* wild-type strain (WA-P) or a virulence plasmid-cured strain (WA-C) and the behaviour of the cytoskeleton was monitored by antibody labellings of selected cytoskeletal proteins of the

infected cells. Additionally, the *in vivo* dynamics of actin, cofilin and profilin II in infected cells were examined via fusion of these proteins to GFP with the aid of the highly resolving confocal laser scanning microscopy (CLSM).

4.4.1 Indirect immunofluorescence study of selected cytoskeletal proteins in *Y. enterocolitica* infected cells

Antibodies specific for human vinculin or talin showed no difference in their labellings in both the uninfected and the WA-P or WA-C infected mammalian cells, suggesting there is no alterations for example in the size or distribution of these focal adhesion proteins in the presence or absence of the Yop effectors. Similarly, an anti-ß-COP antibody revealed in the WA-P or WA-C infected cells Golgi stainings which resembled those of the uninfected cells, leading to the suggestion that the Golgi network is not affected by the Yops. So far, a translocated *Yersinia* effector, YopH has been known to dephosphorylate the focal adhesion proteins, $p130^{Cas}$ (Sakai *et al*., 1994; Burnham *et al*., 1996) and FAK (Richardson and Parsons, 1995), leading to dissembly of focal contacts and impairing bacterial uptake by host cells. Using the antibody approach in this study did not reveal any disruption of the focal adhesion proteins, at least not for vinculin and talin. Alternatively, the remodelling of cytoskeletal proteins could be investigated by their fusions to GFP so that artefacts generated via immunolabelling could be avoided, and abovemost, GFP-tagged proteins allow direct observation of their dynamics in living cells which could be easily resolved with confocal microscopy.

4.4.2 *Y. enterocolitica* infection disrupts the actin cytoskeleton

The behaviours of GFP-tagged actin, cofilin and profilin II in mammalian cells during *Y. enterocolitica* infection were investigated using CLSM. GFP-profilin was observed to have an uniform cytoplasmic distribution as supported by data obtained with various anti-profilin antibodies which labelled the cytoplasm of amoebas (Tseng *et al*., 1984; Kaiser *et al*., 1999), plant cells (Vidali and Hepler, 1997) and vertebrate cells (Buss *et al*., 1992; Watanabe *et al*., 1997). In addition, nuclear labels were observed for cells transfected with GFP-profilin. The significance of GFP-profilin in the nucleus is unclear, however, some profilin antibodies were found capable of staining the nuclei of fixed cells (Tseng *et al*., 1984; Mayboroda *et al*., 1997; Schlueter *et al*., 1998). Like the uninfected cells, mammalian cells infected with either a *Yersinia* wild-type strain or a Yops secretion minus strain showed similar overall cytoplasmic localization of GFP-profilin, suggesting that the translocated Yop effectors do not have any

major effect on the distribution of GFP-profilin and that profilin might not be the host's target of Yops.

For the study of actin dynamics during *Y. enterocolitica* infection, the distribution of GFP-actin fluorescence of transfected mammalian cells was compared with the F-actin localization via phalloidin staining. Data showed similar actin labellings with both approaches in the uninfected cells and also in the WA-P or WA-C infected cells, indicating the authenticity of the GFP-actin staining. At the sites of bacterial attachment, actin-rich phagocytic cup-like structures were observed for both WA-P and WA-C infected cells, suggesting that the mammalian cells respond already upon adhesion of *Y. enterocolitica*, and that this is a non-specific reaction of the host cells in response to bacterial infection independent of the Yop effectors since similar F-actin structures were generated in the presence or absence of secreted Yops. This remodelling of the actin cytoskeleton could perhaps involve the Rho family of small GTPases, as Rac and Cdc42 have been shown to be required for phagocytic cup formation and membrane ruffling in macrophages and leukocytes (Cox *et al*., 1997; Dharmawardhane *et al*., 1999).

In addition, after about 30 min of infection with WA-P, the GFP-actin staining started to disappear and dispersed actin patches were observed whereby up to 2 h of infection, the actin cytoskeleton was completely disrupted and reorganized for the rounding up of cells, brought about by the cytotoxic effect of the Yops. On the contrary, cells infected with a Yop secretion minus strain exhibited similar actin labelling as the uninfected cells with a cytoplasmic distribution of actin concentrated at the cortical regions whereby up to 2 h of infection, the cells still retained their spreading, flattened phenotype. These data showing the actin-disrupting activity of Yops with the use of GFP-tagged actin are in agreement with that obtained with phalloidin staining of actin, whereby two particular secreted *Yersinia* proteins, YopE (Rosqvist *et al*., 1991) and YopT (Iriarte and Cornelis, 1998) have been shown to dissemble actin filaments with YopT being suggested to exert a stronger cytotoxic effect than YopE (Iriarte and Cornelis, 1998; Zumbihl *et al*., 1999). The existence of homology between YopE and exoenzyme S (ExoS), a *Pseudomonas* ADP-ribosylating exotoxin (Kreuger and Barbieri, 1995; Yahr *et al*., 1996) harbouring also actin disrupting activity (Frithz-Lindsten *et al*., 1997), suggests the likelihood that YopE targets the small GTPases since ExoS has been reported to modify these signalling molecules (Coburn *et al*., 1989b; Pederson *et al*., 1999). In fact, YopT of *Y. enterocolitica* has recently been shown to be the first intracellularly translocated cytotoxin to act via modification of the small GTP-binding protein RhoA

(Zumbihl *et al*., 1999) whereby the use of a YopE mutant still expressing the cytotoxic activity of YopT led to the disruption of RhoA-mediated actin stress fibres.

As for the small actin-binding protein, cofilin, which formed actin-cofilin rods as observed via GFP-cofilin fluorescence, it was found to have similar distribution both in the uninfected cells and cells infected with a Yop secretion minus strain. However, infection of mammalian cells with the wild-type *Y. enterocolitica* after 1 h revealed a decrease in the length of the actin-cofilin rods, leading to several possible proposals. Firstly, the actin dissembling activity of the translocated Yops might prevent formation of long actin-cofilin rods. Secondly, since cofilin has been known to reversibly mediate actin polymerization and depolymerization in a pH-dependent way (Yonezawa *et al*., 1985; Abe *et al*., 1989; Hawkins *et al*., 1993), the Yops could perhaps regulate cofilin's ability to disrupt actin filaments via alteration of the host's cellular pH, thus forming shorter actin-cofilin rods. Last but not least, it has been suggested that in higher vertebrates, the subcellular distribution of cofilin as well as its interaction with actin *in vivo* is mediated by its phosphorylation and dephosphorylation (Nagaoka *et al*., 1996; Obinata *et al*., 1997). The actin-binding activity of cofilin has been demonstrated to be negatively regulated by phosphorylation on its Ser 3 residue (Abe *et al*., 1992; Agnew *et al*., 1995; Moriyama *et al*., 1996; Nagaoka *et al*., 1996) and that phosphorylated cofilin failed to interact with actin and showed only diffuse cytoplasmic distribution. Hence the Yops could possibly lead to modification of cofilin via phosphorylation, whereby this phosphorylated form of cofilin could no longer associate with actin, leading to its diffuse distribution in the cytoplasm and the lack of visible long actin-cofilin rods.

Further studies of the influence of *Yersinia* infection on the actin cytoskeleton could include the use of selected Yop mutants for correlation of particular Yop effector with its target host's cytoskeletal protein. It will also be useful to express simultaneously GFP-fused Yops with selected cytoskeletal proteins tagged with variants of GFP to allow direct observation of their interactions with Yops, and to examine the actin dynamics in the *Dictyostelium* amoeba system as its actin-based motile processes are similar to that of the leukocytes.

5 REFERENCES

Abe, H., Ohshima, S. and Obinata, T. (1989). A cofilin-like protein is involved in the regulation of actin assembly in developing skeletal muscle. *J. Biochem*. (Tokyo) **106**:696-702.

Abe, H., Okada, K. and Obinata, T. (1992). Localization of cofilin and its interaction with actin in cultured fibroblasts. *Cell Struct. Funct*. **17**:482.

Adachi, H., Hasebe, T., Yoshinaga, K., Ohta, T. and Sutoh, K. (1994). Isolation of *Dictyostelium discoideum* cytokinesis mutants by restriction enzyme-mediated integration of the blasticidin S resistance marker. *Biochem. Biophys. Res. Comm*. **205**:1808-1814.

Adessi, C., Chapel, A., Vincon, M., Rabilloud, T., Klein, G., Satre, M. and Garin, J. (1995). Identification of major proteins associated with *Dictyostelium discoideum* endocytic vesicles. *J. Cell Sci*. **108**:3331-3337.

Agnew, B.J., Minamide, L.S. and Bamburg, J.R. (1995). Reactivation of phosphorylated actin depolymerizing factor and identification of the regulatory site. *J. Biol. Chem*. **270**:17582-17587.

Aizawa, H., Sutoh, K., Tsubuki, S., Kawashima, S., Ishii, A. and Yahara, I. (1995). Identification, characterization, and intracellular distribution of cofilin in *Dictyostelium discoideum*. *J. Biol. Chem*. **270**:10923-10932.

Aizawa, H., Fukui, Y. and Yahara, I. (1997). Live dynamics of *Dictyostelium* cofilin suggests a role in remodeling actin latticework into bundles. *J. Cell Sci*. **110**:2333-2344.

Aktories, K. (1997). Bacterial toxins that target Rho proteins. *J. Clin. Invest*. **99**:827-829.

Aktories, K., Weller, U. and Chhatwal, G.S. (1987). *Clostridium botulinum* type C produces a novel ADP-ribosyltransferase distinct from *botulinum* C2 toxin. *FEBS Lett*. **212**:109-113.

Aktories, K., Mohr, C. and Koch, G. (1992). *Clostridium botulinum* C3 ADP-ribosyltransferase. *Curr. Top. Microbiol. Immunol*. **175**:115-131.

Allaoui, A., Schulte, R. and Cornelis, G.R. (1995). Mutational analysis of the *Yersinia enterocolitica virC* operon: characterization of *yscE*, *F*, *G*, *I*, *J*, *K* required for Yop secretion and *yscH* encoding YopR. *Mol. Microbiol*. **18**:343-355.

Allen, L.H. and Aderem, A. (1995). A role for MARCKS, the alpha isozyme of protein kinase C and myosin I in zymosan phagocytosis by macrophages. *J. Exp. Med*. **182**:829-840.

André, E., Lottspeich, F., Schleicher, M. and Noegel, A.A. (1988). Severin, gelsolin, and villin share a homologous sequence in regions presumed to contain F-actin severing domains. *J. Biol. Chem*. **263**:722-727.

André, E., Brink, M., Gerisch, G., Isenberg, G., Noegel, A., Schleicher, M., Segall, J.E. and Wallraff, E. (1989). A *Dictyostelium* mutant deficient in severin, an F-actin fragmenting protein, shows normal motility and chemotaxis. *J. Cell Biol*. **108**:985-995.

Archer, S.J., Vinson, V.K., Pollard, T.D. and Torchia, D.A. (1994). Elucidation of the poly-L-proline binding site in *Acanthamoeba* profilin I by NMR spectroscopy. *FEBS Lett*. **337**:145-151.

Baker, J.P. and Titus, M.A. (1998). Myosins: matching functions with motors. *Curr. Biol*. **10**:80-86.

Balasubramanian, M.K., Hirani, B.R., Burke, J.D. and Gould, K.L. (1994). The *Schizosaccharomyces pombe* cdc3+ gene encodes a profilin essential for cytokinesis. *J. Cell Biol*. **125**:1289-1301.

Barkalow, K. and Hartwig, J.H. (1995). Setting the pace of cell movement. *Curr. Biol*. **5**:1000-1002.

Bergman, T., Erickson, K., Galyov, E., Persson, C. and Wolf-Watz, H. (1994). The *lcrB* (*yscN/U*) gene cluster of *Yersinia pseudotuberculosis* is involved in Yop secretion and shows high homology to the *spa* gene cluster of *Shigella flexneri* and *Salmonella typhimurium*. *J. Bacteriol*. **176**:2619-2626.

Bergman, T., Hakansson, S., Forsberg, A., Norlander, L., Macellaro, A., Baeckman, A., Boelin, I. and Wolf-Watz, H. (1991). Analysis of the V antigen *lcrGVH-yopBD* operon of *Yersinia pseudotuberculosis*: evidence for a regulatory role of LcrH and LcrV. *J. Bacteriol*. **173**:1607-1616.

Bernardini, M.L., Mounier, J., D'Hauteville, H., Coquis-Rondon, M. and Sansonetti, P.J. (1989). Identification of *icsA*, a plasmid locus of *Shigella flexneri* that governs bacterial intra- and intercellular spread through interaction with F-actin. *Proc. Natl. Acad. Sci. USA* **86**:3867-3871.

Bjoerkegren, C., Rozycki, M., Schutt, C.E., Lindberg, U. and Karlsson, R. (1993). Mutagenesis of human profilin locates its poly(L-proline)-binding site to a hydrophobic patch of aromatic amino acids. *FEBS Lett*. **333**:123-126.

Bjoerkegren-Sjoegren, C., Korenbaum, E., Nordberg, P., Lindberg, U. and Karlsson, R. (1997). Isolation and characterization of two mutants of human profilin I that do not bind poly(L-proline). *FEBS Lett*. **418**:258-264.

Black, D.S. and Bliska, J.B. (1997). Identification of $p130^{Cas}$ as a substrate of *Yersinia* YopH (Yop51), a bacterial protein tyrosine phosphatase that translocates into mammalian cells and targets focal adhesions. *EMBO J*. **16**:2730-2744.

Bliska, J.B., Galan, J.E. and Falkow, S. (1993). Signal transduction in the mammalian cell during bacterial attachment and entry. *Cell* **73**:903-920.

Boelin, I., Norlander, L. and Wolf-Watz, H. (1982). Temperature-inducible outer membrane protein of *Yersinia pseudotuberculosis* and *Yersinia enterocolitica* is associated with the virulence plasmid. *Infect. Immun*. **37**:506-512.

Boland, A., Sory, M.P., Iriarte, M., Kerbourch, C., Wattiau, P. and Cornelis, G.R. (1996). Status of YopM and YopN in the *Yersinia* Yop virulon: YopM of *Y. enterocolitica* is internalized inside the cytosol of PU5-1.8 macrophages by the YopB, D, N delivery apparatus. *EMBO J*. **15**:5191-5201.

Bradford, M.M. (1976). A rapid and sensitive method for the quantitation of microgram quantities of protein utilizing the principle of protein dye-binding. *Anal. Biochem*. **72**:248-254.

Bretscher, A. and Weber, K. (1979). Villin: the major microfilament associated protein of the intestinal microvillus. *Proc. Natl. Acad. Sci. USA* **76**:2321-2325.

Bretscher, A. and Weber, K. (1980). Villin is a major protein of the microvillus cytoskeleton which binds both G and F actin in a calcium-dependent manner. *Cell* **20**:839-847.

Brink, M., Gerisch, G., Isenberg, G., Noegel, A.A., Segall, J.E., Wallraff, E. and Schleicher, M. (1990). A *Dictyostelium* mutant lacking an F-actin cross-linking protein, the 120-kD gelation factor. *J. Cell Biol*. **111**:1477-1489.

Brock, A.M. and Pardee, J.D. (1988). Cytoimmunofluorescent localization of severin in *Dictyostelium* amoebae. *Dev. Biol*. **128**:30-39.

Brown, S.S., Yamamoto, K. and Spudich, J.A. (1982). A 40,000-dalton protein from *Dictyostelium discoideum* affects assembly properties of actin in a Ca^{2+}-dependent manner. *J. Cell Biol*. **93**:205-210.

Burnham, M.R., Harte, M.T., Richardson, A., Parsons, J.T. and Bouton, A.H. (1996). The identification of $p130^{Cas}$-binding proteins and their role in cellular transformation. *Oncogene* **12**:2467-2472.

Buss, F., Temm-Grove, C., Henning, S. and Jockusch, B. (1992). Distribution of profilin in fibroblasts correlates with the presence of highly dynamic actin filaments. *Cell Motil. Cytoskel*. **22**:51-61.

Carlier, M.F. and Pantaloni, D. (1994). Actin assembly in response to extracellular signals: role of capping proteins, thymosin ß4 and profilin. *Sem. Cell Biol*. **5**:183-191.

Carlier, M.F. and Pantaloni, D. (1997). Control of actin dynamics in cell motility. *J. Mol. Biol*. **269**:459-467.

Carlsson, L., Nystrom, L.E., Sundkvist, I., Markey, F. and Lindberg, U. (1977). Actin polymerizability is influenced by profilin, a low molecular weight protein in nonmuscle cells. *J. Mol. Biol*. **115**:465-483.

Cassel, D. and Selinger, Z. (1977). Mechanism of adenylate cyclase activation by *cholera* toxin: Inhibition of GTP hydrolysis at the regulatory site. *Proc. Natl. Acad. Sci. USA* **74**:3307-3311.

Castrillon, D.H. and Wasserman, S.A. (1994). Diaphanous is required for cytokinesis in *Drosophila* and shares domains of similarity with the products of the limb deformity gene. *Development* **120**:3367-3377.

Cedegren-Zeppezauer, E.S., Goonesekere, N.C., Rozycki, M.D., Myslik, J.C., Dauter, Z., Lindberg, U. and Schutt, C.E. (1994). Crystallization and structure determination of bovine profilin at 2.0 A resolution. *J. Mol. Biol*. **240**:459-475.

Chakraborty, T., Ebel, F., Domann, E., Niebuhr, K., Gerstel, B., Pistor, S., Temm-Grove, C.J., Jockusch, B.M., Reinhard, M. and Walter, U. (1995). A focal adhesion factor directly linking intracellularly motile *Listeria monocytogenes* and *Listeria ivanovii* to the actin-based cytoskeleton of mammalian cells. *EMBO J*. **14**:1314-1321.

Chalfie, M., Tu, Y., Euskirchen, G., Ward, W.W. and Prasher, D.C. (1994). Green fluorescent protein as a marker for gene expression. *Science* **263**:802-805.

Choidas, A., Jungbluth, A., Sechi, A., Murphy, J., Ullrich, A. and Marriott, G. (1998). The suitability and application of a GFP-actin fusion protein for long-term imaging of the organization and dynamics of the cytoskeleton in mammalian cells. *Eur. J. Cell Biol*. **77**:81-90.

Christensen, H.E.M., Ramachandran, S., Tan, C.T., Surana, U., Dong, C.H. and Chua, N.H. (1996). *Arabidopsis* profilins are functionally similar to yeast profilins- identification of a vascular bundle-specific profilin and a pollen-specific profilin. *Plant J*. **10**:269-279.

Chubb, J.R., Wilkins, A., Thomas, G.M. and Insall, R.H. (2000). The *Dictyostelium* RasS protein is required for macropinocytosis, phagocytosis and the control of cell movement. *J. Cell Sci*. **113**:709-719.

Claviez, M., Pagh, K., Maruta, H., Baltes, W., Fisher, P. and Gerisch, G. (1982). Electron microscopic mapping of monoclonal antibodies on the tail region of *Dictyostelium* myosin. *EMBO J*. **1**:1017-1022.

Coburn, J. and Gill, D.M. (1991). ADP-ribosylation of $p21^{ras}$ and related proteins by *Pseudomonas aeruginosa* exoenzyme S. *Infect. Immun*. **59**:4259-4262.

Coburn, J., Dillon, S., Iglewski, B.H. and Gill, D.M. (1989a). Exoenzyme S of *Pseudomonas aeruginosa* ADP-ribosylates the intermediate filament protein vimentin. *Infect. Immun*. **57**:996-998.

Coburn, J., Wyatt, R.T., Iglewski, B.H. and Gill, D.M. (1989b). Several GTP-binding proteins, including p21c-H-ras are preferred substrates of *Pseudomonas aeruginosa* exoenzyme S. *J. Biol. Chem*. **264**:9004-9008.

Condeelis, J. and Vahey, M. (1982). A calcium- and pH-regulated protein from *Dictyostelium discoideum* that cross-links actin filaments. *J. Cell Biol*. **94**:466-471.

Cooley, L., Verheyen, E. and Ayers, K. (1992). Chickadee encodes a profilin required for intercellular cytoplasm transport during *Drosophila* oogenesis. *Cell* **69**:173-184.

Cornelis, G.R. and Wolf-Watz, H. (1997). The *Yersinia* Yop virulon: a bacterial system for subverting eukaryotic cells. *Mol. Microbiol*. **23**:861-867.

Cornelis, G.R., Boland, A., Boyd, A.P., Geuijen, C., Iriarte, M., Neyt, C., Sory, M.P. and Stainier, I. (1998). The virulence plasmid of *Yersinia*, an antihost genome. *Microbiol. Mol. Biol. Rev*. **62**:1315-1352.

Cossart, P. and Kocks, C. (1994). The actin-based motility of the facultative intracellular pathogen *Listeria monocytogenes*. *Mol. Microbiol*. **13**:395-402.

Cox, D., Ridsdale, J.A., Condeelis, J. and Hartwig, J. (1995). Genetic deletion of ABP-120 alters the three-dimensional organization of actin filaments in *Dictyostelium* pseudopods. *J. Cell Biol*. **128**:819-835.

Cox, D., Wessels, D., Soll, D.R., Hartwig, J. and Condeelis, J. (1996). Re-expression of ABP-120 rescues cytoskeletal, motility, and phagocytosis defects of ABP-120 *Dictyostelium* mutants. *Mol. Biol. Cell* **7**:803-823.

Cox, D., Chang, P., Zhang, Q., Reddy, P.G., Bokoch, G.M. and Greenberg, S. (1997). Requirements for both Rac1 and Cdc42 in membrane ruffling and phagocytosis in leukocytes. *J. Exp. Med*. **186**:1487-1494.

Critchley, D.R. (2000). Focal adhesions- the cytoskeletal connection. *Curr. Opin. Cell Biol*. **12**:133-139.

Cudmore, S., Cossart, P., Griffiths, G. and Way, M. (1995). Actin-based motility of *vaccinia* virus. *Nature* **378**:636-638.

Cudmore, S., Reckmann, I., Griffiths, G. and Way, M. (1996). *Vaccinia* virus: a model system for actin-membrane interactions. *J. Cell Sci*. **109**:1739-1747.

De Lozanne, A. and Spudich, J.A. (1987). Disruption of the *Dictyostelium* myosin heavy chain gene by homologous recombination. *Science* **236**:1086-1091.

DePasquale, J.A. and Izzard, C.S. (1991). Accumulation of talin in nodes at the edge of the lamellipodium and separate incorporation into adhesion plaques at focal contacts in fibroblasts. *J. Cell Biol*. **113**:1351-1359.

Devereux, J., Haeberli, P. and Smithies, O. (1984). A comprehensive set of sequence analysis programs for the VAX. *Nucl. Acids Res*. **12**:387-395.

Devreotes, P.N. and Zigmond, S.H. (1988). Chemotaxis in eukaryotic cells: a focus on leukocytes and *Dictyostelium. Ann. Rev. Cell Biol*. **4**:649-686.

Dharmawardhane, S., Brownson, D., Lennartz, M. and Bokoch, G.M. (1999). Localization of p21-activated kinase 1 (PAK1) to pseudopodia, membrane ruffles, and phagocytic cups in activated human neutrophils. *J. Leukoc. Biol*. **66**:521-527.

Doering, V., Schleicher, M. and Noegel, A.A. (1991). *Dictyostelium* annexin VII (synexin) cDNA sequence and isolation of a gene disruption mutant. *J. Biol. Chem*. **266**:17509-17515.

Domann, E., Wehland, J., Rohde, M., Pistor, S., Hartl, M., Goebel, W., Leimeister-Wachter, M., Wuenscher, M. and Chakraborty, T. (1992). A novel bacterial virulence gene in *Listeria monocytogenes* required for host cell microfilament interaction with homology to the proline-rich region of vinculin. *EMBO J*. **11**:1981-1990.

Doyle, T. and Botstein, D. (1996). Movement of yeast cortical actin cytoskeleton visualized *in vivo*. *Proc. Natl. Acad. Sci. USA* **93**:3886-3891.

Duden, R., Griffiths, G., Frank, R., Argos, P. and Kreis, T.E. (1991). Beta-COP, a 110 kd protein associated with non-clathrin-coated vesicles and the Golgi complex, shows homology to beta-adaptin. *Cell* **64**:649-665.

Duden, R., Hosobuchi, M., Hamamoto, S., Winey, M., Byers, B. and Schekman, R. (1994). Yeast beta- and beta‘-coat proteins (COP). Two coatomer subunits essential for endoplasmic reticulum-to-Golgi protein traffic. *J. Biol. Chem*. **269**:24486-24495.

Eddy, R.J., Han, J., Sauterer, R.A. and Condeelis, J.S. (1996). A major agonist-regulated capping activity in *Dictyostelium* is due to the capping protein, cap32/34. *Biochim. Biophys. Acta* **1314**:247-259.

Egelhoff, T.T., Brown, S.S., Manstein, D.J. and Spudich, J.A. (1989). Hygromycin as a selectable marker in *Dictyostelium discoideum*. *Mol. Cell Biol*. **9**:1965-1968.

Egile, C., Loisel, T.P., Laurent, V., Li, R., Pantaloni, D., Sansonetti, P.J. and Carlier, M.F. (1999). Activation of the Cdc42 effector N-WASP by the *Shigella flexneri* IcsA protein promotes actin nucleation by Arp2/3 complex and bacterial actin-based motility. *J. Cell Biol*. **146**:1319-1332.

Eichinger, L. and Schleicher, M. (1992). Characterization of actin- and lipid-binding domains in severin, a Ca^{2+}-dependent F-actin fragmenting protein. *Biochemistry* **31**:4779-4787.

Eichinger, L., Noegel, A.A. and Schleicher, M. (1991). Domain structure in actin-binding proteins: expression and functional characterization of truncated severin. *J. Cell Biol*. **112**:665-676.

Eichinger, L., Lee, S.S. and Schleicher, M. (1999). *Dictyostelium* as model system for studies of the actin cytoskeleton by molecular genetics. *Microscopy Res. Technique* **47**:124-134.

Eichinger, L., Baehler, M., Dietz, M., Eckerskorn, C. and Schleicher, M. (1998). Characterization and cloning of a *Dictyostelium* Ste20-like protein kinase that phosphorylates the actin-binding protein severin. *J. Biol. Chem*. **273**:12952-12959.

Emmons, S., Phan, H., Calley, J., Chen, W., James, B. and Manseau, L. (1995). *cappuccino*, a *Drosophila* maternal effect gene required for polarity of the egg and embryo, is related to the vertebrate *limb deformity* locus. *Genes Dev*. **9**:2482-2494.

Endow, S.A. and Komma, D.J. (1997). Spindle dynamics during meiosis in *Drosophila* oocytes. *J. Cell Biol*. **137**:1321-1336.

Faellman, M., Andersson, K., Hakansson, S., Magnusson, K.E., Stendahl, O. and Wolf-Watz, H. (1995). *Yersinia pseudotuberculosis* inhibits Fc receptor-mediated phagocytosis in J774 cells. *Infect. Immun*. **63**:3117-3124.

Faix, J., Gerisch, G. and Noegel, A.A. (1992). Overexpression of the csA cell adhesion molecule under its own cAMP-regulated promoter impairs morphogenesis in *Dictyostelium*. *J. Cell Sci*. **102**:203-214.

Faix, J., Steinmetz, M., Boves, H., Kammerer, R.A., Lottspeich, F., Mintert, U., Murphy, J., Stock, A., Aebi, U. and Gerisch, G. (1996). Cortexillins, major determinants of cell

shape and size, are actin-bundling proteins with a parallel coiled-coil tail. *Cell* **86**:631-642.

Falkow, S., Isberg, R.R. and Portnoy, D.A. (1992). The interaction of bacteria with mammalian cells. *Ann. Rev. Cell Biol*. **8**:333-363.

Fechheimer, M., Brier, J., Rockwell, E., Luna, E.J. and Taylor, D.L. (1982). A calcium- and pH-regulated actin-binding protein from *D. discoideum*. *Cell Motil*. **2**:287-308.

Fedorov, A.A., Magnus, K.A., Graupe, M.H., Lattman, E.E., Pollard, T.D. and Almo, S.C. (1994). X-ray structures of isoforms of the actin-binding protein profilin that differ in their affinity for phosphatidylinositol phosphates. *Proc. Natl. Acad. Sci. USA* **91**:8636-8640.

Finidori, J., Friedrich, E., Kwiatkowski, D.J. and Louvard, D. (1992). *In vivo* analysis of functional domains from villin and gelsolin. *J. Cell Biol*. **116**:1145-1155.

Fisher, P.F., Noegel, A.A., Fechheimer, M., Rivero, F., Prassler, J. and Gerisch, G. (1997). Photosensory and thermosensory responses in *Dictyostelium* slugs are specifically impaired by absence of the F-actin cross-linking gelation factor (ABP-120). *Curr. Biol*. **7**:889-892.

Flatau, G., Lemichez, E., Gauthier, M., Chardin, P., Paris, S., Fiorentini, C. and Boquet, P. (1997). Toxin-induced activation of the G protein p21 Rho by deamidation of glutamine. *Nature* **387**:729-733.

Forsberg, A. and Wolf-Watz, H. (1990). Genetic analysis of the *yopE* region of *Yersinia* spp.: identification of a novel conserved locus, *yerA*, regulating *yopE* expression. *J. Bacteriol*. **172**:1547-1555.

Forsberg, A., Viitanen, A.M., Skurnik, M. and Wolf-Watz, H. (1991). The surface-located YopN protein involved in calcium signal transduction in *Yersinia pseudotuberculosis*. *Mol. Microbiol*. **5**:977-986.

Forsberg, A., Rosqvist, R. and Wolf-Watz, H. (1994). Regulation and polarized transfer of the *Yersinia* outer proteins (Yops) involved in antiphagocytosis. *Trends Microbiol*. **2**:14-19.

Frischknecht, F., Cudmore, S., Moreau, V., Reckmann, I., Roettger, S. and Way, M. (1999). Tyrosine phosphorylation is required for actin-based motility of *vaccinia* but not *Listeria* or *Shigella*. *Curr. Biol*. **9**:89-92.

Frithz-Lindsten, E., Du, Y., Rosqvist, R. and Forsberg, A. (1997). Intracellular targeting of exoenzyme S of *Pseudomonas aeruginosa* via type III-dependent translocation

induces phagocytosis resistance, cytotoxicity and disruption of actin microfilaments. *Mol. Microbiol*. **25**:1125-1139.

Fucini, P., Renner, C., Herberhold, C., Noegel, A.A. and Holak, T.A. (1997). The repeating segments of the F-actin cross-linking gelation factor (ABP-120) have an immunoglobulin-like fold. *Nat. Struct. Biol*. **4**:223-230.

Fukui, Y., Lynch, T.J., Brzeska, H. and Korn, E.D. (1989). Myosin I is located at the leading edges of locomoting *Dictyostelium* amoebae. *Nature* **341**:328-331.

Furukawa, R. and Fechheimer, M. (1994). Differential localization of alpha-actinin and the 30 kD actin-bundling protein in the cleavage furrow, phagocytic cup, and contractile vacuole of *Dictyostelium discoideum*. *Cell Motil. Cytoskel*. **29**:46-56.

Galyov, E.E., Hakansson, S., Forsberg, A. and Wolf-Watz, H. (1993). A secreted protein kinase of *Yersinia pseudotuberculosis* is an indispensable virulence determinant. *Nature* **361**:730-732.

Galyov, E.E., Hakansson, S. and Wolf-Watz, H. (1994). Characterization of the operon encoding the YpkA Ser/Thr protein kinase and the YopJ protein of *Yersinia pseudotuberculosis*. *J. Bacteriol*. **176**:4543-4548.

Ganesan, A.K., Frank, D.W., Misra, R.P., Schmidt, G. and Barbieri, J.T. (1998). *Pseudomonas aeruginosa* exoenzyme S ADP-ribosylates ras at multiple sites. *J. Biol. Chem*. **273**:7332-7337.

Geese, M., Schlueter, K., Rothkegel, M., Jockusch, B.M., Wehland, J. and Sechi, A.S. (2000). Accumulation of profilin II at the surface of *Listeria* is concomitant with the onset of motility and correlates with bacterial speed. *J. Cell Sci*. **113**:1415-1426.

Gerisch, G., Albrecht, R., Heizer, C., Hodgkinson, S. and Maniak, M. (1995). Chemoattractant-controlled accumulation of coronin at the leading edge of *Dictyostelium* cells monitored using a green fluorescent protein-coronin fusion protein. *Curr. Biol*. **5**:1280-1285.

Gertler, F.B., Niebuhr, K., Reinhard, M., Wehland, J. and Soriano, P. (1996). Mena, a relative of VASP and *Drosophila* Enabled, is implicated in the control of microfilament dynamics. *Cell* **87**:227-239.

Gettemans, J., De Ville, Y., Vandekerckhove, J. and Waelkens, E. (1992). *Physarum* actin is phosphorylated as the actin-fragmin complex at residues Thr203 and Thr202 by a specific 80 kDa kinase. *EMBO J*. **11**:3185-3191.

Gibbon, B.C., Zonia, L.E., Kovar, D.R., Hussey, P.J. and Staiger, C.J. (1998). Pollen profilin function depends on interaction with proline-rich motifs. *Plant Cell* **10**:981-993.

Gilmore, A.P. and Burridge, K. (1996). Regulation of vinculin binding to talin and actin by phosphatidyl-inositol-4-5-bisphosphate. *Nature* **381**:531-535.

Gilmore, A.P., Jackson, P., Waites, G.T. and Critchley, D.R. (1992). Further characterization of the talin-binding site in the cytoskeletal protein vinculin. *J. Cell Sci*. **103**:719-731.

Goldberg, M., Barzu, O., Parsot, C. and Sansonetti, P.J. (1993). Unipolar localization and ATPase activity of IcsA, a *Shigella flexneri* protein involved in intracellular movement. *J. Bacteriol*. **175**:2189-2196.

Goosney, D.L., de Grado, M. and Finlay, B.B. (1999). Putting *E. coli* on a pedestal: a unique system to study signal transduction and the actin cytoskeleton. *Trends Cell Biol*. **9**:11-14.

Gottwald, U., Brokamp, R., Karakesisoglou, I., Schleicher, M. and Noegel, A.A. (1996). Identification of a cyclase-associated protein (CAP) homologue in *Dictyostelium discoideum* and characterization of its interaction with actin. *Mol. Biol. Cell* **7**:261-272.

Gouin, E., Gantelet, H., Egile, C., Lasa, I., Ohayon, H., Villiers, V., Gounon, P., Sansonetti, P.J. and Cossart, P. (1999). A comparative study of the actin-based motilities of the pathogenic bacteria *Listeria monocytogenes*, *Shigella flexneri* and *Rickettsia conorii*. *J. Cell Sci*. **112**:1697-1708.

Graham, F.L. and van der Eb, A.J. (1973). A new technique for the assay of infectivity of human adenovirus 5 DNA. *Virology* **52**:456.

Haarer, B.K., Lillie, S.H., Adams, A.E.M., Magdolen, V., Bandlow, W. and Brown, S.S. (1990). Purification of profilin from *Saccharomyces cerevisiae* and analysis of profilin-deficient cells. *J. Cell Biol*. **110**:105-114.

Haarer, B.K., Petzold, A.S. and Brown, S.S. (1993). Mutational analysis of yeast profilin. *Mol. Cell Biol*. **13**:7864-7873.

Hacker, U., Albrecht, R. and Maniak, M. (1997). Fluid-phase uptake by macropinocytosis in *Dictyostelium*. *J. Cell Sci*. **110**:105-112.

Hakansson, S., Bergman, T., Vanooteghem, J.C., Cornelis, G.R. and Wolf-Watz, H. (1993). YopB and YopD constitute a novel class of *Yersinia* Yop proteins. *Infect. Immun*. **61**:71-80.

Hakansson, S., Schesser, K., Persson, C., Galyov, E.E., Rosqvist, R., Homble, F. and Wolf-Watz, H. (1996a). The YopB protein of *Yersinia pseudotuberculosis* is essential for the translocation of Yop effector proteins across the target cell plasma membrane and displays a contact dependent membrane disrupting activity. *EMBO J*. **15**:5812-5823.

Hakansson, S., Galyov, E.E., Rosqvist, R. and Wolf-Watz, H. (1996b). The *Yersinia* YpkA Ser/Thr kinase is translocated and subsequently targeted to the inner surface of the HeLa cell plasma membrane. *Mol. Microbiol*. **20**:593-603.

Hanakam, F., Albrecht, R., Eckerskorn, C., Matzner, M. and Gerisch, G. (1996). Myristoylated and non-myristoylated forms of the pH sensor protein hisactophilin II: intracellular shuttling to plasma membrane and nucleus monitored in real time by a fusion with green fluorescent protein. *EMBO J*. **15**:2935-2943.

Hanski, C., Kutschka, U., Schmoranzer, H.P., Naumann, M., Stallmach, A., Hahn, H., Menge, H. and Riecken, E.O. (1989). Immunohistochemical and electron microscopic study of interaction of *Yersinia enterocolitica* serotype O8 with intestinal mucosa during experimental enteritis. *Infect. Immun*. **57**:673-678.

Hartmann, H., Noegel, A.A., Eckerskorn, C., Rapp, S. and Schleicher, M. (1989). Ca^{2+}-independent F-actin capping proteins. *J. Biol. Chem*. **264**:12639-12647.

Hartwig, J.H. and Shevlin, P. (1986). The architecture of actin filaments and the ultrastructural location of actin-binding protein in the periphery of lung macrophages. *J. Cell Biol*. **103**:1007-1020.

Hasegawa, T., Takahashi, S., Hayashi, H. and Hatano, S. (1980). Fragmin: a calcium ion sensitive regulatory factor on the formation of actin filaments. *Biochemistry* **19**:2677-2683.

Haugwitz, M., Noegel, A.A., Rieger, D., Lottspeich, F. and Schleicher, M. (1991). *Dictyostelium discoideum* contains two profilin isoforms that differ in structure and function. *J. Cell Sci*. **100**:481-489.

Haugwitz, M., Noegel, A.A., Karakesisoglou, I. and Schleicher, M. (1994). *Dictyostelium* amoebae that lack G-actin-sequestering profilins show defects in F-actin content, cytokinesis, and development. *Cell* **79**:303-314.

Hawkins, M., Pope, B., Maciver, S.K. and Weeds, A.G. (1993). Human actin depolymerizing factor mediates a pH-sensitive destruction of actin filaments. *Biochemistry* **32**:9985-9993.

Heesemann, J. (1987). Chromosomal-encoded siderophores are required for mouse virulence of enteropathogenic *Yersinia* species. *FEMS. Microbiol. Lett*. **48**:229-233.

Heesemann, J. and Grueter, L. (1987). Genetic evidence that the outer membrane protein YOP1 of *Yersinia enterocolitica* mediates adherence and phagocytosis resistance to human epithelial cells. *FEMS Microbiol. Lett*. **40**:37-41.

Heim, R. and Tsien, R.Y. (1996). Engineering green fluorescent protein for improved brightness, longer wavelengths and fluorescence resonance energy transfer. *Curr. Biol*. **6**:178-182.

Heim, R., Prasher, D.C. and Tsien, R.Y. (1994). Wavelength mutations and posttranslational autooxidation of green fluorescent protein. *Proc. Natl. Acad. Sci. USA* **91**:12501-12504.

Heim, R., Cubitt, A.B. and Tsien, R.Y. (1995). Improved green fluorescence. *Nature* **373**:663-664.

Hemmings, L., Rees, D.J., Ohanian, V., Bolton, S.J., Gilmore, A.P., Patel, B., Priddle, H., Trevithick, J.E., Hynes, R.O. and Critchley, D.R. (1996). Talin contains three actin-binding sites each of which is adjacent to a vinculin-binding site. *J. Cell Sci*. **109**:2715-2726.

Hitt, A.L., Lu, T.H. and Luna, E.J. (1994). Ponticulin is an atypical membrane protein. *J. Cell Biol*. **126**:1421-1431.

Hock, R.S. and Condeelis, J.S. (1987). Isolation of a 240-kilodalton actin-binding protein from *Dictyostelium discoideum*. *J. Biol. Chem*. **262**:394-400.

Hofmann, A., Noegel, A.A., Bomblies, L., Lottspeich, F. and Schleicher, M. (1993). The 100 kDa F-actin capping protein of *Dictyostelium* amoebae is a villin prototype ("protovillin"). *FEBS Lett*. **328**:71-76.

Holmes, D.S. and Quigley, M. (1981). A rapid boiling method for the preparation of bacterial plasmids. *Anal. Biochem*. **114**:193-197.

Holmstroem, A., Rosqvist, R., Wolf-Watz, H. and Forsberg, A. (1995). Virulence plasmid-encoded YopK is essential for *Yersinia pseudotuberculosis* to cause systemic infection in mice. *Infect. Immun*. **63**:2269-2276.

Horiguchi, Y., Senda, T., Sugimoto, N., Katahira, J. and Matsuda, M. (1995). *Bordetella bronchiseptica* dermonecrotizing toxin stimulates assembly of actin stress fibers and focal adhesions by modifying the small GTP-binding protein rho. *J. Cell Sci*. **108**:3243-3251.

Horiguchi, Y., Inoue, N., Masuda, M., Kashimoto, T., Katahira, J., Sugimoto, N. and Matsuda, M. (1997). *Bordetella bronchiseptica* dermonecrotizing toxin induces reorganization of actin stress fibers through deamidation of Gln-63 of the GTP-binding protein Rho. *Proc. Natl. Acad. Sci. USA* **94**:11623-11626.

Howard, T.H. and Watts, R.G. (1994). Actin polymerization and leukocyte function. *Curr. Opin. Hematol*. **1**:61-68.

Howard, P.K., Ahern, K.G. and Firtel, R.A. (1988). Establishment of a transient expression system for *Dictyostelium discoideum*. *Nucleic Acids Res*. **16**:2613-2623.

Imamura, H., Tanaka, K., Hihara, T., Umikawa, M., Kamei, T., Takahashi, K., Sasaki, T. and Takai, Y. (1997). Bni1p and Bnr1p: downstream targets of the Rho family small G-proteins which interact with profilin and regulate actin cytoskeleton in *Saccharomyces cerevisiae*. *EMBO J*. **16**:2745-2755.

Iriarte, M. and Cornelis, G.R. (1998). YopT, a new *Yersinia* effector protein, affects the cytoskeleton of host cells. *Mol. Microbiol*. **29**:915-929.

Iriarte, M., Sory, M.-P., Boland, A., Boyd, A.P., Mills, S.D., Lambermont, I. and Cornelis, G.R. (1998). TyeA, a protein involved in control of Yop release and in translocation of *Yersinia* Yop effectors. *EMBO J*. **17**:1907-1918.

Isberg, R.R. (1989). Determinants for thermoinducible cell binding and plasmid-encoded cell entry detected in the absence of the *Yersinia pseudotuberculosis* invasin protein. *Infect. Immun*. **57**:1998-2005.

Isberg, R.R. and Leong, J.M. (1990). Multiple $ß_1$ chain integrins are receptors for invasin, a protein that promotes bacterial penetration into mammalian cells. *Cell* **60**:861-871.

Isberg, R.R., Voorhis, D.L. and Falkow, S. (1987). Identification of invasin: a protein that allows enteric bacteria to penetrate cultured mammalian cells. *Cell* **50**:769-778.

Isberg, R.R., Swain, A. and Falkow, S. (1988). Analysis of expression and thermoregulation of *Yersinia pseudotuberculosis inv* gene with hybrid proteins. *Infect. Immun*. **59**:2133-2138.

Janmey, P.A. and Matsudaira, P.T. (1988). Functional comparison of villin and gelsolin. *J. Biol. Chem*. **263**:16738-16743.

Johnson, R.P. and Craig, S.W. (1995). F-actin binding site masked by the intramolecular association of vinculin head and tail domains. *Nature* **373**:261-264.

Jung, E., Fucini, P., Stewart, M., Noegel, A.A. and Schleicher, M. (1996a). Linking microfilaments to intracellular membranes: the actin-binding and vesicle-associated protein comitin exhibits a mannose-specific lectin activity. *EMBO J*. **15**:1238-1246.

Jung, G., Wu, X.F. and Hammer, J.A. (1996b). *Dictyostelium* mutants lacking multiple classic myosin I isoforms reveal combinations of shared and distinct functions. *J. Cell Biol*. **133**:305-323.

Just, I., Selzer, J., Wilm, M., von Eichel-Streiber, C., Mann, M. and Aktories, K. (1995). Glucosylation of Rho proteins by *Clostridium difficile* toxin B. *Nature* **375**:500-503.

Kadurugamuwa, J.L., Rohde, M., Wehland, J. and Timmis, K.N. (1991). Intercellular spread of *Shigella flexneri* through a monolayer mediated by membranous protrusions and associated with reorganization of the cytoskeletal protein vinculin. *Infect. Immun*. **59**:3463-3471.

Kaiser, D.A. and Pollard, T.D. (1996). Characterization of actin and poly-L-proline binding sites of *Acanthamoeba* profilin with monoclonal antibodies and by mutagenesis. *J. Mol. Biol*. **256**:89-107.

Kaiser, D.A., Sato, M., Ebert, R. and Pollard, T.D. (1986). Purification and characterization of two isoforms of *Acanthamoeba* profilin. *J. Cell Biol*. **102**:221-226.

Kaiser, D.A., Goldschmidt-Clermont, P.J., Levine, B.A. and Pollard, T.D. (1989). Characterization of renatured profilin purified by urea elution from poly-L-proline agarose columns. *Cell Motil. Cytoskel*. **14**:251-262.

Kaiser, D.A., Vinson, V.K., Murphy, D.B. and Pollard, T.D. (1999). Profilin is predominantly associated with monomeric actin in *Acanthamoeba*. *J. Cell Sci*. **112**:3779-3790.

Kalderon, D., Richardson, W.D., Markham, A.F. and Smith, A.E. (1984). Sequence requirements for nuclear location of simian virus 40 large-T antigen. *Nature* **311**:33-38.

Kalpaxis, D., Zundorf, I., Werner, H., Reindl, N., Boy-Marcotte, E., Jacquet, M. and Dingermann, T. (1991). Positive selection for *Dictyostelium discoideum* mutants lacking UMP synthase activity based on resistance to 5-fluoroorotic acid. *Mol. Gen. Genet*. **225**:492-500.

Kapperud, G., Namork, E., Skurnik, M. and Nesbakken, T. (1987). Plasmid-mediated surface fibrillae of *Yersinia pseudotuberculosis* and *Yersinia enterocolitica*: relationship to the outer membrane protein YOP1 and possible importance for pathogenesis. *Infect. Immun*. **55**:2247-2254.

Karakesisoglou, I., Schleicher, M., Gibbon, B.C. and Staiger, C.J. (1996). Plant profilins rescue the aberrant phenotype of profilin-deficient *Dictyostelium* cells. *Cell Motil. Cytoskel*. **34**:36-47.

Karakesisoglou, I., Janssen, K.-P., Eichinger, L., Noegel, A.A. and Schleicher, M. (1999). Identification of a suppressor of the *Dictyostelium* profilin-minus phenotype as a CD36/LIMPII homologue. *J. Cell Biol*. **145**:167-181.

Katada, T. and Ui, M. (1982). ADP-ribosylation of the specific membrane protein of C6 cells by islet-activating protein associated with modification of adenylate cyclase activity. *J. Biol. Chem*. **257**:7210-7216.

Kaufmann, S., Kas, J., Goldmann, W.H., Sackman, E. and Isenberg, G. (1992). Talin anchors and nucleates actin filaments at lipid membranes. A direct demonstration. *FEBS Lett*. **314**:203-205.

Kelly, C.P., Pothoulakis, C. and LaMont, J.T. (1994). *Clostridium difficile* colitis. *New Engl. J. Med*. **330**:257-262.

Knecht, D.A. and Loomis, W.F. (1987). Antisense RNA inactivation of myosin heavy chain gene expression in *Dictyostelium discoideum*. *Science* **236**:1081-1086.

Kocks, C., Gouin, E., Tabouret, M., Berche, P., Ohayon, H. and Cossart, P. (1992). *Listeria monocytogenes*-induced actin assembly requires the actA gene product, a surface protein. *Cell* **68**:521-531.

Kouyama, T. and Mihashi, K. (1981). Fluorimetry study of N-(1-pyrenyl)iodoacetamide-labelled F-actin. Local structural change of actin protomer both on polymerization and on binding of heavy meromyosin. *Eur. J. Biochem*. **114**:33-38.

Kreitmeier, M., Gerisch, G., Heizer, C. and Mueller-Taubenberger, A. (1995). A talin homologue of *Dictyostelium* rapidly assembles at the leading edge of cells in response to chemoattractant. *J. Cell Biol*. **129**:179-188.

Kreuger, K.M. and Barbieri, J.T. (1995). The family of bacterial ADP-ribosylating exotoxins. *Clin. Microbiol. Rev*. **8**:34-37.

Kuebler, E. and Riezman, H. (1993). Actin and fimbrin are required for the internalization step of endocytosis in yeast. *EMBO J*. **12**:2855-2862.

Kuspa, A. and Loomis, W.F. (1992). Tagging developmental genes in *Dictyostelium* by restriction enzyme-mediated integration of plasmid DNA. *Proc. Natl. Acad. Sci. USA* **89**:8803-8807.

Kwiatkowski, D.J. (1999). Function of gelsolin: motility, signaling, apoptosis, cancer. *Curr. Opin. Cell Biol*. **11**:103-108.

Lacerda, H.M., Lax, A.J. and Rozengurt, E. (1996). *Pasteurella multocida* toxin, a potent intracellularly acting mitogen, induces p125 FAK and paxillin tyrosine phosphorylation, actin stress fiber formation, and focal contact assembly in Swiss 3T3 cells. *J. Biol. Chem*. **271**:439-445.

Laemmli, U.K. (1970). Cleavage of structural proteins during assembly of the head of bacteriophage T4. *Nature* **227**:680-685.

Laine, R.O., Zeile, W., Kang, F., Purich, D.L. and Southwick, F.S. (1997). Vinculin proteolysis unmasks an ActA homolog for actin-based *Shigella* motility. *J. Cell Biol*. **138**:1255-1264.

Lambert de Rouvroit, C., Sluiters, C. and Cornelis, G.R. (1992). Role of the transcriptional activator, VirF, and temperature in the expression of the pYV plasmid genes of *Yersinia enterocolitica*. *Mol. Microbiol*. **6**:395-409.

Lambrechts, A., Verschelde, J.-L., Jonckheere, V., Goethals, M., Vandekerckhove, J. and Ampe, C. (1997). The mammalian profilin isoforms display complementary affinities for PIP_2 and proline-rich sequences. *EMBO J*. **16**:484-494.

Lassing, I. and Lindberg, U. (1985). Specific interaction between phosphatidylinositol 4,5-bisphosphate and profilactin. *Nature* **314**:472-474.

Lassing, I. and Lindberg, U. (1988). Specificity of the interaction between phosphatidylinositol 4,5-bisphosphate and the profilin:actin complex. *J. Cell Biochem*. **37**:255-267.

Lee, C.A. (1997). Type III secretion systems: machines to deliver bacterial proteins into eukaryotic cells? *Trends Microbiol*. **5**:148-156.

Lee, S.W., Wulfkuhle, J.D. and Otto, J.J. (1992). Vinculin binding site mapped on talin with an anti-idiotypic antibody. *J. Biol. Chem*. **267**:16355-16358.

Lee, S.S., Karakesisoglou, I., Noegel, A.A., Rieger, D. and Schleicher, M. (2000). Dissection of functional domains by expression of point mutated profilins in *Dictyostelium* mutants. *Eur. J. Cell Biol*. **79**:92-103.

Lehman, W., Craig, R. and Vibert, P. (1994). Ca(2+)-induced tropomyosin movement in *Limulus* thin filaments revealed by three-dimensional reconstruction. *Nature* **368**:65-67.

Leiting, B. and Noegel, A.A. (1991). The *ble* gene of *Streptoalloteichus hindustanus* as a new selectable marker for *Dictyostelium discoideum* confers resistance to phleomycin. *Biochem. Biophys. Res. Comm*. **180**:1403-1407.

Lian, C.-H., Hwang, W.S. and Pai, C.H. (1987). Plasmid-mediated resistance to phagocytosis in *Yersinia enterocolitica*. *Infect. Immun*. **55**:1176-1183.

Lindberg, U., Schutt, C.E., Hellsten, E., Tjader, A.C. and Hult, T. (1988). The use of poly(L-proline)-Sepharose in the isolation of profilin and profilactin complexes. *Biochim. Biophys. Acta* **967**:391-400.

Liu, T., Williams, J.G. and Clarke, M. (1992). Inducible expression of calmodulin antisense RNA in *Dictyostelium* cells inhibits the completion of cytokinesis. *Mol. Biol. Cell* **3**:1403-1413.

Loomis, W.F. (1996). Genetic networks that regulate development in *Dictyostelium* cells. *Microbiol. Rev*. **60**:135-150.

Ludin, B. and Matus, A. (1998). GFP illuminates the cytoskeleton. *Trends Cell Biol*. **8**:72-77.

Lyerly, D.M., Krivan, H.C. and Wilkins, T.D. (1988). *Clostridium difficile*: its disease and toxins. *Clin. Microbiol. Rev*. **1**:1-18.

Ma, X., Ehrhardt, D.W. and Margolin, W. (1996). Colocalization of cell division proteins FtsZ and FtsA to cytoskeletal structures in living *Escherichia coli* cells by using green fluorescent protein. *Proc. Natl. Acad. Sci. USA* **93**:12998-13003.

Machesky, L.M. (1997). Cell motility: complex dynamics at the leading edge. *Curr. Biol.* **7**:R164-R167.

Machesky, L.M., Cole, N.B., Moss, B. and Pollard, T.D. (1994). *Vaccinia* virus expresses a novel profilin with a higher affinity for polyphosphoinositides than actin. *Biochemistry* **33**:10815-10824.

MacLean-Fletcher, S. and Pollard, T.D. (1980). Viscometric analysis of the gelation of *Acanthamoeba* extracts and purification of two gelation factors. *J. Cell Biol*. **85**:414-428.

Malchow, D., Naegele, B., Schwarz, H. and Gerisch, G. (1972). Membrane-bound cyclic AMP phosphodiesterase in chemotactically responding cells of *Dictyostelium discoideum*. *Eur. J. Biochem*. **28**:136-142.

Maniak, M., Rauchenberger, R., Albrecht, R., Murphy, J. and Gerisch, G. (1995). Coronin involved in phagocytosis: dynamics of particle-induced relocalization visualized by a green fluorescent protein tag. *Cell* **83**:915-924.

Mannherz, H.G., Barrington-Leigh, J., Leberman, R. and Pfrang, H. (1975). A specific 1:1 G-actin: DNase I complex formed by the action of DNase I on F-actin. *FEBS Lett*. **60**:34-38.

Manstein, D.J. (1993). Myosin function in the motile behaviour of cells. *Symp. Soc. Exp. Biol*. **47**:375-381.

Manstein, D.J., Titus, M.A., De Lozanne, A. and Spudich, J.A. (1989). Gene replacement in *Dictyostelium*: Generation of myosin null mutants. *EMBO J*. **8**:923-932.

Marhoul, J.F. and Adams, T.H. (1995). Identification of developmental regulatory genes in *Aspergillus nidulans* by overexpression. *Genetics* **139**:537-547.

Matsudaira, P. and Janmey, P. (1988). Pieces in the actin-severing protein puzzle. *Cell* **54**:139-140.

Matsudaira, P., Mandelkow, E., Renner, W., Hesterberg, L.K. and Weber, K. (1983). Role of fimbrin and villin in determining the interfilament distances of actin bundles. *Nature* **301**:209-214.

Mayboroda, O., Schlueter, K. and Jockusch, B. (1997). Differential colocalization of profilin with microfilaments in PtK2 cells. *Cell Motil. Cytoskel*. **37**:166-177.

McGuffie, E.M., Frank, D.W., Vincent, T.S. and Olson, J.C. (1998). Modification of Ras in eukaryotic cells by *Pseudomonas aeruginosa* exoenzyme S. *Infect. Immun*. **66**:2607-2613.

Metzler, W.J., Constantine, K.L., Friedrichs, M.S., Bell, A.J., Ernst, E.G., Lavoie, T.B. and Mueller, L. (1993). Characterization of the three-dimensional solution structure of human profilin: ^{1}H, ^{13}C, and ^{15}N NMR assignments and global folding pattern. *Biochemistry* **32**:13818-13829.

Metzler, W.J., Bell, A.J., Ernst, E., Lavoie, T.B. and Mueller, L. (1994). Identification of the poly-L-proline-binding site on human profilin. *J. Biol. Chem*. **269**:4620-4625.

Michiels, T. and Cornelis, G. (1988). Nucleotide sequence and transcription analysis of *yop51* from *Yersinia enterocolitica* W22703. *Microb. Pathog*. **5**:449-459.

Michiels, T. and Cornelis, G.R. (1991). Secretion of hybrid proteins by the *Yersinia* Yop export system. *J. Bacteriol*. **173**:1677-1685.

Michiels, T., Wattiau, P., Brasseur, R., Ruysschaert, J.M. and Cornelis, G.R. (1990). Secretion of Yop proteins by *yersiniae*. *Infect. Immun*. **58**:2840-2849.

Michiels, T., Vanooteghem, J. C., Lambert de Rouvroit, C., China, B., Gustin, A., Boudry, P. and Cornelis, G.R. (1991). Analysis of *virC*, an operon involved in the secretion of Yop proteins by *Yersinia enterocolitica*. *J. Bacteriol*. **173**:4994-5009.

Mills, S., Boland, A., Sory, M., van der Smissen, P., Kerbourch, C., Finlay, B.B. and Cornelis, G.R. (1997). *Yersinia enterocolitica* induces apoptosis in macrophages by a process requiring functional type III secretion and translocation mechanisms and involving YopP, presumably acting as an effector protein. *Proc. Natl. Acad. Sci. USA* **94**:12638-12643.

Mishima, M. and Nishida, E. (1999). Coronin localizes to leading edges and is involved in cell spreading and lamellipodium extension in vertebrate cells. *J. Cell Sci*. **112**:2833-2842.

Mockrin, S.C. and Korn, E.D. (1980). *Acanthamoeba* profilin interacts with G-actin to increase the rate of actin-bound adenosine 5‘-trisphosphate. *Biochemistry* **19**:5359-5362.

Mohrs, M.R., Janssen, K.-P., Kreis, T., Noegel, A.A. and Schleicher, M. (2000). Cloning and characterization of ß-COP from *Dictyostelium discoideum*. *Eur. J. Cell Biol*. **79**:1-8.

Moores, S.L., Sabry, J.H. and Spudich, J.A. (1996). Myosin dynamics in live *Dictyostelium* cells. *Proc. Natl. Acad. Sci. USA* **93**:443-446.

Moriyama, K., Iida, K. and Yahara, I. (1996). Phosphorylation of Ser-3 of cofilin regulates its essential function on actin. *Genes Cells* **1**:73-86.

Nachmias, V.T. (1993). Small actin-binding proteins: the ß-thymosin family. *Curr. Opin. Cell Biol*. **5**:56-62.

Nagaoka, R., Abe, H. and Obinata, T. (1996). Site-directed mutagenesis of the phosphorylation site of cofilin: its role in cofilin-actin interaction and cytoplasmic localization. *Cell Motil. Cytoskel*. **35**:200-209.

Nefsky, B. and Bretscher, A. (1989). Preparation of immobilized monomeric actin and its use in the isolation of protease-free and ribonuclease-free pancreatic deoxyribonuclease I. *Eur. J. Biochem*. **179**:215-219.

Nellen, W., Silan, C. and Firtel, R.A. (1984). DNA-mediated transformation in *Dictyostelium discoideum*: Regulated expression of an actin gene fusion. *Mol. Cell Biol*. **4**:2890-2898.

Neujahr, R., Heizer, C. and Gerisch, G. (1997). Myosin II-independent processes in mitotic cells of *Dictyostelium discoideum*: redistribution of the nuclei, rearrangement of the actin system, and formation of the cleavage furrow. *J. Cell Sci*. **110**:123-137.

Neujahr, R., Albrecht, R., Koehler, J., Matzner, M., Schwartz, J.M., Westphal, M. and Gerisch, G. (1998). Microtubule-mediated centrosome motility and the positioning of cleavage furrows in multinucleate myosin II-null cells. *J. Cell Sci*. **111**:1227-1240.

Niewoehner, J., Weber, I., Maniak, M., Mueller-Taubenberger, A. and Gerisch, G. (1997). Talin-null cells of *Dictyostelium* are strongly defective in adhesion to particle and substrate surfaces and slightly impaired in cytokinesis. *J. Cell Biol*. **138**:349-361.

Nishida, E. (1985). Opposite effects of cofilin and profilin from porcine brain on rate of exchange of actin-bound adenosine 5‘-trisphosphate. *Biochemistry* **24**:1160-1164.

Nishida, E., Iida, K., Yonezawa, N., Koyasu, S., Yahara, I. and Sakai, H. (1987). Cofilin is a component of intranuclear and cytoplasmic actin rods induced in cultured cells. *Proc. Natl. Acad. Sci. USA* **84**:5262-5266.

Nodelman, I.M., Bowman, G.D., Lindberg, U. and Schutt, C.E. (1999). X-ray structure determination of human profilin II: A comparative structural analysis of human profilins. *J. Mol. Biol*. **294**:1271-1285.

Noegel, A.A. and Luna, J.E. (1995). The *Dictyostelium* cytoskeleton. *Experientia* **51**:1135-1143.

Noegel, A.A., Witke, W. and Schleicher, M. (1987). Calcium-sensitive non-muscle α-actinin contains EF-hand structures and highly conserved regions. *FEBS Lett*. **221**:391-396.

Noegel, A.A., Rapp, S., Lottspeich, F., Schleicher, M. and Stewart, M. (1989). The *Dictyostelium* gelation factor shares a putative actin-binding site with alpha-actinins and dystrophin and also has a rod domain containing six 100-residue motifs that appear to have a cross-beta conformation. *J. Cell Biol*. **109**:607-618.

Nolta, K.V., Rodriguez-Paris, J.M. and Steck, T.L. (1994). Analysis of successive endocytic compartments isolated from *Dictyostelium discoideum* by magnetic fractionation. *Biochim. Biophys. Acta* **1224**:237-246.

Novak, K.D., Peterson, M.D., Reedy, M.C. and Titus, M.A. (1995). *Dictyostelium* myosin I double mutants exhibit conditional defects in pinocytosis. *J. Cell Biol*. **131**:1205-1221.

Obinata, T., Nagaoka, R., Ono, S., Kusano, K., Mohri, K., Ohtaka, Y., Yamashiro, S., Okada, K. and Abe, H. (1997). Low molecular-weight G-actin binding proteins involved in the regulation of actin assembly during myofibrillogenesis. *Cell Struct. Funct*. **22**:181-189.

Olson, K.R., McIntosh, J.R. and Olmsted, J.B. (1995). Analysis of MAP4 function in living cells using green fluorescent protein (GFP) chimeras. *J. Cell Biol*. **130**:639-650.

Ostrander, D.B., Ernst, E.G., Lavoie, T.B. and Gorman, J.A. (1999). Polyproline binding is an essential function of human profilin in yeast. *Eur. J. Biochem*. **262**:26-35.

Oswald, E., Sugai, M., Labigne, A., Wu, H.C., Fiorentini, C., Boquet, P. and O'Brien, A.D. (1994). Cytotoxic necrotizing factor type 2 produced by virulent *Escherichia coli* modifies the small GTP-binding proteins Rho involved in assembly of actin stress fibers. *Proc. Natl. Acad. Sci. USA* **91**:3814-3818.

Pang, K.M., Lee, E. and Knecht, D.A. (1998). Use of a fusion protein between GFP and an actin-binding domain to visualize transient filamentous-actin structures. *Curr. Biol*. **8**:405-408.

Pantaloni, D. and Carlier, M.F. (1993). How profilin promotes actin filament assembly in the presence of thymosin ß4. *Cell* **75**:1007-1014.

Pardee, J.D. and Spudich, J.A. (1982). Purification of muscle actin. *Meth. Enzym*. **85**:164-181.

Pederson, K.J., Vallis, A.J., Aktories, K., Frank, D.W. and Barbieri, J.T. (1999). The amino-terminal domain of *Pseudomonas aeruginosa* ExoS disrupts actin filaments via small-molecular-weight GTP-binding proteins. *Mol. Microbiol*. **32**:393-401.

Pepperkok, R., Scheel, J., Horstmann, H., Hauri, H.-P., Griffiths, G. and Kreis, T.E. (1993). Beta-COP is essential for biosynthetic membrane transport from the endoplasmic reticulum to the Golgi complex *in vivo*. *Cell* **74**:71-82.

Persson, C., Carballeira, N., Wolf-Watz, H and Faellman, M. (1997). The PTPase YopH inhibits uptake of *Yersinia*, tyrosine phosphorylation of $p130^{Cas}$ and FAK, and the associated accumulation of these proteins in peripheral focal adhesions. *EMBO J*. **16**:2307-2318.

Petersen, J., Weilguny, D., Egel, R. and Nielsen, O. (1995). Characterization of *fus1* in *Schizosaccharomyces pombe*; a developmentally controlled function needed for conjugation. *Mol. Cell Biol*. **15**:3697-3707.

Pierce, D.W., Hom-Booher, N. and Vale, R.D. (1997). Imaging individual green fluorescent proteins. *Nature* **388**: 338.

Pistor, S., Chakraborty, T., Niebuhr, K., Domann, E. and Wehland, J. (1994). The ActA protein of *L. monocytogenes* acts as a nucleator inducing reorganization of the actin cytoskeleton. *EMBO J*. **13**:758-763.

Pollard, T.D. and Cooper, J.A. (1984). Quantitative analysis of the effect of *Acanthamoeba* profilin on actin filament nucleation and elongation. *Biochemistry* **23**:6631-6641.

Pollard, T.D. and Cooper, J.A. (1986). Actin and actin-binding proteins. A critical analysis of mechanisms and functions. *Ann. Rev. Biochem*. **55**:987-1035.

Pollard, T.D., Almo, A., Quirk, S., Vinson, V. and Lattman, E.E. (1994). Structure of actin-binding proteins: insights about function at atomic resolution. *Ann. Rev. Cell Biol*. **10**:207-249.

Pollenz, R.S., Chen, T.L., Trivinos-Lagos, L. and Chisholm, R.L. (1992). The *Dictyostelium* essential light chain is required for myosin function. *Cell* **69**:951-962.

Pope, B., Way, M., Matsudaira, P.T. and Weeds, A. (1994). Characterization of the F-actin binding domains of villin: classification of F-actin binding proteins into two groups according to their binding sites on actin. *FEBS Lett*. **338**:58-62.

Prasher, D.C., Eckenrode, V.K., Ward, W.W., Prendergast, F.G. and Cormier, M.J. (1992). Primary structure of the *Aequorea victoria* green fluorescent protein. *Gene* **111**:229-233.

Prassler, J., Stocker, S., Marriott, G., Heidecker, M., Kellermann, J. and Gerisch, G. (1997). Interaction of a *Dictyostelium* member of the plastin/fimbrin family with actin filaments and actin-myosin complexes. *Mol. Biol. Cell* **8**:83-95.

Raper, K.B. (1935). *Dictyostelium discoideum*, a new species of slime mold from decaying forest leaves. *J. Agric. Res*. **50**:133-147.

Reaven, E.P. and Axline, S.G. (1973). Subplasmalemmal microfilaments and microtubules in resting and phagocytizing cultivated macrophages. *J. Cell Biol*. **59**:12-27.

Reinhard, M., Giehl, K., Abel, K., Haffner, C., Jarchau, T., Hoppe, V., Jockusch, B.M. and Walter, U. (1995). The proline-rich focal adhesion and microfilament protein VASP is a ligand for profilins. *EMBO J*. **14**:1583-1589.

Richardson, A. and Parsons, J.T. (1995). Signal transduction through integrins: a central role for focal adhesion kinase? *Bioessays* **17**:229-236.

Ridley, A.J. and Hall, A. (1992). The small GTP-binding protein rho regulates the assembly of focal adhesions and actin stress fibers in response to growth factors. *Cell* **70**:389-399.

Rimpilaeinen, M., Forsberg, A. and Wolf-Watz, H. (1992). A novel protein, LcrQ, involved in the low-calcium response of *Yersinia pseudotuberculosis* shows extensive homology to YopH. *J. Bacteriol*. **174**:3355-3363.

Rivero, F., Koeppel, B., Peracino, B., Bozzaro, S., Siegert, F., Weijer, C.J., Schleicher, M., Albrecht, R. and Noegel A.A. (1996). The role of the cortical cytoskeleton: F-actin crosslinking proteins protect against osmotic stress, ensure cell size, cell shape and motility, and contribute to phagocytosis and development. *J. Cell Sci*. **109**:2679-2691.

Rivero, F., Kuspa, A., Brokamp, R., Matzner, M. and Noegel, A.A. (1998). Interaptin, an actin-binding protein of the alpha-actinin superfamily in *Dictyostelium discoideum*, is developmentally and cAMP-regulated and associates with intracellular membrane compartments. *J. Cell Biol*. **142**:735-750.

Rivero, F., Albrecht, A., Dislich, H., Bracco, E., Graciotti, L., Bozzaro, S. and Noegel, A.A. (1999). RacF1, a novel member of the Rho protein family, associates transiently with cell contact areas, macropinosomes and phagosomes. *Mol. Biol. Cell* **10**:1205-1219.

Rizzuto, R., Brini, M., De Giorgi, F., Rossi, R., Heim, R., Tsien, R.Y. and Pozzan, T. (1996). Double labelling of subcellular structures with organelle-targeted GFP mutants *in vivo*. *Curr. Biol*. **6**:183-188.

Rosqvist, R., Boelin, I. and Wolf-Watz, H. (1988). Inhibition of phagocytosis in *Yersinia pseudotuberculosis*: a virulence plasmid-encoded ability involving the Yop2b protein. *Infect. Immun*. **56**:2139-2143.

Rosqvist, R., Forsberg, A., Rimpilaeinen, M., Bergman, T. and Wolf-Watz, H. (1990). The cytotoxic protein YopE of *Yersinia* obstructs the primary host defence. *Mol. Microbiol*. **4**:657-667.

Rosqvist, R., Forsberg, A. and Wolf-Watz, H. (1991). Intracellular targeting of the *Yersinia* YopE cytotoxin in mammalian cells induces actin microfilament disruption. *Infect. Immun*. **59**:4562-4569.

Rosqvist, R., Magnusson, K.E. and Wolf-Watz, H. (1994). Target cell contact triggers expression and polarized transfer of *Yersinia* YopE cytotoxin into mammalian cells. *EMBO J*. **13**:964-972.

Rosqvist, R., Hakansson, S., Forsberg, A. and Wolf-Watz, H. (1995). Functional conservation of the secretion and translocation machinery for virulence proteins of *yersiniae*, *salmonellae* and *shigellae*. *EMBO J*. **14**:4187-4195.

Rothkegel, M., Mayboroda, O., Rohde, M., Wucherpfennig, C., Valenta, R. and Jockusch, B.M. (1996). Plant and animal profilins are functionally equivalent and stabilize microfilaments in living animal cells. *J. Cell Sci*. **109**:83-90.

Rottner, K., Behrendt, B., Small, J.V. and Wehland, J. (1999). VASP dynamics during lamellipodia protrusion. *Nature Cell Biol*. **1**:321-322.

Rubin, E.J., Gill, D.M., Boquet, P. and Popoff, M.R. (1988). Functional modification of a 21-kilodalton G protein when ADP-ribosylated by exoenzyme C3 of *Clostridium botulinum*. *Mol. Cell Biol*. **8**:418-426.

Ruckdeschel, K., Roggenkamp, A., Schubert, S. and Heesemann, J. (1996). Differential contribution of *Yersinia enterocolitica* virulence factors to evasion of microbicidal action of neutrophils. *Infect. Immun*. **64**:724-733.

Russel, M. (1994). Mutants at conserved positions in gene IV, a gene required for assembly and secretion of filamentous phages. *Mol. Microbiol*. **14**:357-369.

Sakai, R., Iwamatsu, A., Hirano, N., Ogawa, S., Tanaka, T., Mano, H., Yazaki, Y. and Hirai, H. (1994). A novel signaling molecule, p130, forms stable complexes *in vivo* with v-Crk and v-Src in a tyrosine phosphorylation-dependent manner. *EMBO J*. **13**:3748-3756.

Sambrook, J., Fritsch, E.F. and Maniatis, T. (1989). "Molecular cloning". *Cold Spring Harbor Laboratory Press*, Cold Spring Harbor, New York.

Sanger, J.M., Chang, R., Ashton, F., Kaper, J.B. and Sanger, J.W. (1996). Novel form of actin-based motility transports bacteria on the surfaces of infected cells. *Cell Motil. Cytoskelet*. **34**:279-287.

Sarker, M.R., Sory, M.P., Boyd, A.P., Iriarte, M. and Cornelis, G.R. (1998). LcrG is required for efficient translocation of *Yersinia* Yop effector proteins into eukaryotic cells. *Infect. Immun*. **66**:2976-2979.

Scheel, J., Ziegelbauer, K., Kupke, T., Humbel, B.M., Noegel, A.A., Gerisch, G. and Schleicher, M. (1989). Hisactophilin, a histidine-rich actin-binding protein from *Dictyostelium discoideum*. *J. Biol. Chem*. **264**:2832-2839.

Schesser, K., Spiik, A.K., Dukuzumuremyi, J.M., Neurath, M.F., Pettersson, S. and Wolf-Watz, H. (1998). The *yopJ* locus is required for *Yersinia*-mediated inhibition of NF-kB activation and cytokine expression: YopJ contains a eukaryotic SH2-like domain that is essential for its repressive activity. *Mol. Microbiol*. **28**:1067-1079.

Schleicher, M., Gerisch, G. and Isenberg, G. (1984). New actin-binding proteins from *Dictyostelium discoideum*. *EMBO J*. **3**:2095-2100.

Schleicher, M., Noegel, A.A., Schwarz, T., Wallraff, E., Brink, M., Faix, J., Gerisch, G. and Isenberg, G. (1988). A *Dictyostelium* mutant with severe defects in alpha-actinin: its characterization using cDNA probes and monoclonal antibodies. *J. Cell Sci*. **90**:59-71.

Schleicher, M., Andre, B., Andreoli, C., Eichinger, L., Haugwitz, M., Hofmann, A., Karakesisoglou, I., Stoeckelhuber, M. and Noegel, A.A. (1995). Structure/function studies on cytoskeletal proteins in *Dictyostelium* amoebae as a paradigm. *FEBS Lett*. **369**:38-42.

Schlueter, K., Jockusch, B.M. and Rothkegel, M. (1997). Profilins as regulators of actin dynamics. *Biochim. Biophys. Acta* **1359**:97-109.

Schlueter, K., Schleicher, M. and Jockusch, B.M. (1998). Effects of single amino acid substitutions in the actin-binding site on the biological activity of bovine profilin I. *J. Cell Sci*. **111**:3261-3273.

Schmidt, G., Sehr, P., Wilm, M., Selzer, J., Mann, M. and Aktories, K. (1997). Gln 63 of Rho is deamidated by *Escherichia coli* cytotoxic necrotising factor-1. *Nature* **387**:725-728.

Schnuchel, A., Wiltscheck, R., Eichinger, L., Schleicher, M. and Holak, T.A. (1995). Structure of severin domain 2 in solution. *J. Mol. Biol*. **247**:21-27.

Schulze-Koops, H., Burkhardt, H., Heesemann, J., Kirsch, T., Swoboda, B., Bull, C., Goodman, S. and Emmrich, F. (1993). Outer membrane protein YadA of enteropathogenic *yersiniae* mediates specific binding to cellular but not plasma fibronectin. *Infect. Immun*. **61**:2513-2519.

Schutt, C.E., Myslik, J.C., Rozycki, M.D., Goonesekere, N.C. and Lindberg, U. (1993). The structure of crystalline profilin-ß-actin. *Nature* **365**:810-816.

Schutt, D.C., Wessels, D., Wagenkenecht, K., Chandrasekar, A., Hitt, A.L., Luna, E.J. and Soll, D.R. (1995). Ponticulin plays a role in the positional stabilization of pseudopods. *J. Cell Biol*. **131**:1495-1506.

Sells, M.A., Knaus, U.G., Bagrodia, S., Ambrose, D.M., Bokoch, G.M. and Chernoff, J. (1997). Human p21-activated kinase (Pak1) regulates actin organization in mammalian cells. *Curr. Biol*. **7**:202-210.

Serafini, T., Orci, L., Amherdt, M., Brunner, M., Kahn, R.A. and Rothman, J.E. (1991). ADP-ribosylation factor is a subunit of the coat of Golgi-derived COP-coated vesicles: a novel role for a GTP-binding protein. *Cell* **67**:239-253.

Simon, M.-N., Mutzel, R., Mutzel, H. and Veron, M. (1988). Vectors for expression of truncated coding sequences in *Escherichia coli*. *Plasmid* **19**:94-102.

Simonet, M. and Falkow, S. (1992). Invasin expression in *Yersinia pseudotuberculosis*. *Infect. Immun*. **60**:4414-4417.

Simpson, P.A., Spudich, J.A. and Parham, P. (1984). Monoclonal antibodies prepared against *Dictyostelium* actin: characterization and interactions with actin. *J. Cell Biol*. **99**:287-295.

Sixma, T.K., Pronk, S.E., Kalk, K.H., Wartna, E.S., van Zanten, B.A.M., Witholt, B. and Hol, W.G.J. (1991). Crystal structure of a *cholera* toxin-related heat-labile enterotoxin from *E. coli*. *Nature* **351**:371-377.

Smilenov, L.B., Mikhailov, A., Pelham Jr., R.J., Marcantonio, E.E. and Gundersen, G.G. (1999). Focal adhesion motility revealed in stationary fibroblasts. *Science* **286**:1172-1174.

Sohn, R.H. and Goldschmidt-Clermont, P.J. (1994). Profilin: at the crossroads of signal transduction and the actin cytoskeleton. *Bioessays* **16**:465-472.

Sohn, R.H., Chen, J., Koblan, K.S., Bray, P.F., Goldschmidt-Clermont, P.J. (1995). Localization of a binding site for phosphatidylinositol 4,5-bisphosphate on human profilin. *J. Biol. Chem*. **270**:21114-21120.

Sory, M.P. and Cornelis, G.R. (1994). Translocation of a hybrid YopE-adenylate cyclase from *Yersinia enterocolitica* into HeLa cells. *Mol. Microbiol*. **14**:583-594.

Sory, M.P., Boland, A., Lambermont, A. and Cornelis, G.R. (1995). Identification of the YopE and YopH domains required for secretion and internalization into the cytosol of macrophages, using the *cyaA* gene fusion approach. *Proc. Natl. Acad. Sci. USA* **92**:11998-12002.

Spudich, J.A. and Watt, S. (1971). The regulation of rabbit skeletal muscle contraction. Biochemical studies on the interaction of tropomyosin-troponin complex with actin and the proteolytic fragments of myosin. *J. Biol. Chem*. **246**:4866-4871.

Staiger, C.J., Yuan, M., Valenta, R., Shaw, P.J., Warn, R.M. and Lloyd, C.W. (1994). Microinjected profilin affects cytoplasmic streaming in plant cells by rapidly depolymerizing actin microfilaments. *Curr. Biol*. **4**:215-219.

Stainier, I., Iriarte, M. and Cornelis, G.R. (1997). YscM1 and YscM2, two *Yersinia enterocolitica* proteins causing downregulation of *yop* transcription. *Mol. Microbiol*. **26**:833-843.

Stendahl, O.I., Hartwig, J.H., Brotschi, E.A. and Stossel, T.P. (1980). Distribution of actin-binding protein and myosin in macrophages during spreading and phagocytosis. *J. Cell Biol*. **84**:215-224.

Stoeckelhuber, M., Noegel, A.A., Eckerskorn, C., Koehler, J., Rieger, D. and Schleicher, M. (1996). Structure/function studies on the pH-dependent actin-binding protein hisactophilin in *Dictyostelium* mutants. *J. Cell Sci*. **109**:1825-1835.

Stossel, T.P., Chaponnier, C., Ezzell, R.M., Hartwig, J.H., Janmey, P.A., Kwiatkowski, D.J., Lind, S.E., Smith, D.B., Southwick, F.S., Yin, H.L. and Zaner, K.S. (1985). Nonmuscle actin-binding proteins. *Ann. Rev. Cell Biol*. **1**:353-402.

Straight, A.F., Marshall, W.F., Sedat, J.W. and Murray, A.W. (1997). Mitosis in living budding yeast: anaphase A but no metaphase plate. *Science* **277**:574-578.

Straley, S.C., Skrzypek, E., Plano, G.V. and Bliska, J.B. (1993). Yops of *Yersinia* spp. pathogenic for humans. *Infect. Immun*. **61**:3105-3110.

Sugai, M., Enomoto, T., Hashimoto, K., Matsumoto, K., Matsuo, Y., Ohgai, H., Hong, Y.M., Inoue, S., Yoshikawa, K. and Suginaka, H. (1990). A novel epidermal cell differentiation inhibitor (EDIN): purification and characterization from *Staphylococcus aureus*. *Biochem. Biophys. Res. Commun*. **173**:92-98.

Suggs, S.V., Hirose, T., Miyake, T., Kawashima, E.H., Johnson, M.J., Itakura, K. and Wallace, R.B. (1981). Use of synthetic oligodeoxy-ribonucleotides for the isolation of specific cloned DNA sequences using purified genes. In: "Developmental Biology" (Brown, D.D. and Fox, C.F.). *Academic Press*, New York. pp683-693.

Sun, H.Q., Kwiatkowska, K. and Yin, H.L. (1995). Actin monomer binding proteins. *Curr. Biol*. **7**:102-110.

Sun, H.Q., Lin, K.M. and Yin, H.L. (1997). Gelsolin modulates phospholipase C activity *in vivo* through phospholipid binding. *J. Cell Biol*. **138**:811-820.

Sussman, M. (1987). Cultivation and synchronous morphogenesis of *Dictyostelium* under controlled experimental conditions. *Methods Cell Biol*. **28**:9-29.

Suzuki, T., Shinsuke, S. and Sasakawa, C. (1996). Functional analysis of *Shigella* VirG domains essential for interaction with vinculin and actin-based motility. *J. Biol. Chem*. **271**:21878-21885.

Suzuki, T., Miki, H., Takenawa, T. and Sasakawa, C. (1998). Neural Wiskott-Aldrich syndrome protein is implicated in the actin-based motility of *Shigella flexneri*. *EMBO J*. **17**:2767-2776.

Swanson, J.A. and Baer, S.C. (1995). Phagocytosis by zippers and triggers. *Trends Cell Biol*. **5**:89-93.

Tanaka, M. and Shibata, H. (1985). Poly(L-proline)-binding proteins from chick embryos are a profilin and a profilactin. *Eur. J. Biochem*. **151**:291-297.

Tapon, N. and Hall, A. (1997). Rho, Rac and Cdc42 GTPases regulate the organization of the actin cytoskeleton. *Curr. Opin. Cell Biol*. **9**:86-92.

Tarachandani, A. and Wang, Y.L. (1996). Site-directed mutagenesis enabled preparation of a functional fluorescent analog of profilin: biochemical characterization and localization in living cells. *Cell Motil. Cytoskel*. **34**:313-323.

Theriot, J.A. (1997). Accelerating on a treadmill: ADF/cofilin promotes rapid actin filament turnover in the dynamic cytoskeleton. *J. Cell Biol*. **136**:1165-1168.

Theriot, J.A. and Mitchison, T.J. (1993). The three faces of profilin. *Cell* **75**:835-838.

Tilney, L.G. and Portnoy, D.A. (1989). Actin filaments and the growth, movement, and spread of the intracellular bacterial parasite, *Listeria monocytogenes*. *J. Cell Biol*. **109**:1597-1608.

Tilney, L.G., Bonder, E.M., Coluccio, L.M. and Mooseker, M.S. (1983). Actin from Thyone sperm assembles on only one end of an actin filament: a behaviour regulated by profilin. *J. Cell Biol*. **97**:112-124.

Towbin, H., Staehelin, T. and Gordon, J. (1979). Electrophoretic transfer of proteins from polyacrylamide gels to nitrocellulose sheets: procedure and some applications. *Proc. Natl. Acad. Sci. USA* **76**:4350-4354.

Tseng, P.C.H., Runge, M.S., Cooper, J.A., Williams, Jr., R.C. and Pollard, T.D. (1984). Physical, immunochemical and functional properties of *Acanthamoeba* profilin. *J. Cell Biol*. **98**:214-221.

Uyeda, T.Q.P. and Titus, M.A. (1997). The myosins of *Dictyostelium*. In: Maeda, Y., Inouye, K., Takeuchi, I. (eds). *Dictyostelium*: A model system for cell and developmental biology. Universal Academy Press Inc., Tokyo, Japan, pp43-64.

Valerius, N.H., Stendahl, O., Hartwig, J.H. and Stossel, T.P. (1981). Distribution of actin-binding protein and myosin in polymorphonuclear leukocytes during locomotion and phagocytosis. *Cell* **24**:195-202.

Vandekerckhove, J.S., Kaiser, D.A. and Pollard, T.D. (1989). *Acanthamoeba*-actin and profilin can be cross-linked between glutamic acid 364 of actin and lysine 115 of profilin. *J. Cell Biol*. **109**:619-626.

Verheyen, E.M. and Cooley, L. (1994). Profilin mutations disrupt multiple actin-dependent processes during *Drosophila* development. *Development* **120**:717-728.

Vidali, L. and Hepler, P.K. (1997). Characterization and localization of profilin in pollen grains and tubes of *Lilium longiflorum*. *Cell Motil. Cytoskel*. **36**:323-338.

Vieira, J. and Messing, J. (1982). The pUC plasmid, a M13mp7-derived system for insertion mutagenesis and sequencing with synthetic universal primers. *Gene (Amst.)* **19**:259-268.

Vinson, V.K., Archer, S.J., Lattman, E.E., Pollard, T.D. and Torchia, D.A. (1993). Three dimensional solution structure of *Acanthamoeba* profilin-I. *J. Cell Biol*. **122**:1277-1283.

Visser, L.G., Annema, A. and van Furth, R. (1995). Role of Yops in inhibition of phagocytosis and killing of opsonized *Yersinia enterocolitica* by human granulocytes. *Infect. Immun*. **63**:2570-2575.

Wang, S. and Hazelrigg, T. (1994). Implications for *bcd* mRNA localization from spatial distribution of exu protein in *Drosophila* oogenesis. *Nature* **369**:400-403.

Watanabe, N., Madaule, P., Reid, T., Ishizaki, T., Watanabe, G., Kakizuka, A., Saito, Y., Nakao, K., Jockusch, B.M. and Narumiya, S. (1997). p140mDia, a mammalian homolog of *Drosophila* diaphanous, is a target protein for Rho small GTPase and is a ligand for profilin. *EMBO J*. **16**:3044-3056.

Wattiau, P., Woestyn, S. and Cornelis, G.R. (1996). Customized secretion chaperones in pathogenic bacteria. *Mol. Microbiol*. **20**:255-262.

Weber, I., Gerisch, G., Heizer, C., Murphy, J., Badelt, K., Stock, A., Schwartz, J.-M. and Faix, J. (1999). Cytokinesis mediated through the recruitment of cortexillins into the cleavage furrow. *EMBO J*. **18**:586-594.

Wegner, A. (1976). Head-to-tail polymerization of actin. *J. Mol. Biol*. **108**:139-150.

Wegner, A. and Isenberg, G. (1983). 12-fold difference between the critical monomer concentrations of the two ends of actin filaments in physiological salt conditions. *Proc. Natl. Acad. Sci. USA* **80**:4922-4925.

Weiner, O.H., Murphy, J., Griffiths, G., Schleicher, M. and Noegel, A.A. (1993). The actin-binding protein comitin (p24) is a component of the Golgi apparatus. *J. Cell Biol*. **123**:23-34.

Welch, M.D., Iwamatsu, A. and Mitchison, T.J. (1997). Actin polymerization is induced by Arp2/3 protein complex at the surface of *Listeria monocytogenes*. *Nature* **385**:265-269.

Welch, M.D., Rosenblatt, J., Skoble, J., Portnoy, D.A. and Mitchison, T.J. (1998). Interaction of human Arp2/3 complex and the *Listeria monocytogenes* ActA protein in actin filament nucleation. *Science* **281**:105-108.

Westphal, M., Jungbluth, A., Heidecker, M., Muehlbauer, B., Heizer, C., Schwartz, J.-M., Marriott, G. and Gerisch, G. (1997). Microfilament dynamics during cell movement and chemotaxis monitored using a GFP-actin fusion protein. *Curr. Biol*. **7**:176-183.

Williams, C. and Newell, G. (1976). A genetic study of aggregation in the cellular slime mold *Dictyostelium discoideum* using complementation analysis. *Genetics* **82**:287-307.

Witke, W., Schleicher, M. and Noegel, A.A. (1992). Redundancy in the microfilament system: abnormal development of *Dictyostelium* cells lacking two F-actin cross-linking proteins. *Cell* **68**:53-62.

Witke, W., Sharpe, A.H. and Kwiatkowski, D.J. (1993). Profilin deficient mice are not viable. *Mol. Biol. Cell* **4**:149a.

Witke, W., Sharpe, A.H., Hartwig, J.H., Azuma, T., Stossel, T.P. and Kwiatkowski, D.J. (1995). Hemostatic, inflammatory, and fibroblast responses are blunted in mice lacking gelsolin. *Cell* **81**:41-51.

Woychik, R.P., Maas, R.L., Zeller, R., Vogt, T.F. and Leder, P. (1990). "Formins": proteins deduced from the alternative transcripts of the *limb deformity* gene. *Nature* **346**:850-853.

Yahr, T.L., Hovey, A.K., Kulich, S.M. and Frank, D. (1995). Transcriptional analysis of the *Pseudomonas aeruginosa* exoenzyme S structural gene. *J. Bacteriol*. **177**:1169-1178.

Yahr, T.L., Goranson, J. and Frank, D.W. (1996). Exoenzyme S of *Pseudomonas aeruginosa* is secreted by a type III pathway. *Mol. Microbiol*. **22**:991-1003.

Yamamoto, K., Pardee, J.D., Reidler, J., Stryer, L. and Spudich, J.A. (1982). Mechanism of interaction of *Dictyostelium* severin with actin filaments. *J. Cell Biol*. **95**:711-719.

Yanisch-Perron, C., Vieira, J. and Messing, J. (1985). Improved M13 phage cloning vectors and host strains: Nucleotide sequences of the M13mp18 and pUC19 vectors. *Gene* **33**:103-119.

Yin, H.L. and Stossel, T.P. (1979). Control of cytoplasmic actin gel-sol transformation by gelsolin, a calcium-dependent regulatory protein. *Nature* **281**:581-586.

Yonezawa, N., Nishida, E. and Sakai, H. (1985). pH control of actin polymerization by cofilin. *J. Biol. Chem*. **260**:14410-14412.

Yonezawa, N., Nishida, E., Iida, K., Yahara, I. and Sakai, H. (1990). Inhibition of the interactions of cofilin, destrin and deoxyribonuclease I with actin by phosphoinositides. *J. Biol. Chem*. **265**:8382-8386.

Yumura, S. and Fukui, Y. (1998). Spatiotemporal dynamics of actin concentration during cytokinesis and locomotion in *Dictyostelium*. *J. Cell Sci*. **111**:2097-2108.

Zang, J.-H., Cavet, G., Sabry, J.H., Wagner, P., Moores, S.L. and Spudich, J.A. (1997). On the role of myosin II in cytokinesis: division of *Dictyostelium* cells under adhesive and nonadhesive conditions. *Mol. Biol. Cell* **8**:2617-2629.

Zeile, W.L., Purich, D.L. and Southwick, F.S. (1996). Recognition of two classes of oligoproline sequences in profilin-mediated acceleration of actin-based *Shigella* motility. *J. Cell Biol*. **133**:49-59.

Zumbihl, R., Aepfelbacher, M., Andor, A., Jacobi, C.A., Ruckdeschel, K., Rouot, B. and Heesemann, J. (1999). The cytotoxin YopT of *Yersinia enterocolitica* induces modification and cellular redistribution of the small GTP-binding protein RhoA. *J. Biol. Chem*. **274**:29289-29293.

CURRICULUM VITAE

Personal Data

Name:	Soo Sim Lee
Date and place of birth:	10.10.1970; Singapore
Marital status:	single

Education and research experience

1977-1982	Primary school in Singapore
1983-1986	Nanyang Girls' High School
1987-1988	Hwa Chong Junior College
Jul. 1989-Jun. 1992	National University of Singapore Bachelor of Science degree
Jul. 1992-Jun. 1993	National University of Singapore Bachelor of Science with second upper class Honours degree in Microbiology
Sept. 1993-Dec. 1996	National University of Singapore Master of Science degree in Microbiology Title of the Master's thesis: "Isolation and characterization of *DENN*, a novel human gene differentially expressed in normal and neoplastic cells"
Since Apr. 1997	Doctorate candidature at the Adolf-Butenandt-Institut für Zellbiologie in the group of Prof. Dr. M. Schleicher and under the care of Dr. F. Siegert, a representative of the Faculty of Biology, Zoological Institute, Ludwig-Maximilians-Universität Title of PhD thesis: "Functional studies of selected actin binding proteins by point mutations and GFP fusions"

ACKNOWLEDGEMENT

I am very grateful to *Dr. Florian Siegert* from the Zoological Institute, LMU, for his care of my thesis.

I would like to thank *Prof. Dr. Michael Schleicher* for the wonderful opportunity to work in his group and for his guidance and endless patience throughout my doctorate work.

My appreciation to *Prof. Dr. Angelika Noegel* for her advice and generosity in sharing things from her lab.

Special thanks to *Dr. Gerard Marriott* for his GFP-actin construct.

I would also like to thank *Dr. Walter Witke* for his provision of the GFP-fused cytoskeletal constructs.

Especially, I would like to express my gratitude to *Prof. Dr. Dr. J. Heesemann* and *Dr. M. Aepfelbacher* from the Max von Pettenkofer Institut for the use of the confocal microscope and also for providing the *Yersinia* strains.

I am indebted to *Timo Zimmermann* for our collaborative work, his expertise with the confocal microscope and certainly his unselfish support.

Many heartfelt thanks to *Dr. Ludwig Eichinger* for his valuable advice, *Dr. Iakowos Karakesisoglou* for the point-mutated profilins, *Dr. Ralph Gräf* for his useful tips and help in the german translation of the summary, *Dr. Martin Bähler* for the mammalian cell lines, *Daniela Rieger* for her helpful suggestions and assistance, *Mrs E. -M. Praetorius* for the photos, *Mrs M. Beer* and *Mr J. Grimm* for technical support.

A million thanks to *Dr. Klaus-Peter Janssen*, *Annika Gloss*, *Dr. Harald Felgner*, *Andreas Schneider* and *Christian Horn* for their computer expertise and tireless offer of computer assistance.

For my fellow "benchmates" in the Schleicher-group, special thanks go out to my friend from "that place" *Annika Gloss*, *Hyun-Ju Son*, *Klaus-Peter Janssen* "ex-someone", *Lars Israel*, *René Rost*, *Stephan Schwager*, *Stefan Thiel* and *Thomas Giebing*. Thank U all for being there for me and for one of the most pleasant working environment I ever had.

I would like to especially thank *Annika Gloss* and *Klaus-Peter Janssen* for their support and endless patience throughout the entire period of my thesis work.

Last but not least, I would like to thank my family for their support in "all forms" and my friends in Singapore for their encouragement.